

# On the extraction of collinear PDFs

Valerio Bertone

IRFU, CEA, Université Paris-Saclay

université  
PARIS-SACLAY



January 04-08, 2023, Aussois, France, QaT2023 mini-school

# Disclaimer

- When talking about PDFs one often means *unpolarised collinear PDFs of the proton*.
  - They are relevant in processes that involve *unpolarised* protons in the initial state and in which *all hard scales are of the same order* and much larger than  $\Lambda_{\text{QCD}}$ .
  - Typical situation at the **LHC**.
- **Many other kinds of PDFs** exist:
  - collinear *nuclear* PDFs,
  - collinear *longitudinally* polarised PDFs,
  - collinear *transversely* polarised PDFs,
  - transverse-momentum-dependent (*TMD*) PDFs,
  - *unintegrated* PDFs
  - *diffractive* PDFs,
  - ...
- All these different PDFs are appropriate in **other contexts** different from that mentioned above.

# Everything starts from...

A collinear factorisation theorem:

$$d\sigma_{\text{had}} = W_{\{i\}} \otimes \mathcal{L}_{\{i\}} d\Phi$$

# Everything starts from...

A collinear factorisation theorem:

$$d\sigma_{\text{had}} = W_{\{i\}} \otimes \mathcal{L}_{\{i\}} d\Phi$$

**Hard cross sections:**

- process dependent,
- high-energy dominated,
- computable in perturbation theory.

**Parton distribution functions (PDFs):**

- universal,
- low-energy dominated,
- perturbation theory inapplicable.

How do we determine PDFs?

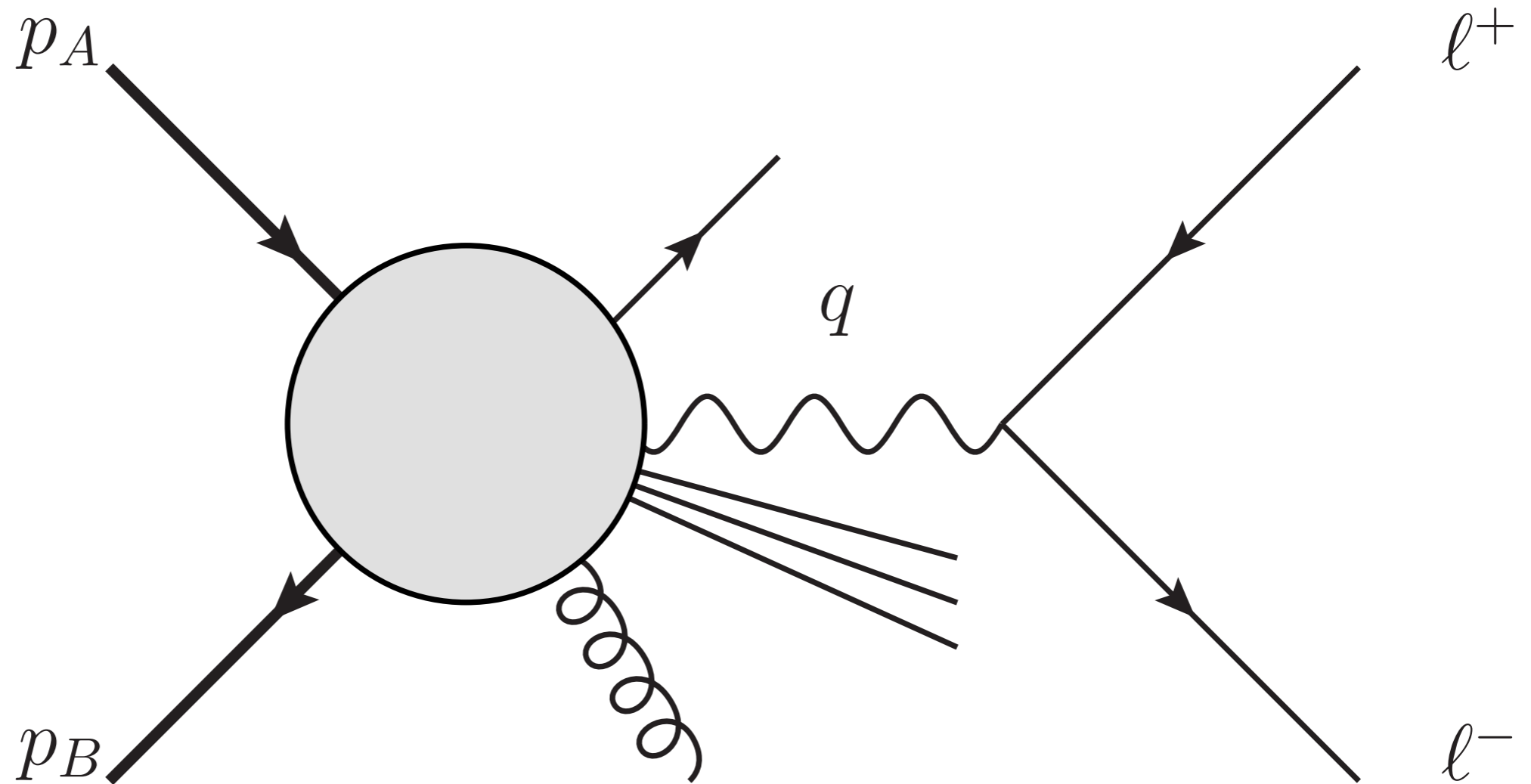


Currently, the most accurate and reliable way is through **fits to data.**

# Diagrammatic power counting

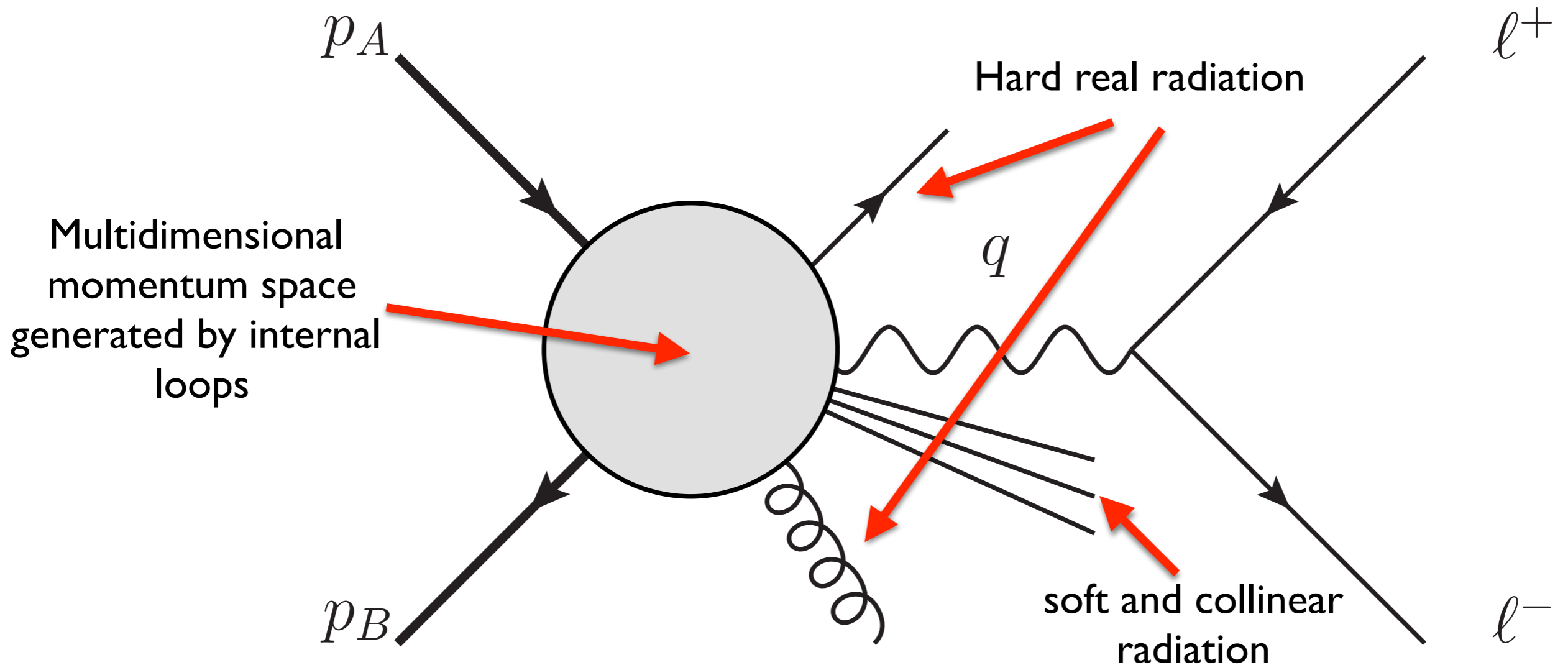


Let us use Drell-Yan production (*i.e. inclusive* production of a lepton pair in hadron-hadron collisions) to sketch the main steps:



# Diagrammatic power counting

🍏 Let us use Drell-Yan production (*i.e. inclusive* production of a lepton pair in hadron-hadron collisions) to sketch the main steps:



🍏 Relevant scales:

$$Q = \sqrt{q^2}, \quad \Lambda_{\text{QCD}} \ll Q$$

# Diagrammatic power counting

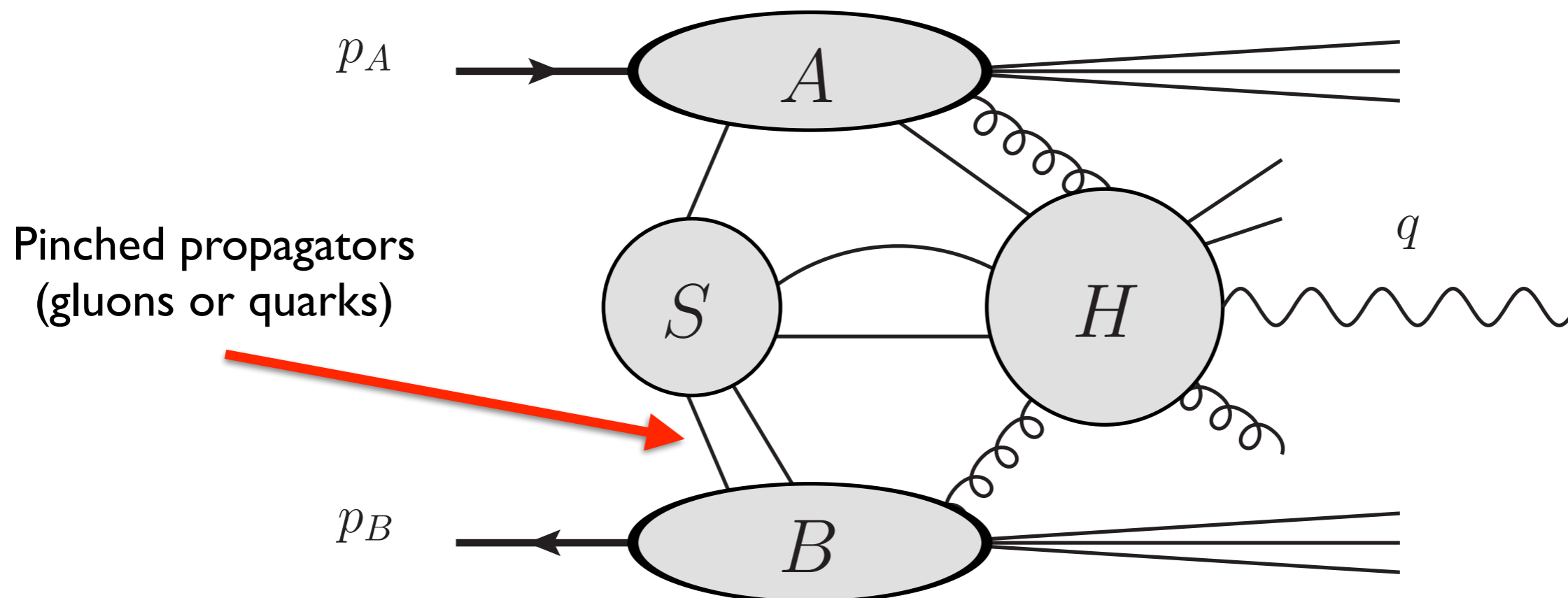
Let us work in **massless** QCD and, for each *single* graph, identify the regions in the integration momentum space where the integrand is large:

🍏 **pinched** propagators  $\Rightarrow$  Landau criterion and **reduced graphs**,

🍏 soft modes (**S**),

🍏 (anti)collinear modes (**A** and **B**),

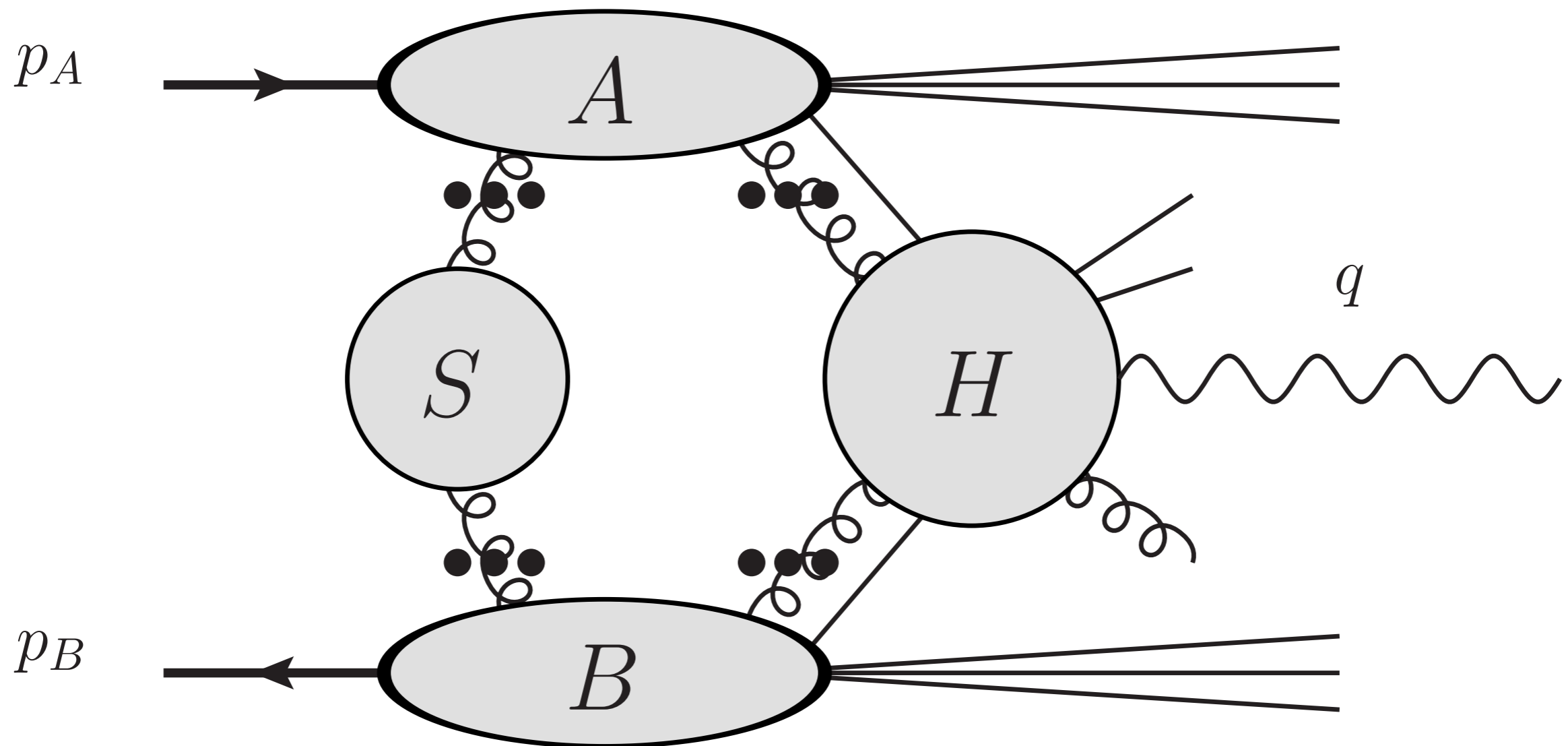
🍏 hard modes (**H**) (not pinched but large integration region).



# Diagrammatic power counting

[G. Sterman, Phys. Rev. D 17 (1978) 2773]

- 🍏 Apply Libby-Sterman power counting to identify the **asymptote** in  $Q$ :
- 🍏 The result (in a **covariant gauge**) is strikingly simple:

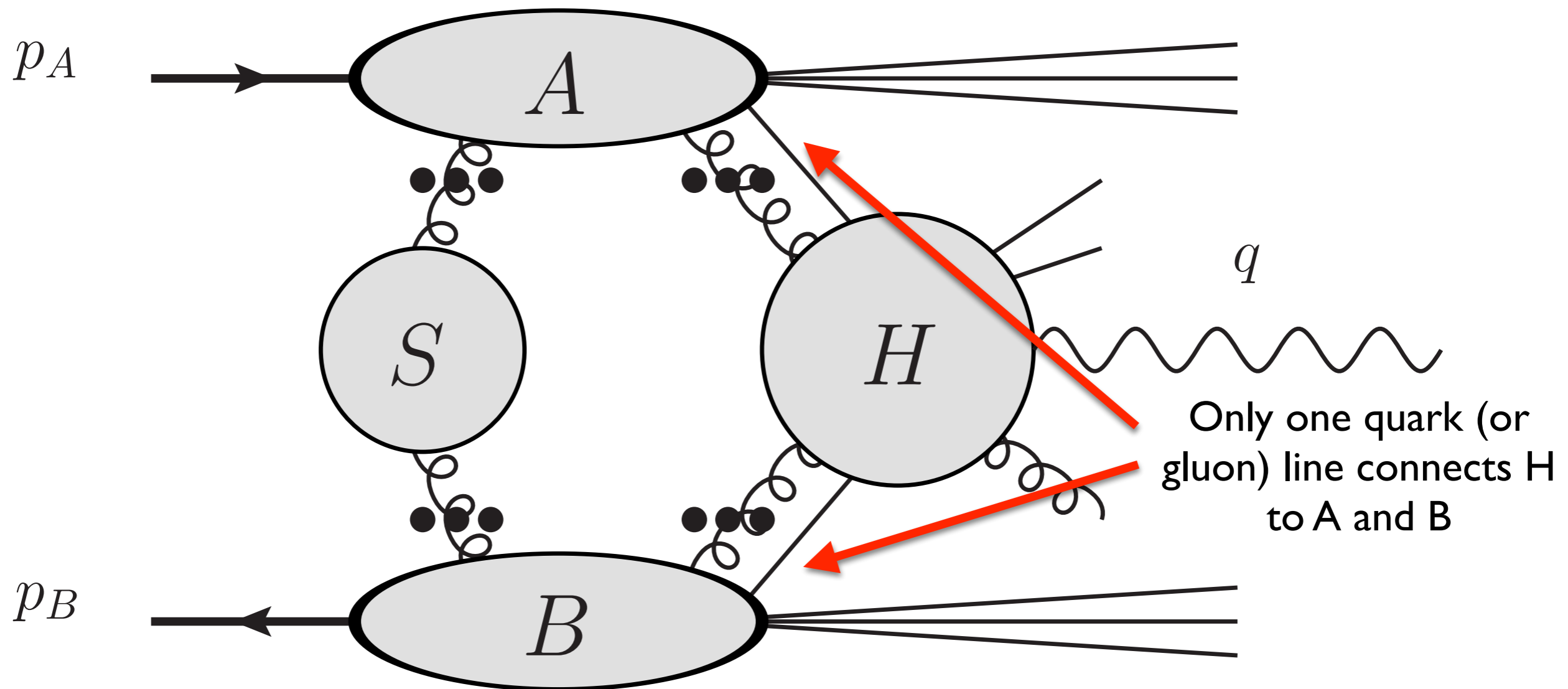




# Diagrammatic power counting

[G. Sterman, Phys. Rev. D 17 (1978) 2773]

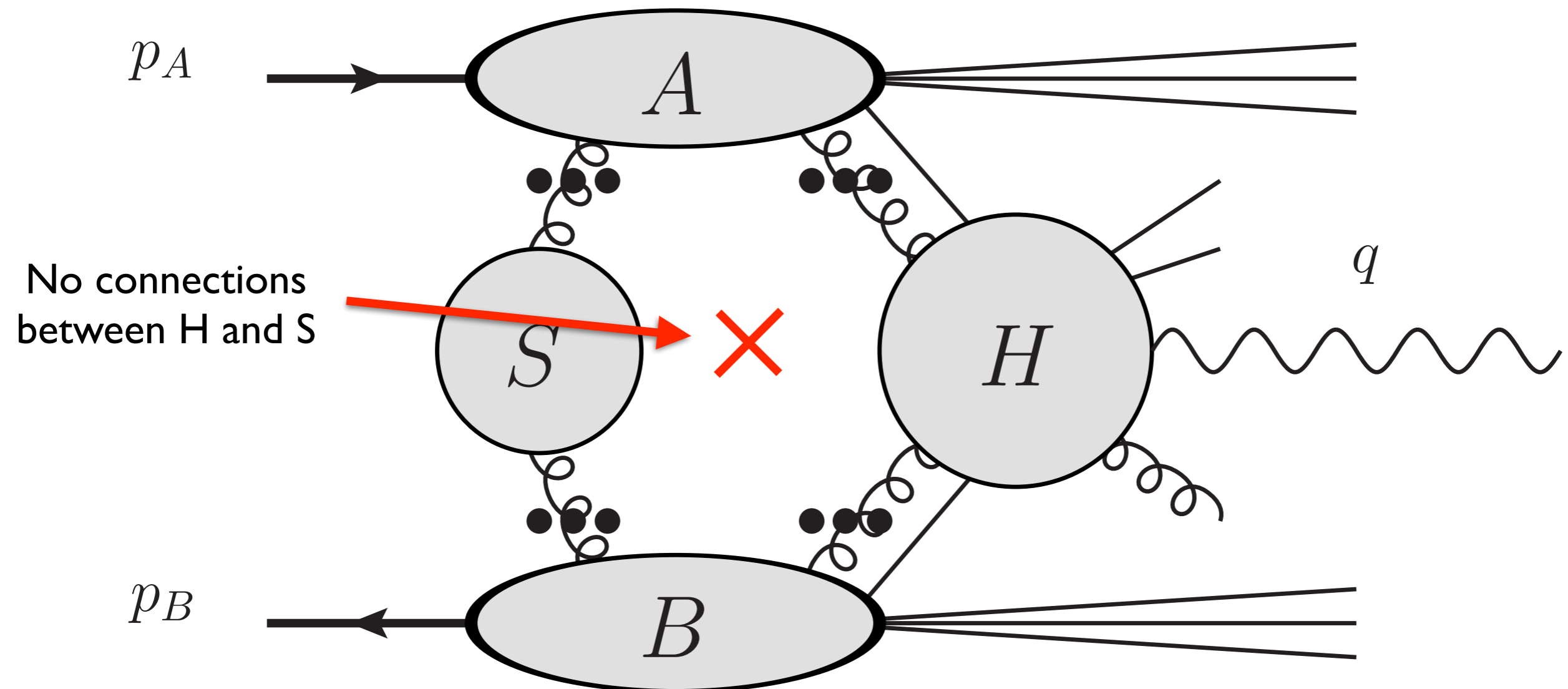
- 🍏 Apply Libby-Sterman power counting to identify the **asymptote** in  $Q$ :
- 🍏 The result (in a **covariant gauge**) is strikingly simple:



# Diagrammatic power counting

[G. Sterman, Phys. Rev. D 17 (1978) 2773]

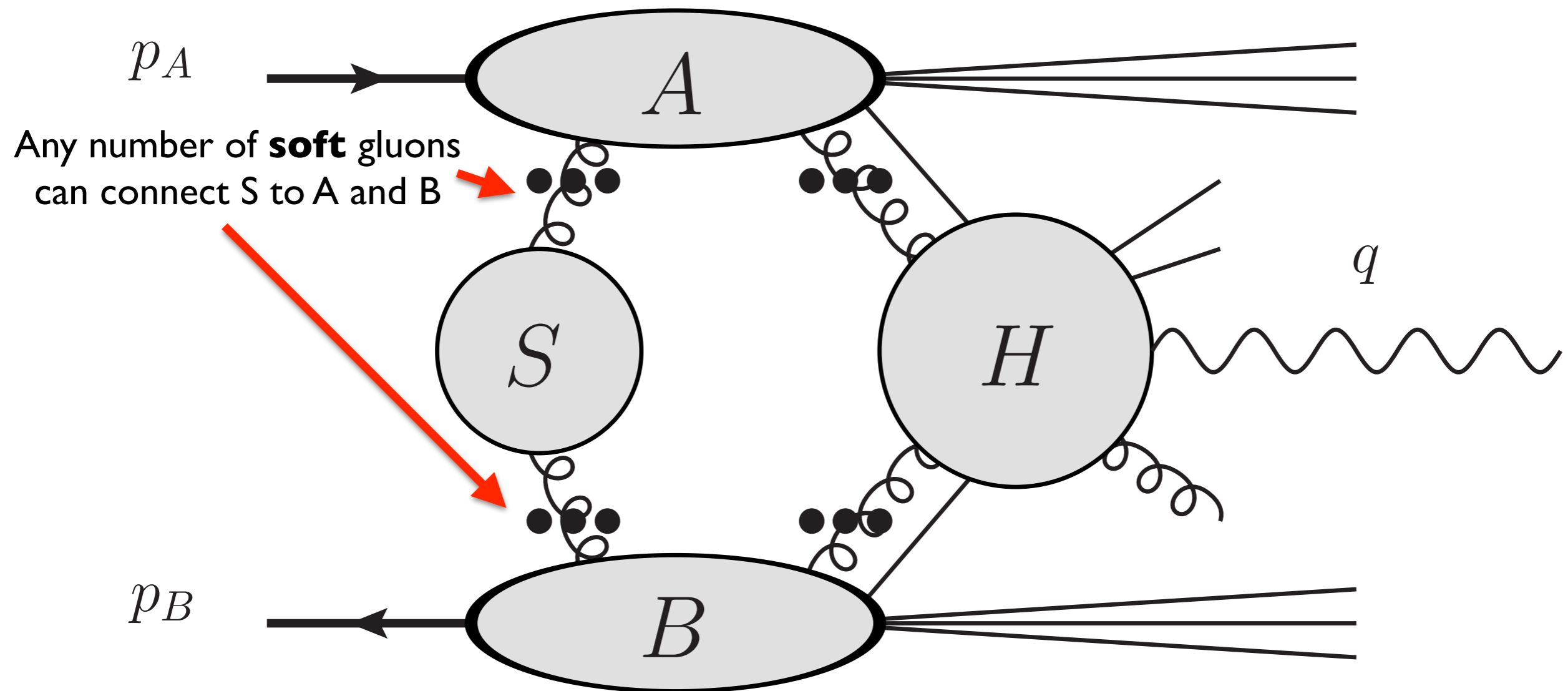
- 🍏 Apply Libby-Sterman power counting to identify the **asymptote** in  $Q$ :
- 🍏 The result (in a **covariant gauge**) is strikingly simple:



# Diagrammatic power counting

[G. Sterman, Phys. Rev. D 17 (1978) 2773]

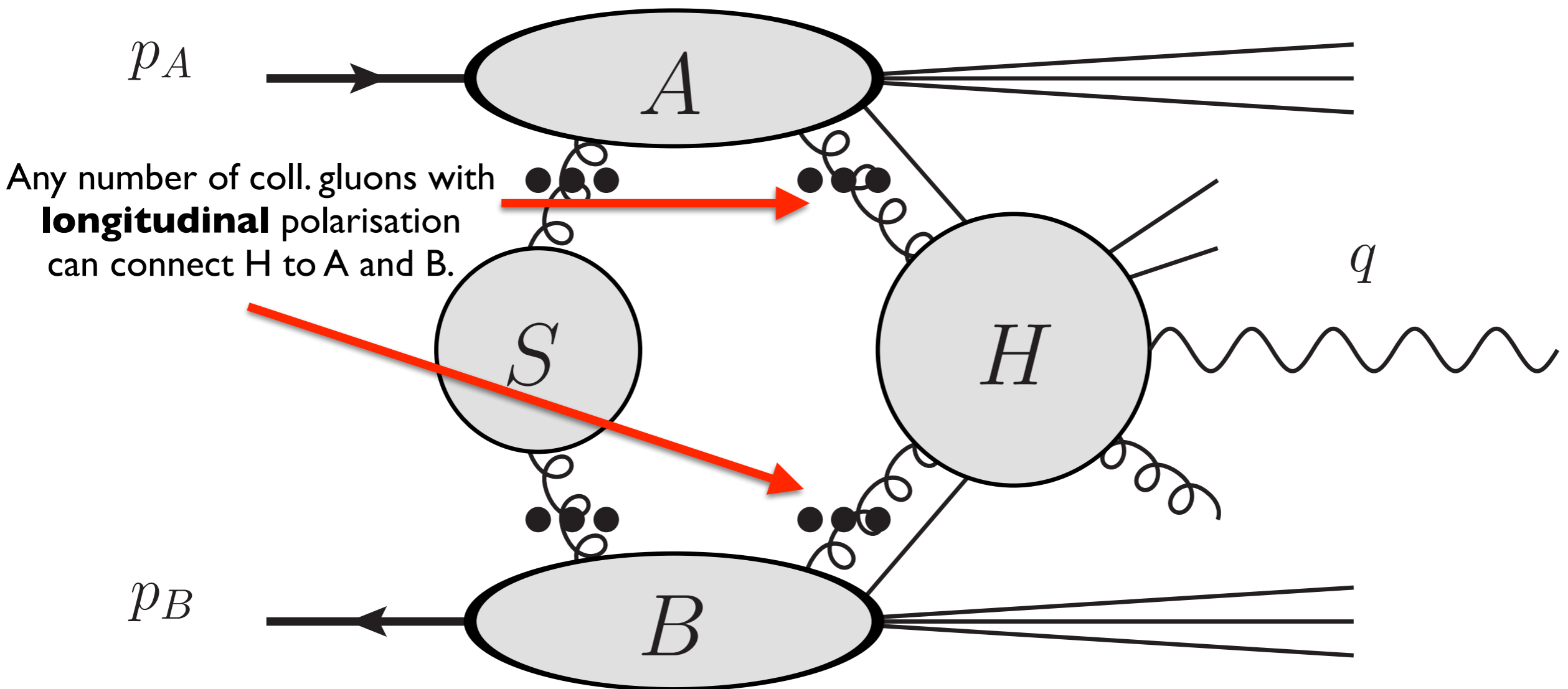
- Apply Libby-Sterman power counting to identify the **asymptote** in  $Q$ :
- The result (in a **covariant gauge**) is strikingly simple:



# Diagrammatic power counting

[G. Sterman, Phys. Rev. D 17 (1978) 2773]

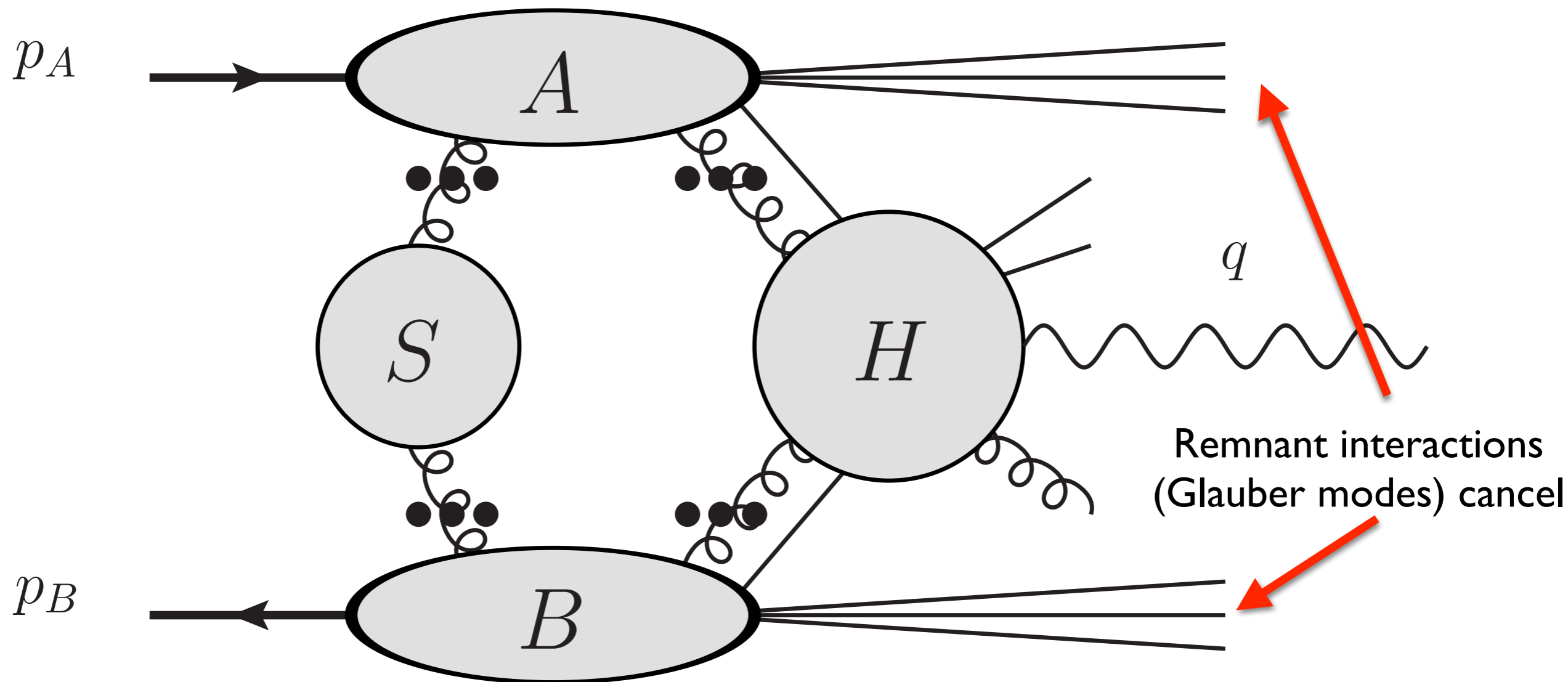
- 🍏 Apply Libby-Sterman power counting to identify the **asymptote** in  $Q$ :
- 🍏 The result (in a **covariant gauge**) is strikingly simple:



# Diagrammatic power counting

[G. Sterman, Phys. Rev. D 17 (1978) 2773]

- 🍏 Apply Libby-Sterman power counting to identify the **asymptote** in  $Q$ :
- 🍏 The result (in a **covariant gauge**) is strikingly simple:



# Diagrammatic power counting

Finally, factorisation is achieved by:

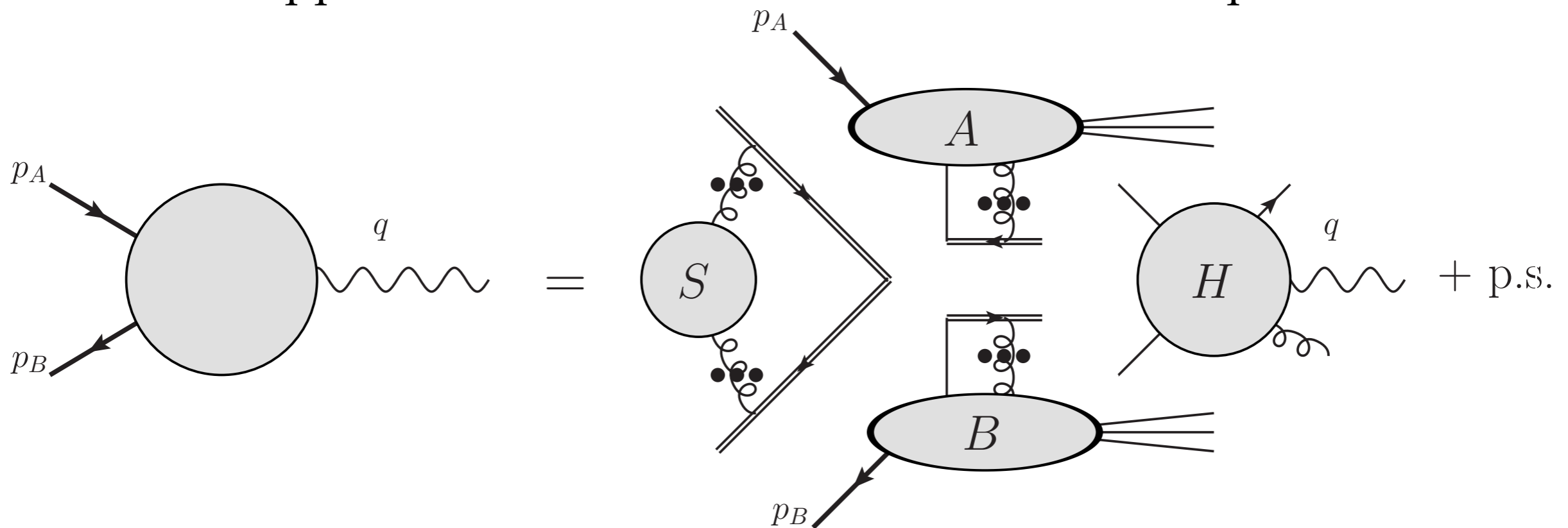
[G. Grammer, D.R. Yennie, *Phys.Rev.D* 8 (1973) 4332-4344]

using **eikonal approximations** for each soft/collinear gluon attachment with momentum  $k$  to write, for example:

$$S^{\mu\dots} g_{\mu\nu} A^{\nu\dots} \sim (\mathbf{k} \cdot \mathbf{S}^{\dots}) \frac{1}{\mathbf{n} \cdot \mathbf{k}} (\mathbf{n} \cdot \mathbf{A}^{\dots})$$

this allows one to use **Ward identities** and introduces **Wilson lines**.

A recursive application leads to factorisation of the amplitude:

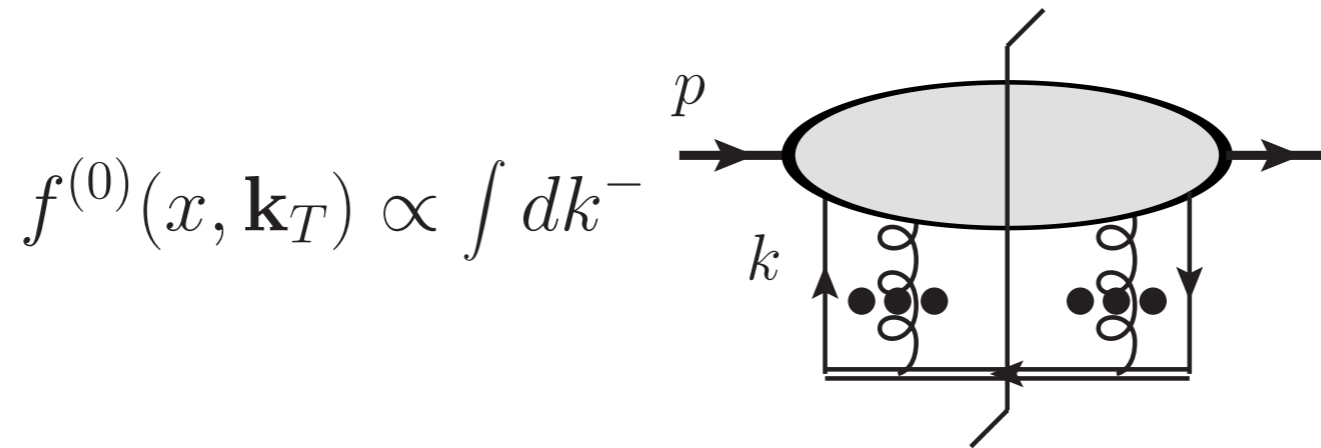


$$A \sim H \cdot A \cdot B \cdot S$$

# Diagrammatic power counting

🍏 Upon squaring, factorisation leads to the operator definition of:

🍏 gauge invariant (unsubtracted) parton-distribution function (**PDF**):

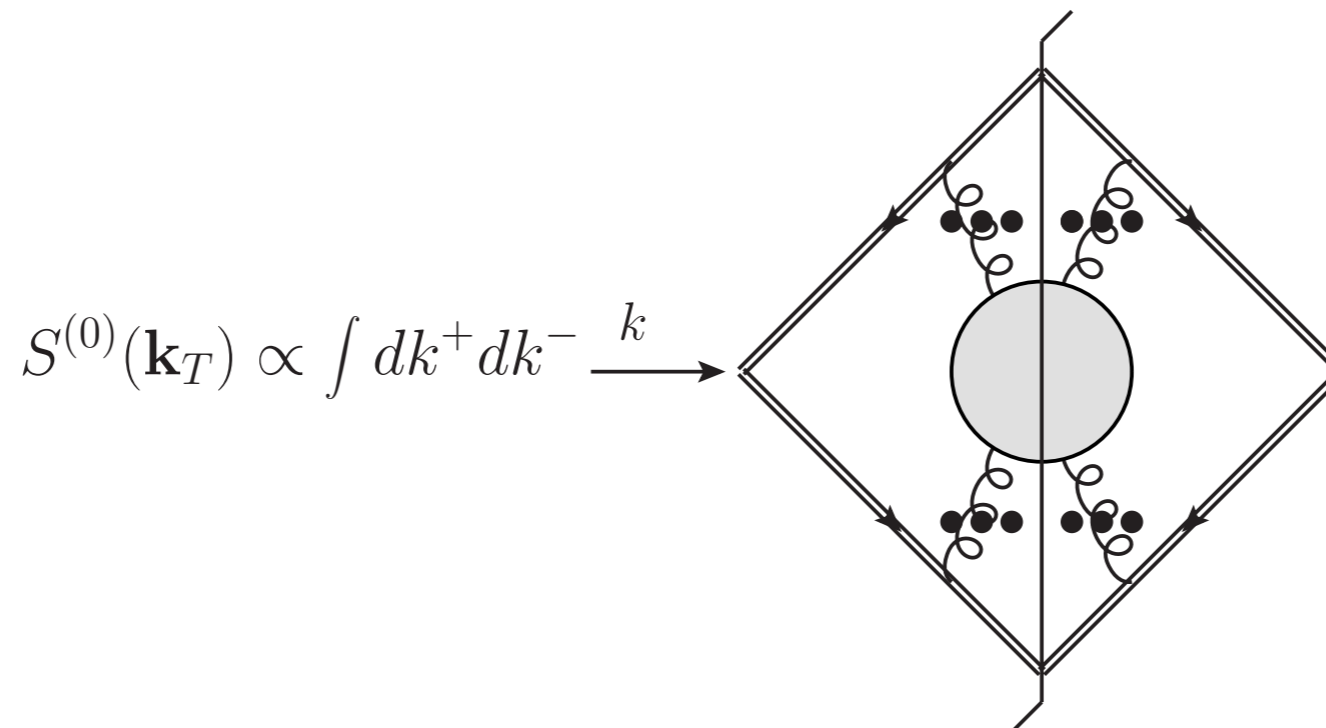


light-cone coordinates:

$$k = (k^+, k^-, \mathbf{k})$$

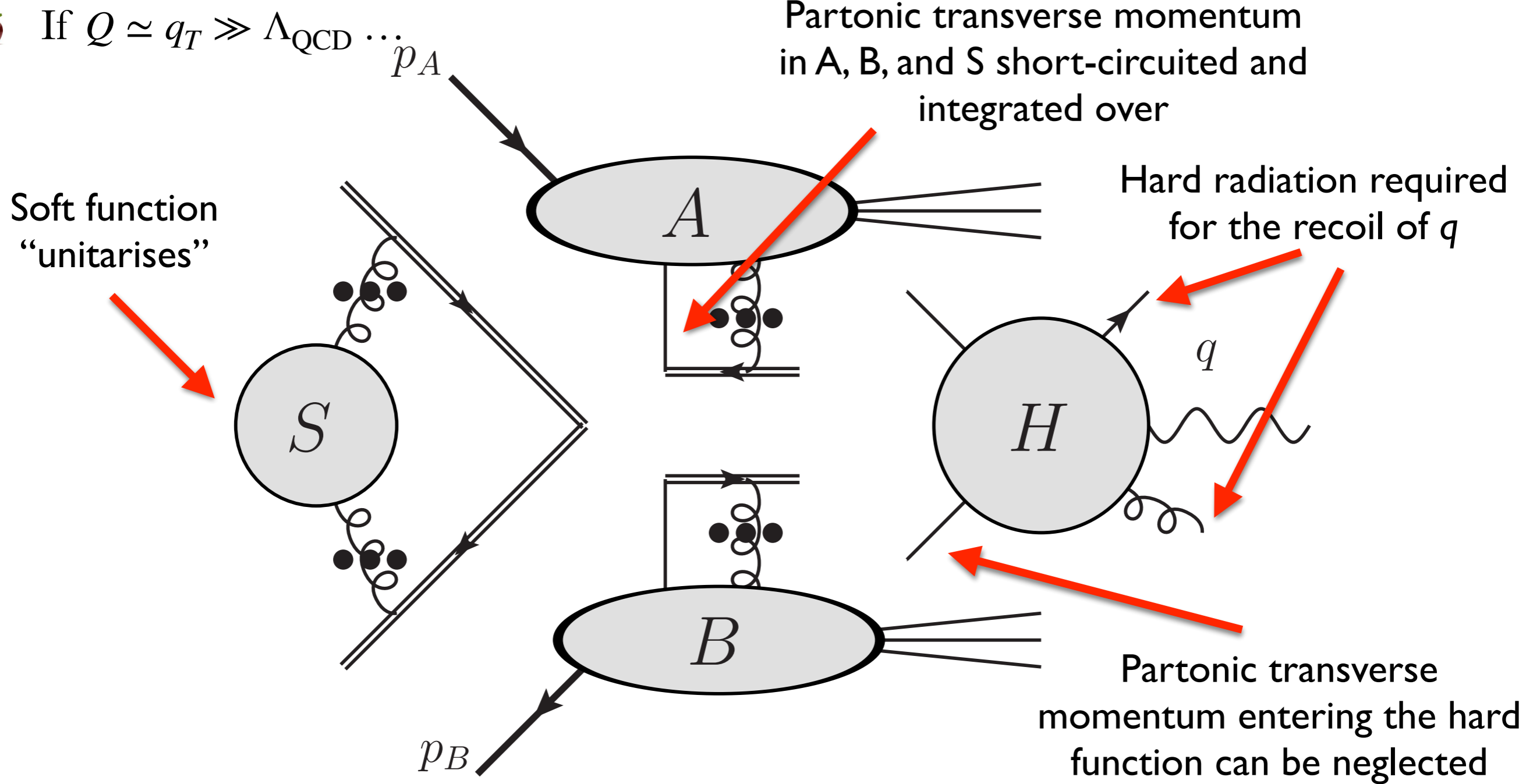
$$k^\pm = \frac{E \pm k_z}{\sqrt{2}}$$

🍏 **soft function:**



🍏 and **hard function.**

# Collinear factorisation



🍎  $H$  is a “complicated” perturbative function accounting for both **real** and **virtual** corrections that depends on the longitudinal momentum fractions  $x$ .

🍎  $k_T$  dependence of A, B, S can be integrated out. This causes “contact” divergences whose removal is responsible for the **DGLAP evolution**.



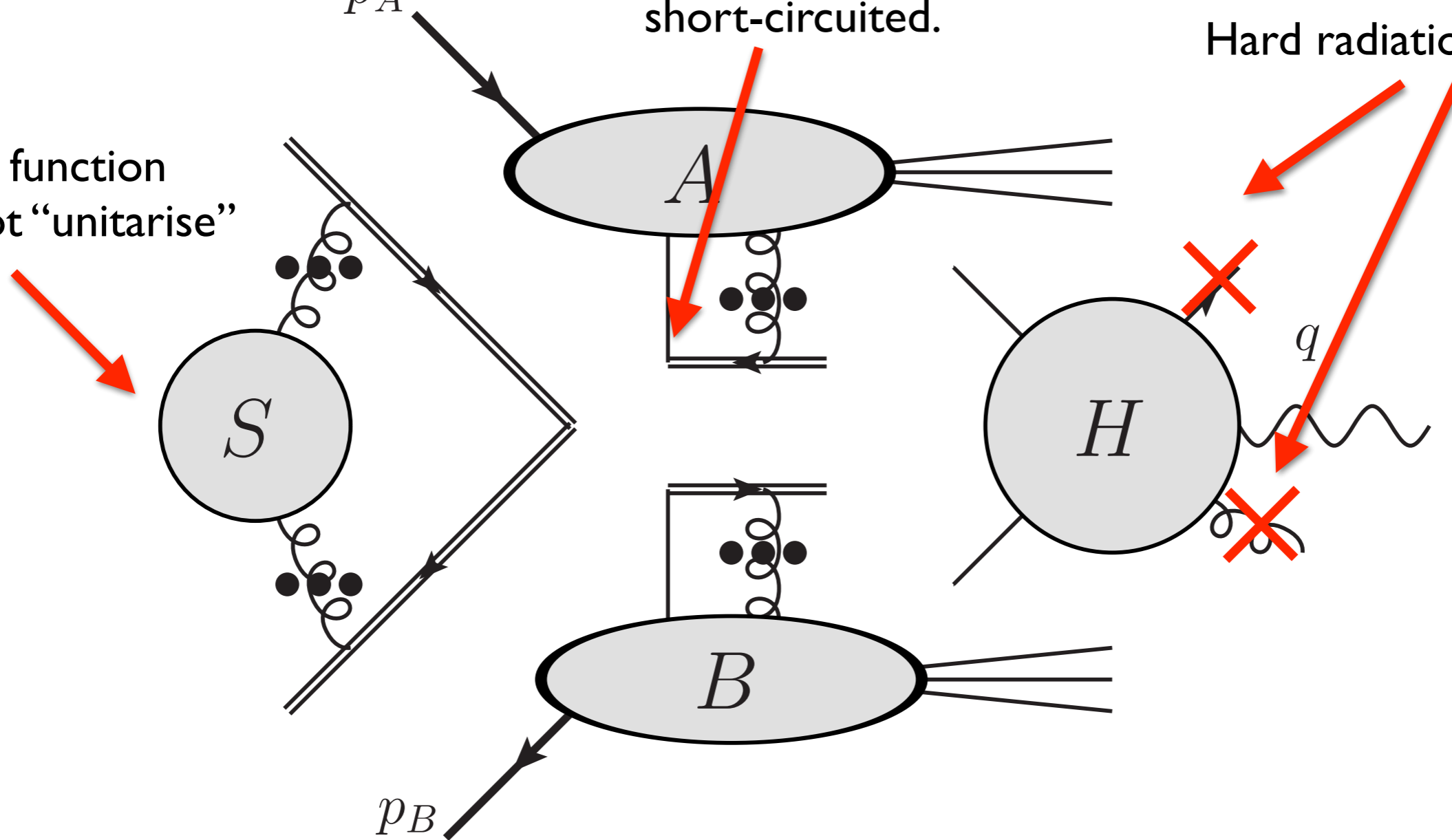
# TMD factorisation

Partonic transverse momentum relevant and cannot be short-circuited.

Hard radiation forbidden

🍏 If  $Q \gg q_T \gg \Lambda_{\text{QCD}} \dots \dot{p}_A$

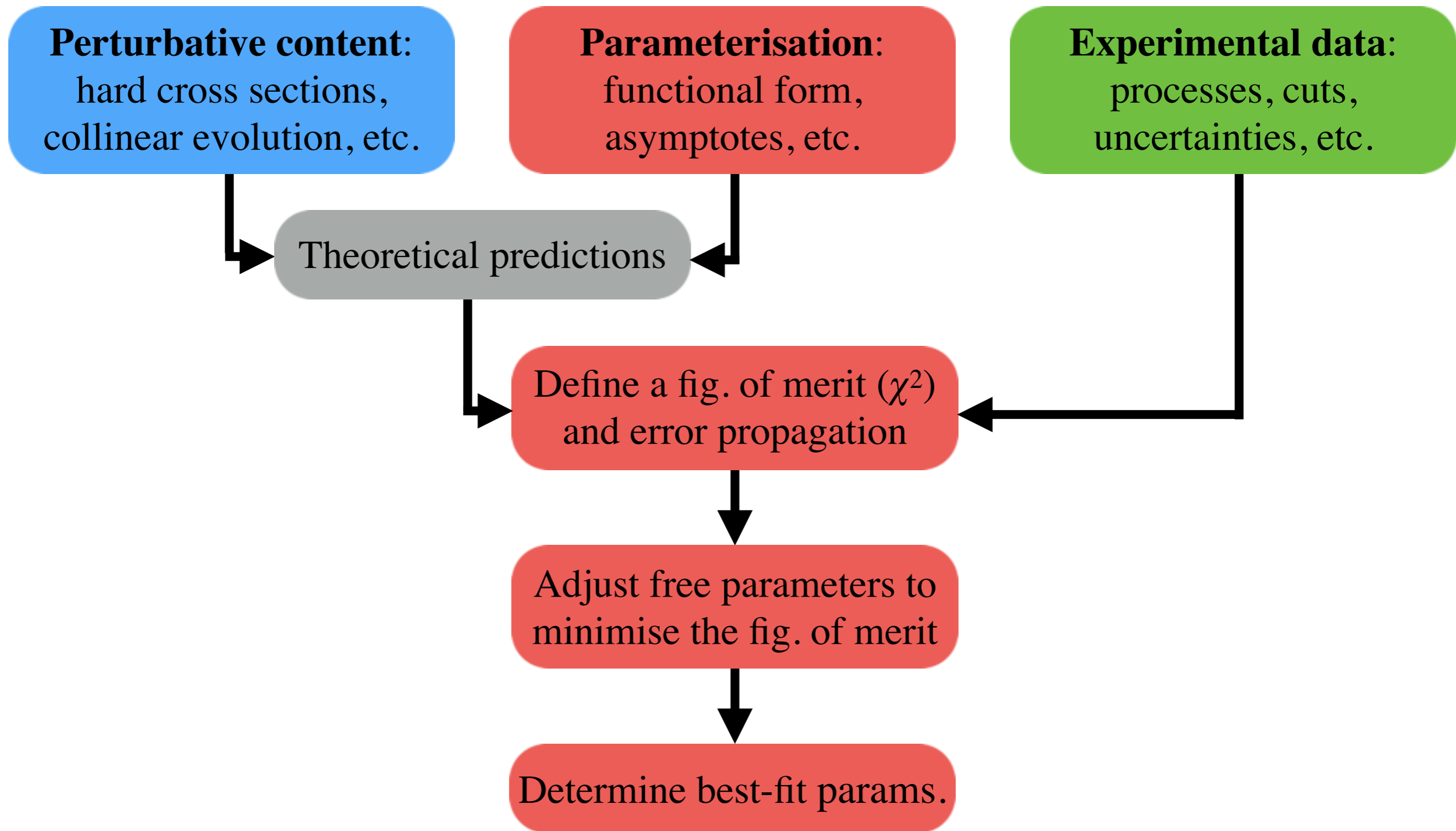
Soft function does not “unitarise”



🍏  $H$  is a “simple” perturbative function that only accounts for **virtual** corrections.

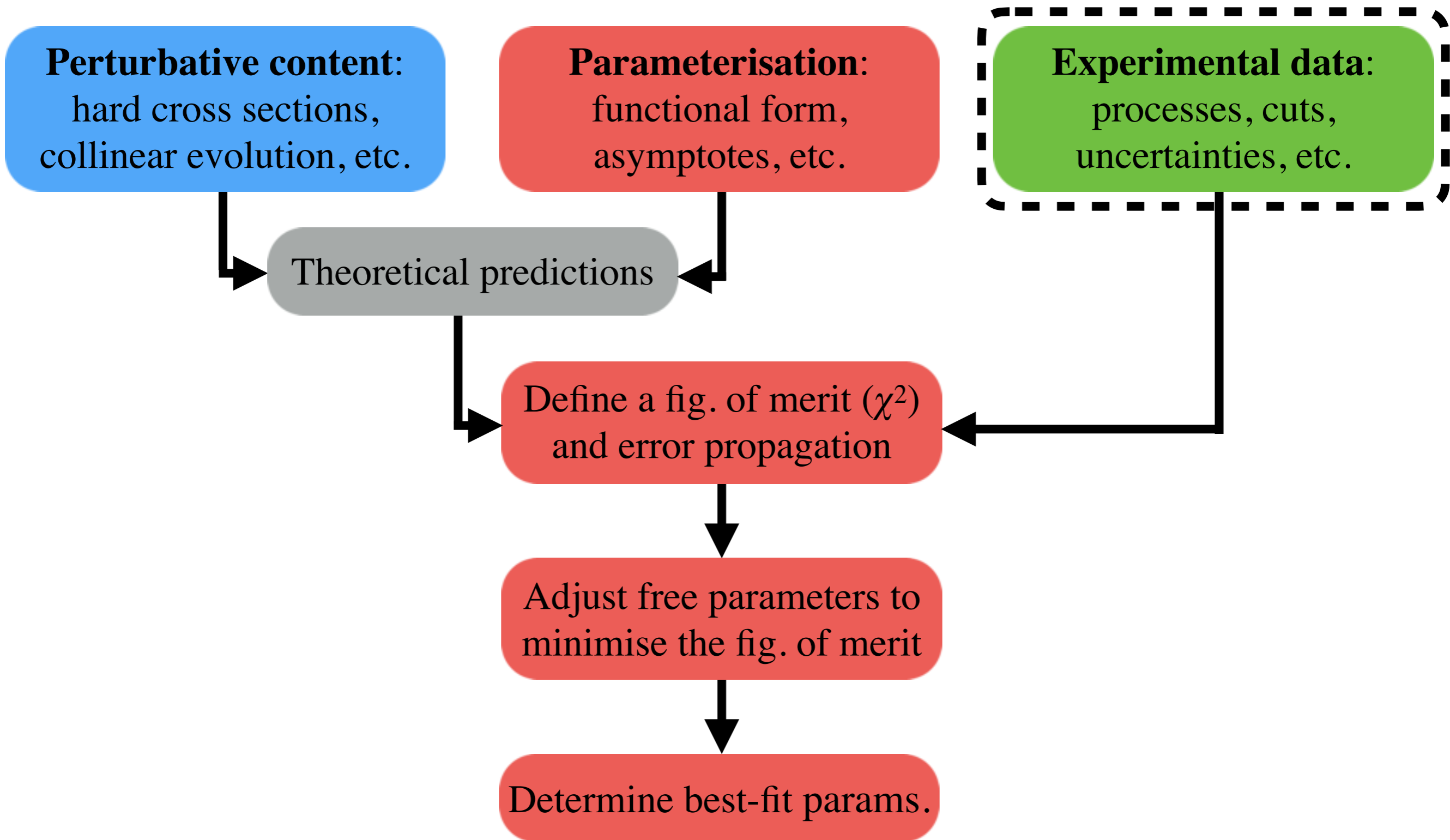
🍏 As opposed to  $q_T \approx Q$  (collinear fact.),  $k_T$  dependence of  $A$ ,  $B$ ,  $S$  cannot be integrated out. Therefore, we need to **treat  $k_T$  exactly**: this is the essence of TMD factorisation.

# The general strategy



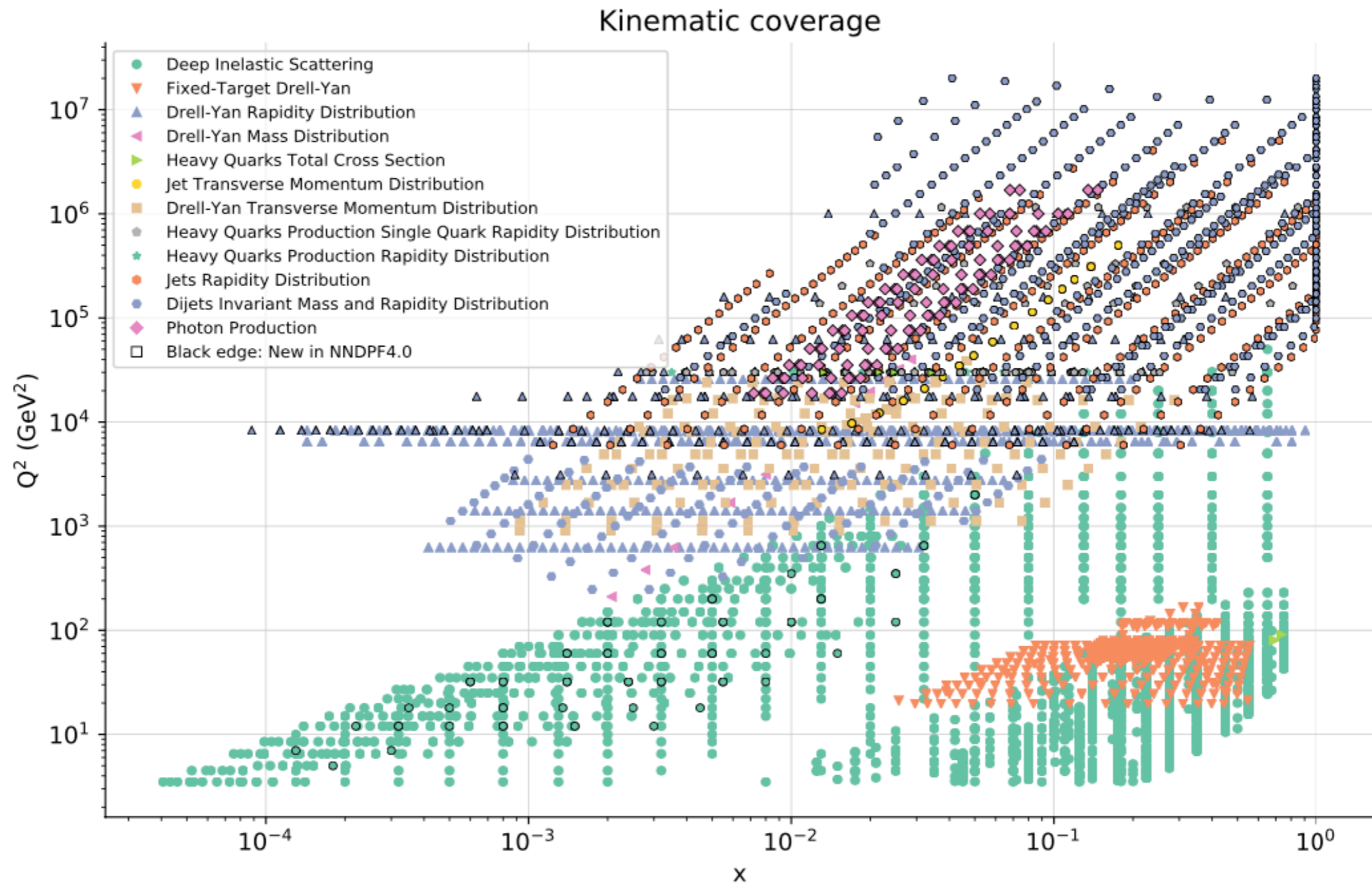
Each box requires a choice. **Different choices** lead to **different determinations**.

# The general strategy



# Experimental data

## NNPDF4.0: data set extension

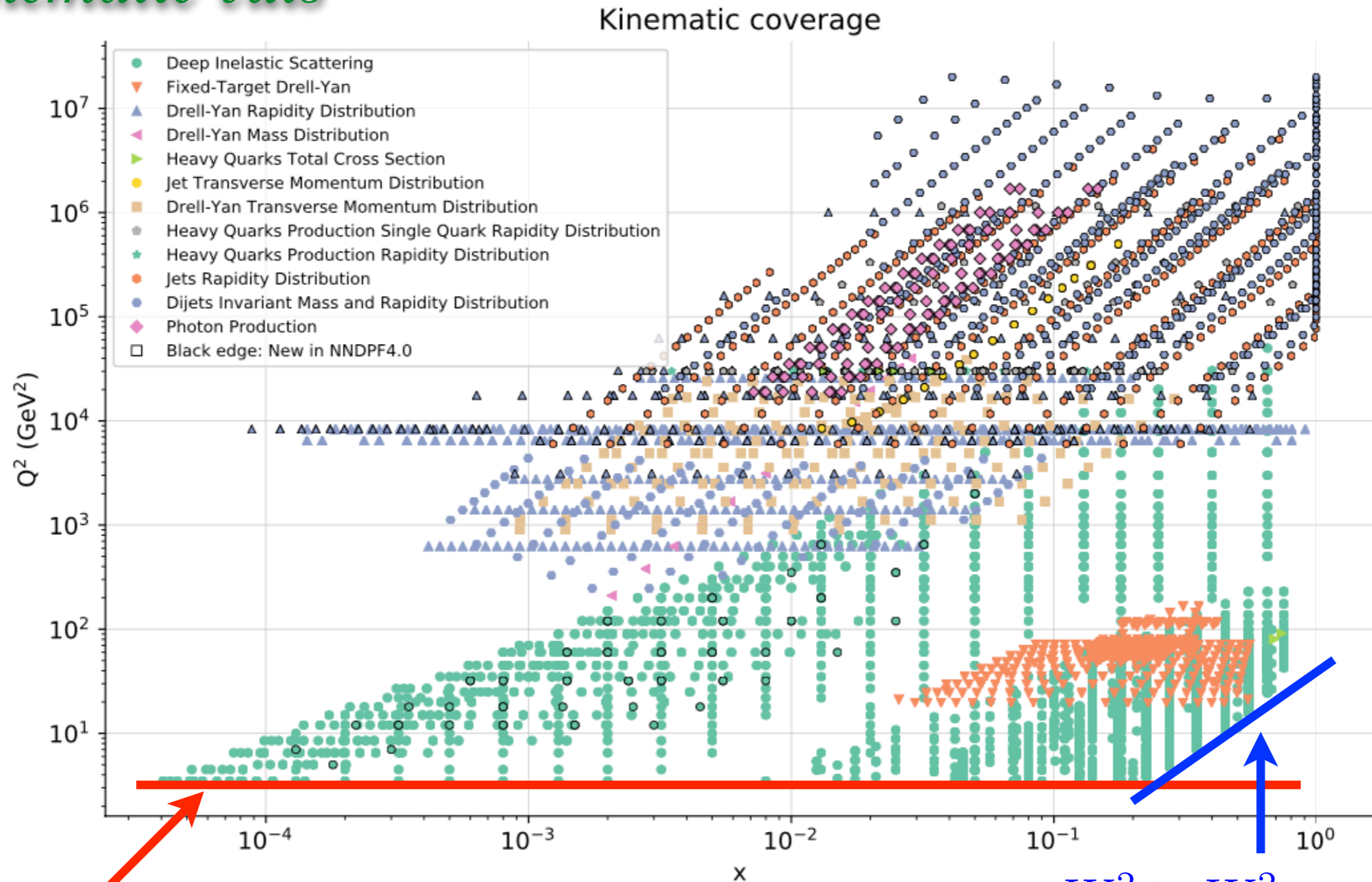


[NNPDF4.0, arXiv:2109.02653]

- Impressive number of processes and data points ( $O(4500)$ ):
  - $ep$  data, *i.e.* DIS (one PDF involved),
  - $pp$  data (two PDFs involved),
  - very wide kinematic coverage:  $10^{-5} \lesssim x \lesssim 1$  and  $2 \text{ GeV} \lesssim Q \lesssim 5 \text{ TeV}$ .

# Experimental data

## *Kinematic cuts*



[NNPDF4.0, arXiv:2109.02653]

$$Q^2 \geq Q_{\min}^2 \quad (Q_{\min} \simeq 2 \text{ GeV})$$

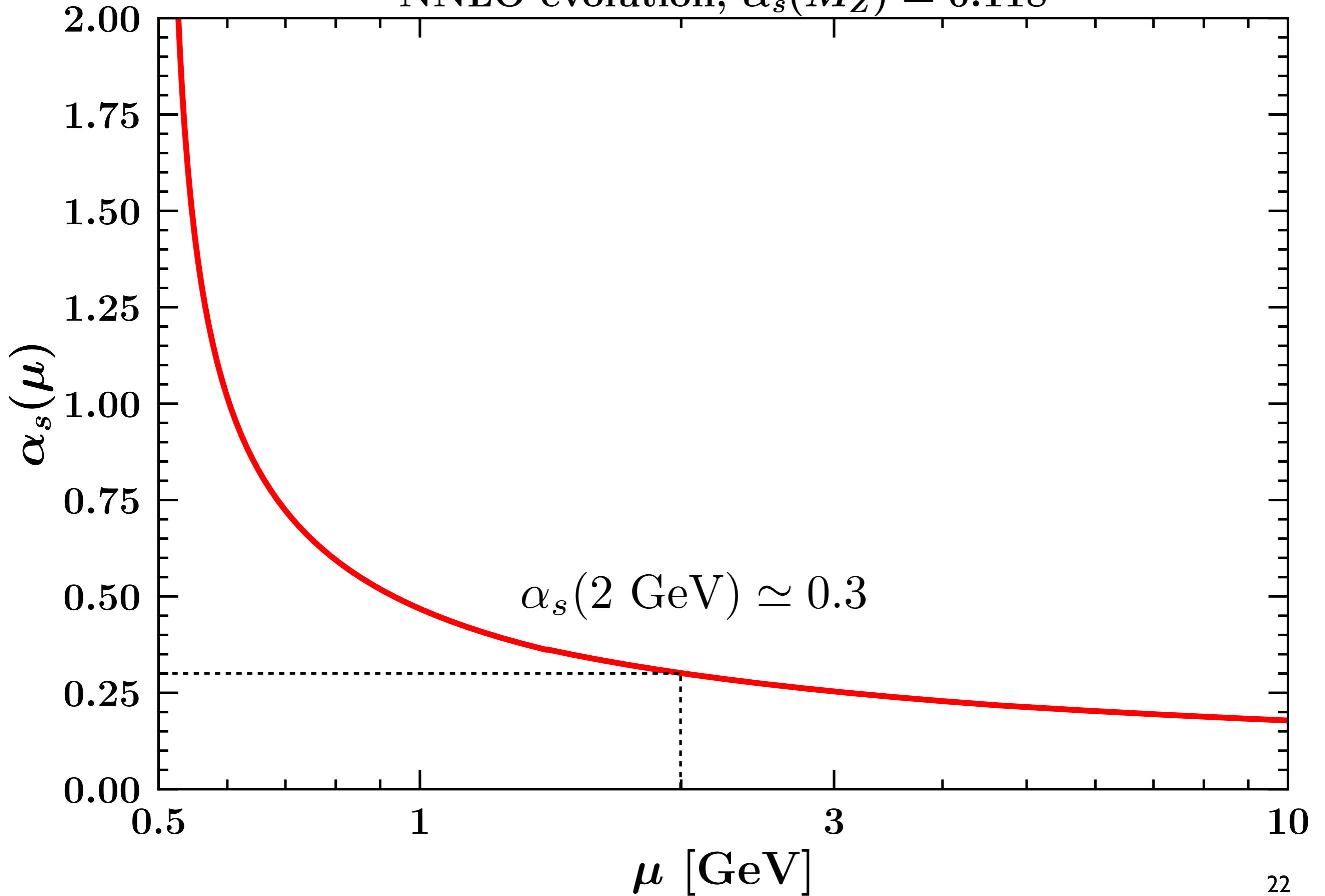
Ensure that perturbation theory is applicable

$$W^2 \geq W_{\min}^2$$

$$\left( W^2 = \frac{Q^2(1-x)}{x}, \quad W_{\min} \simeq 4 \text{ GeV} \right)$$

Remove higher-twist contributions (mostly for DIS and Fixed-target DY data)

NNLO evolution,  $\alpha_s(M_Z) = 0.118$



# Experimental data

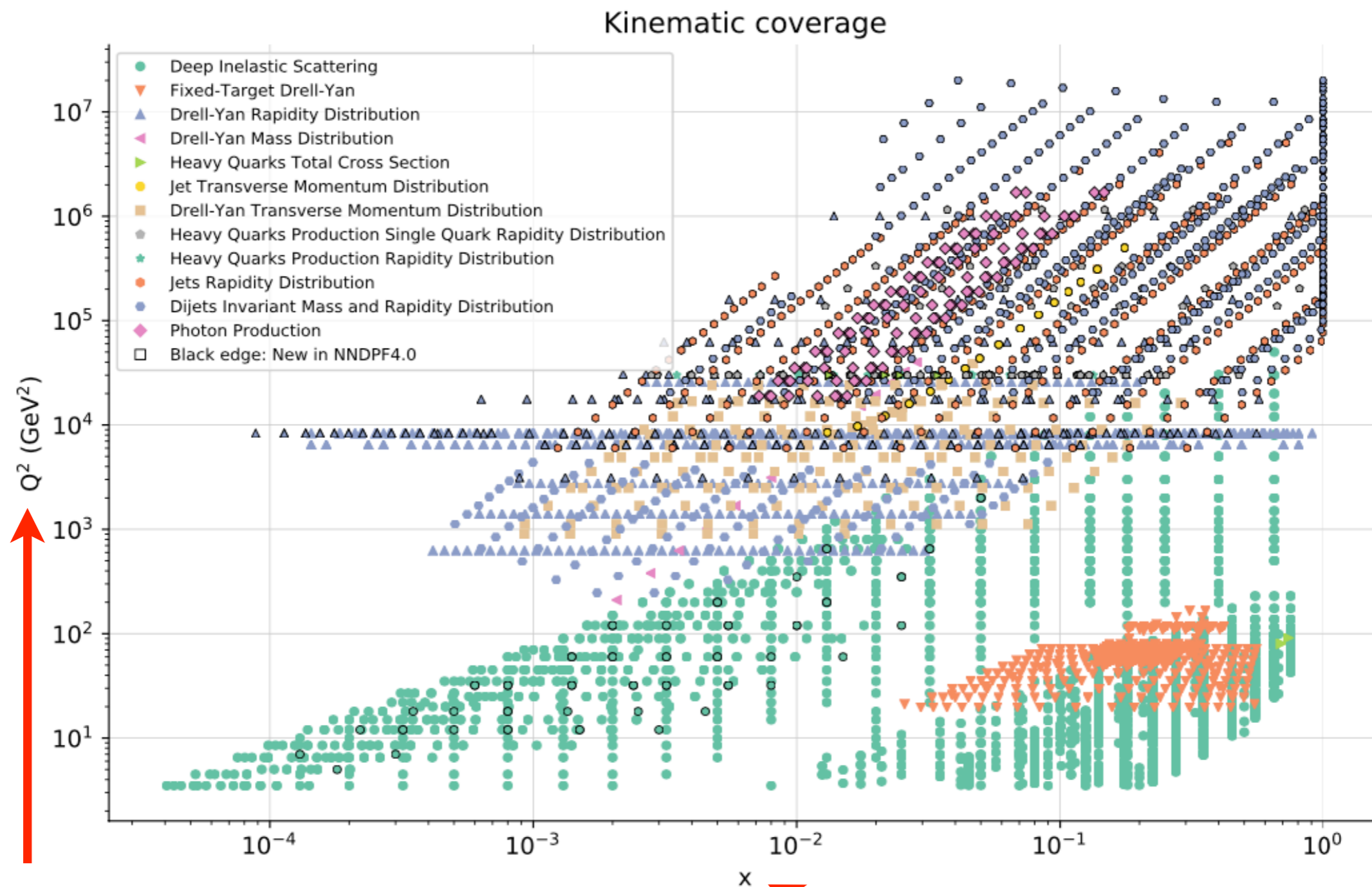
## *Kinematic cuts*

- Usually, many more cuts are enforced...

Dataset	NLO	NNLO
DIS measurements	$W^2 \geq 12.5 \text{ GeV}^2; Q^2 \geq 3.5 \text{ GeV}^2$	$W^2 \geq 12.5 \text{ GeV}^2; Q^2 \geq 3.5 \text{ GeV}^2$
HERA I+II $\sigma_{\text{NC}}^e$ (in addition to the above)	—	$Q^2 \geq 8 \text{ GeV}^2$ (fitted charm)
E866/E605 $\sigma^P$	$\tau \leq 0.08;  y/y_{\text{max}}  \leq 0.0663$	$\tau \leq 0.08;  y/y_{\text{max}}  \leq 0.0663$
D0 $W$ electron/muon asymmetry	—	$ A_\ell  \geq 0.03$
ATLAS low-mass DY 7 TeV	$m_{\ell\ell} > 22 \text{ GeV}$	—
ATLAS high-mass DY 7 TeV	$m_{\ell\ell} < 210 \text{ GeV}$	$m_{\ell\ell} < 210 \text{ GeV}$
CMS DY 2D 7 TeV	$30 \leq m_{\ell\ell} \leq 200 \text{ GeV};  y_{\ell\ell}  \leq 2.2$	$m_{\ell\ell} \leq 200 \text{ GeV};  y_{\ell\ell}  \leq 2.2$
LHCb $W, Z \rightarrow \mu$ 7 TeV	—	$ \eta_\mu / y_{\mu\bar{\mu}}  \geq 2.25$
ATLAS low-mass DY 2D 8 TeV	$m_{\ell\ell} \leq 116 \text{ GeV}$	$m_{\ell\ell} \leq 116 \text{ GeV}$
LHCb $W, Z \rightarrow \mu$ 8 TeV	—	$ \eta_\mu / y_{\mu\bar{\mu}}  \geq 2.25$
LHCb $Z \rightarrow ee/Z \rightarrow \mu\mu$ 13 TeV	—	$ y_{\ell\ell}  \geq 2.25$
ATLAS $W^\pm + \text{jet}$ 8 TeV	$p_T^W \geq 25 \text{ GeV}$	$p_T^W \geq 25 \text{ GeV}$
ATLAS $Z p_T$ 8 TeV ( $p_T, m_{\ell\ell}$ )	$p_T^Z \geq 30 \text{ GeV}$	$p_T^Z \geq 30 \text{ GeV}$
ATLAS $Z p_T$ 8 TeV ( $p_T, y_Z$ )	$30 \leq p_T^Z \leq 150 \text{ GeV}$	$30 \leq p_T^Z \leq 150 \text{ GeV}$
CMS $Z p_T$ 8 TeV	$30 \leq p_T^Z \leq 170 \text{ GeV};  y_Z  \leq 1.6$	$30 \leq p_T^Z \leq 170 \text{ GeV};  y_Z  \leq 1.6$
CMS incl. jets 8 TeV	$p_T^{\text{jet}} \geq 74 \text{ GeV}$	$p_T^{\text{jet}} \geq 74 \text{ GeV}$

# Experimental data

## *How to read the scatter plot*



[NNPDF4.0, arXiv:2109.02653]

Hard scale  $\simeq$  factorisation scale  
(i.e. scale at which PDFs are computed)

Kinematic lower bound 24



# Experimental data

## *How to read the scatter plot*

- Inclusive DIS:  $e(k) + p(P) \rightarrow e(k') + X$

$$q = k - k', \quad Q = \sqrt{-q^2}, \quad x_B = \frac{Q^2}{2q \cdot P}$$

$$\frac{d\sigma}{dx_B dQ} \propto \int_{x_B}^1 \frac{dy}{y} C\left(\frac{x_B}{y}, \alpha_s(Q)\right) f(y, Q)$$

- Drell-Yan:  $p(P_1) + p(P_2) \rightarrow e^+(k) + e^-(k') + X$

$$q = k + k'$$
$$s = (P_1 + P_2)^2, \quad M = \sqrt{q^2}, \quad \tau = \frac{M^2}{s}, \quad x_{1,2} = \sqrt{\tau} e^{\pm y}$$
$$y = \frac{1}{2} \ln \frac{q_0 + q_3}{q_0 - q_3}$$

- Mass-differential distribution:

$$\frac{d\sigma}{dM} \propto \int_{\tau}^1 \frac{dt}{t} C\left(\frac{\tau}{t}, \alpha_s(Q)\right) \int_t^1 \frac{dy}{y} f_1(y, Q) f_2\left(\frac{t}{y}, Q\right)$$

- Rapidity-differential distribution:

$$\frac{d\sigma}{dy dM} \propto \int_{x_1}^1 \frac{dy_1}{y_1} \int_{x_2}^1 \frac{dy_2}{y_2} C\left(\frac{x_1}{y_1}, \frac{x_2}{y_2}, \alpha_s(Q)\right) f_1(y_1, Q) f_2(y_2, Q)$$

# The general strategy

**Perturbative content:**  
collinear evolution,  
hard cross sections, etc.

**Parameterisation:**  
functional form,  
asymptotes, etc.

**Experimental data:**  
processes, cuts,  
uncertainties, etc.

Theoretical predictions

Define a fig. of merit ( $\chi^2$ )  
and error propagation

Adjust free parameters to  
minimise the fig. of merit

Determine best-fit params.

# Perturbative content

## *DGLAP evolution*

- PDFs obey a set of **coupled integro-differential equations**: the DGLAP equations

$$\frac{df_i(x, \mu)}{d \ln \mu^2} = \sum_j \int_x^1 \frac{dy}{y} P_{ij}(y, \alpha_s(\mu)) f_j\left(\frac{x}{y}, \mu\right)$$
$$P_{ij}(y, \alpha_s(\mu)) = \sum_{n=0}^{\infty} \alpha_s^{n+1}(\mu) P_{ij}^{(n)}(y)$$

- Unpolarised space-like splitting functions fully known up to NNLO.

Moch, Vermaseren, Vogt [*Nucl.Phys.B* 688 (2004) 101-134] [*Nucl.Phys.B* 691 (2004) 129-181]

- Several numerical implementations:

- $x$ -space approach:

- QCDNUM, Botje [arXiv:1602.08383]
- HOPPET, Salam [arXiv:0804.3755]
- APFEL(++), Bertone, Carrazza, Rojo [arXiv:1310.1394], Bertone [arXiv:1708.00911]

- $\mathcal{N}$ -space approach:

- PEGASUS, Vogt [hep-ph/0408244]
- MELA, Bertone, Carrazza, Nocera [arXiv:1501.00494]
- EKO, Candido, Hekhorn, Magni [arXiv:2202.02338]

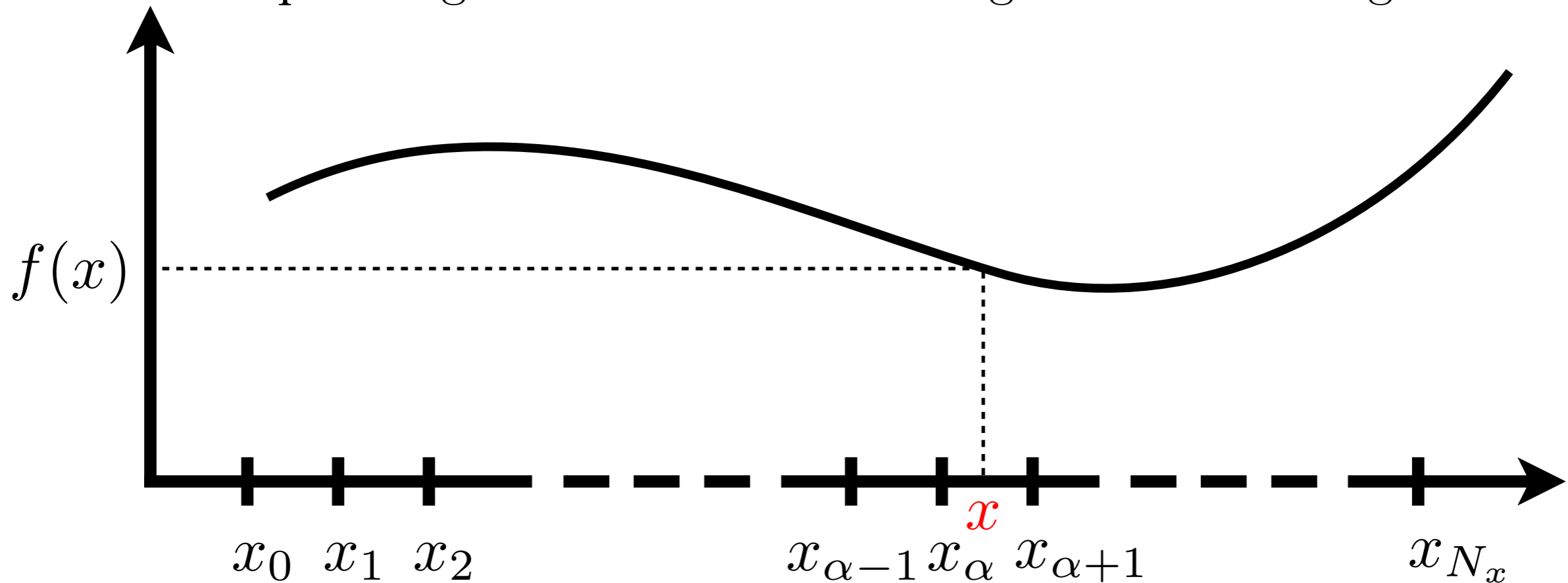
# Perturbative content

## *DGLAP evolution: $x$ -space approach*

- The only possibility to solve the DGLAP equations as they stand is numerically. But the solution must be efficient enough to be used in a fit of PDFs.

# Lagrange interpolation

🍏 Goal: interpolating a 1D function knowing its values on a grid.



🍏 “Moving” polynomial interpolation of degree  $k$ :

$$f(x) = \sum_{\alpha=0}^{N_x} w_{\alpha}^{(k)}(x) f(x_{\alpha}) + \mathcal{O}\left(\frac{f^{(k+1)}(x)}{(k+1)!} h^{k+1}\right)$$

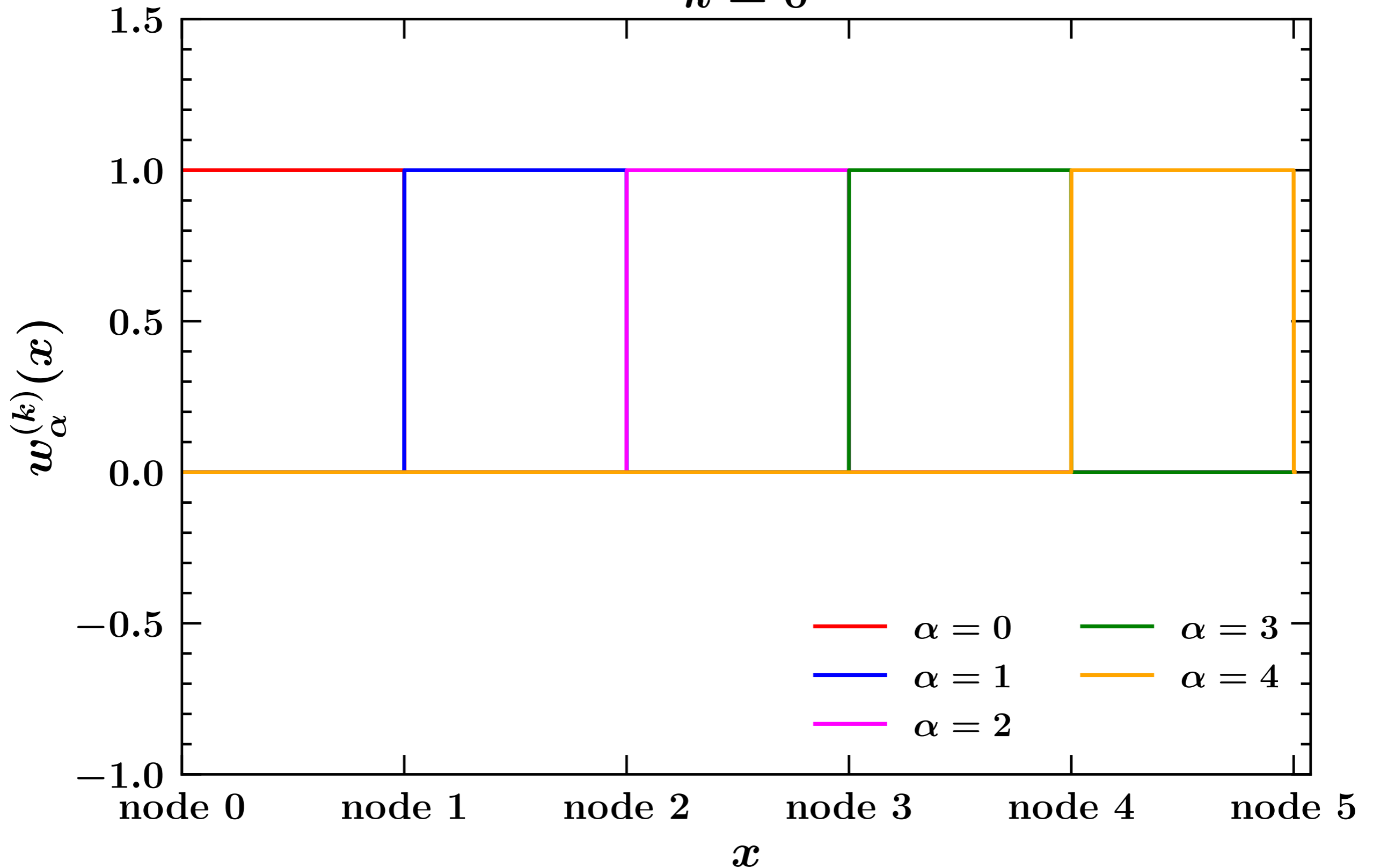
🍏 assuming that  $x_{\alpha} < x \leq x_{\alpha+1}$ :

$$w_{\alpha}^{(k)}(x) = \sum_{i=0, i \leq \alpha}^k \theta(x - x_{\alpha-i}) \theta(x_{\alpha-i+1} - x) \prod_{m=0, m \neq i}^k \frac{x - x_{\alpha-i+m}}{x_{\alpha} - x_{\alpha-i+m}}$$

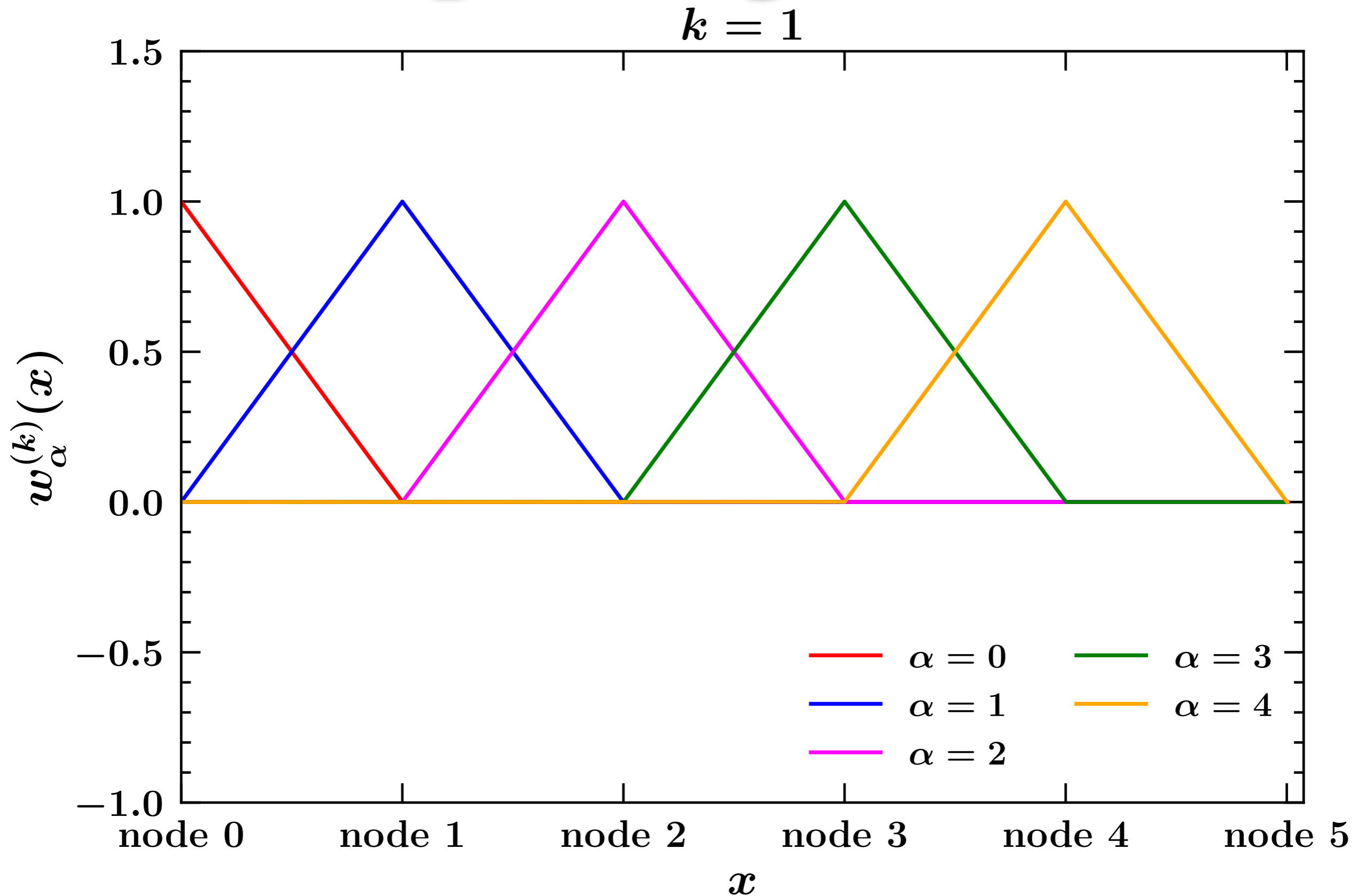
Lagrange polynomials

# The interpolating functions

$k = 0$

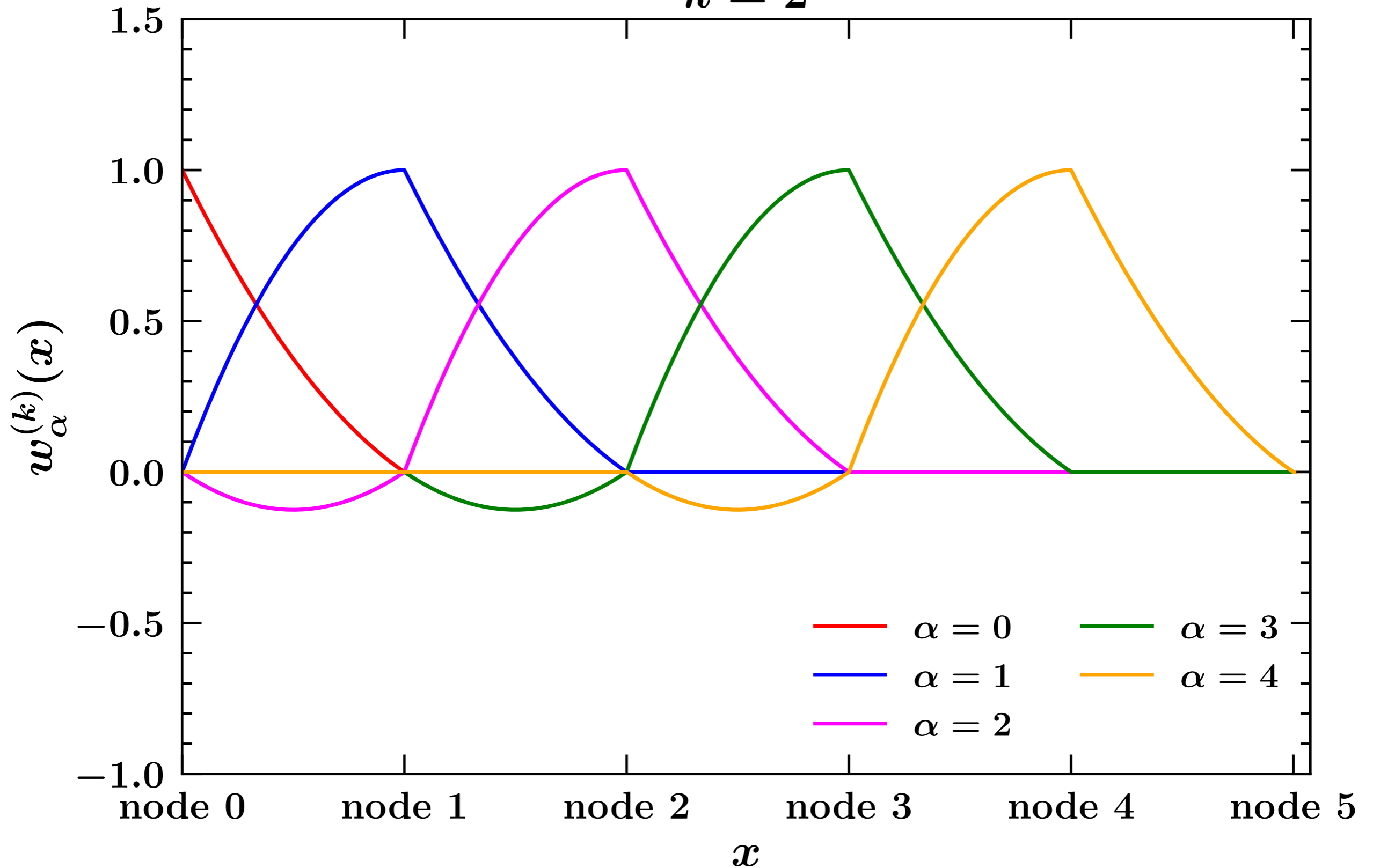


# The interpolating functions



# The interpolating functions

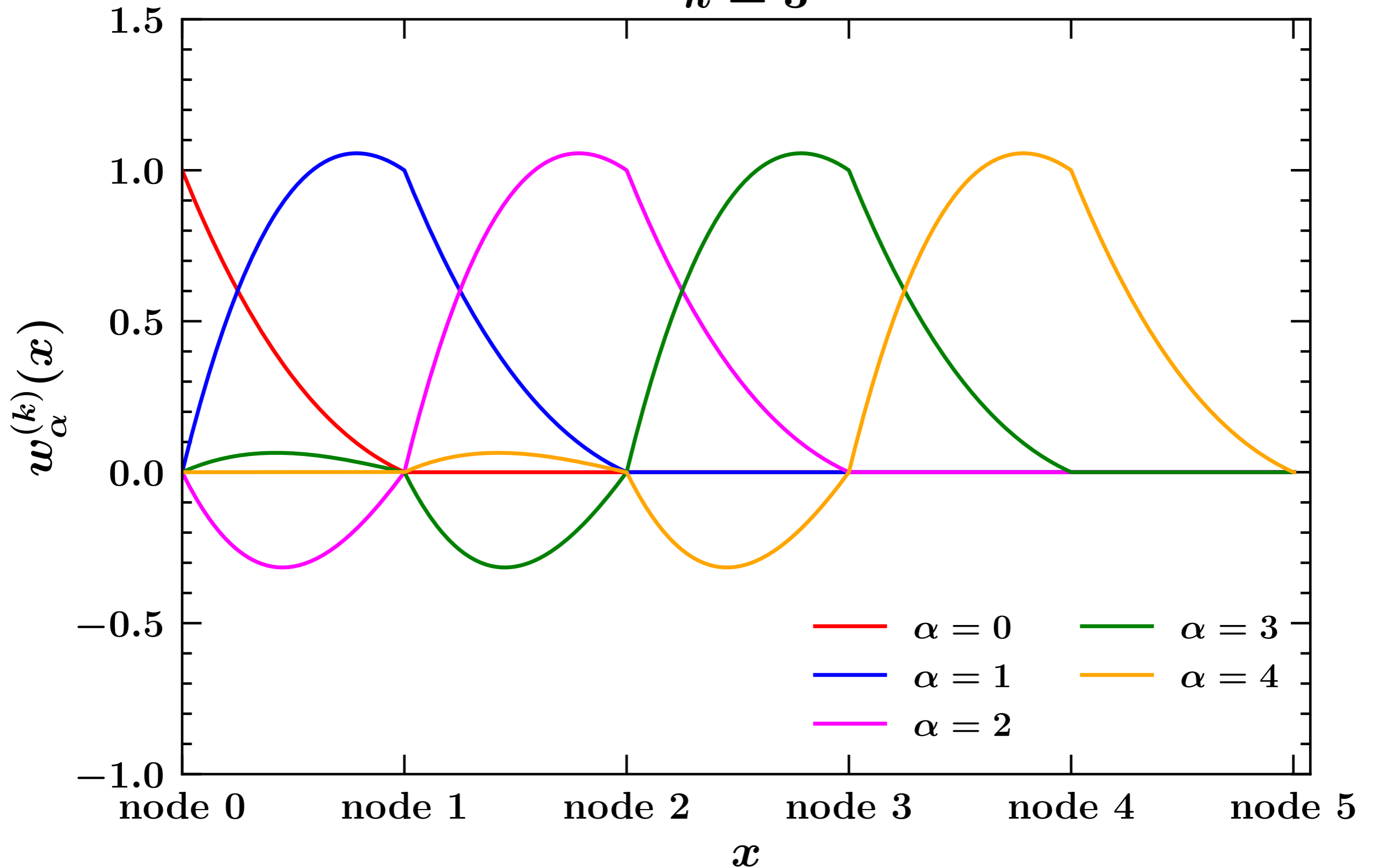
$$k = 2$$





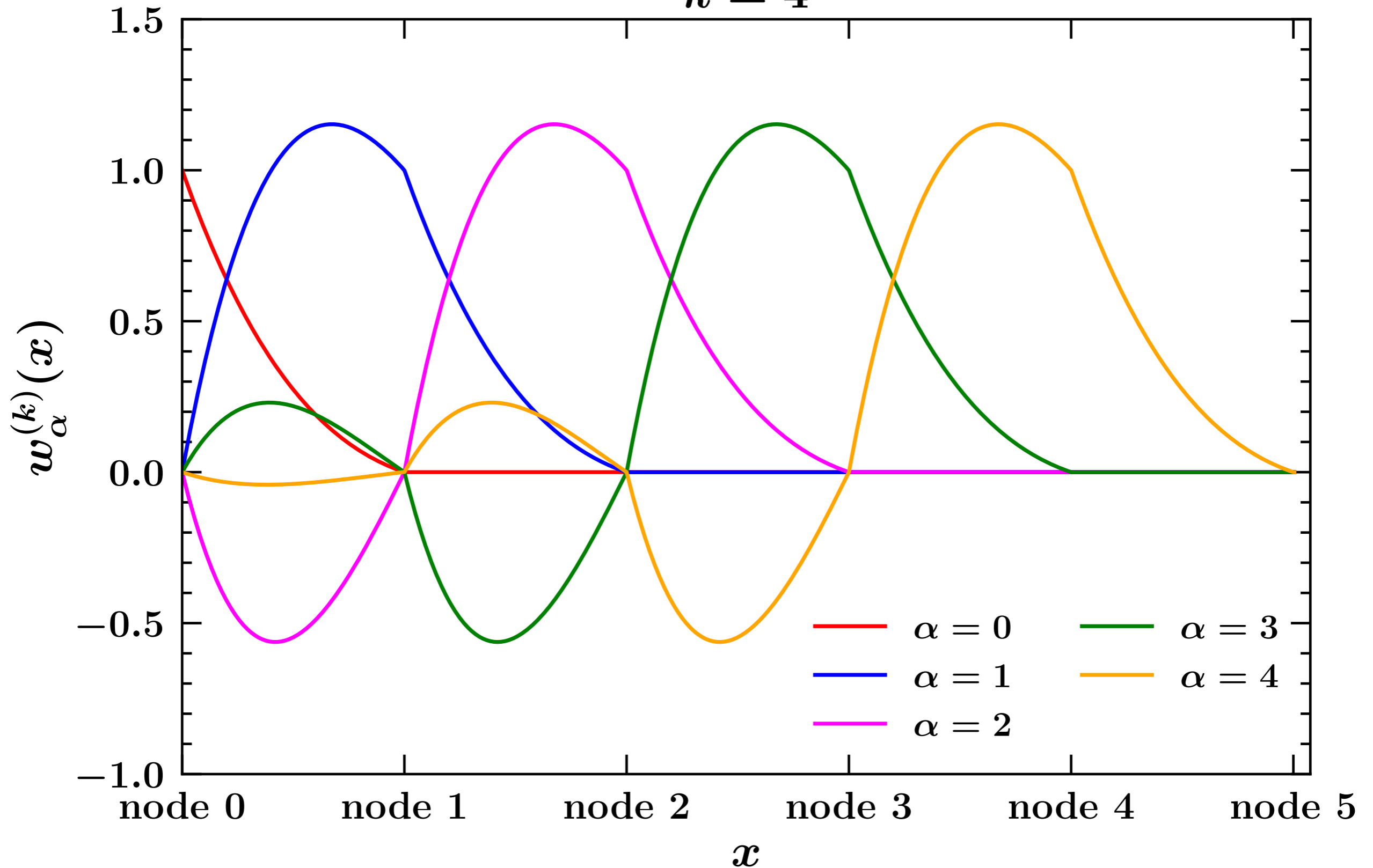
# The interpolating functions

$k = 3$



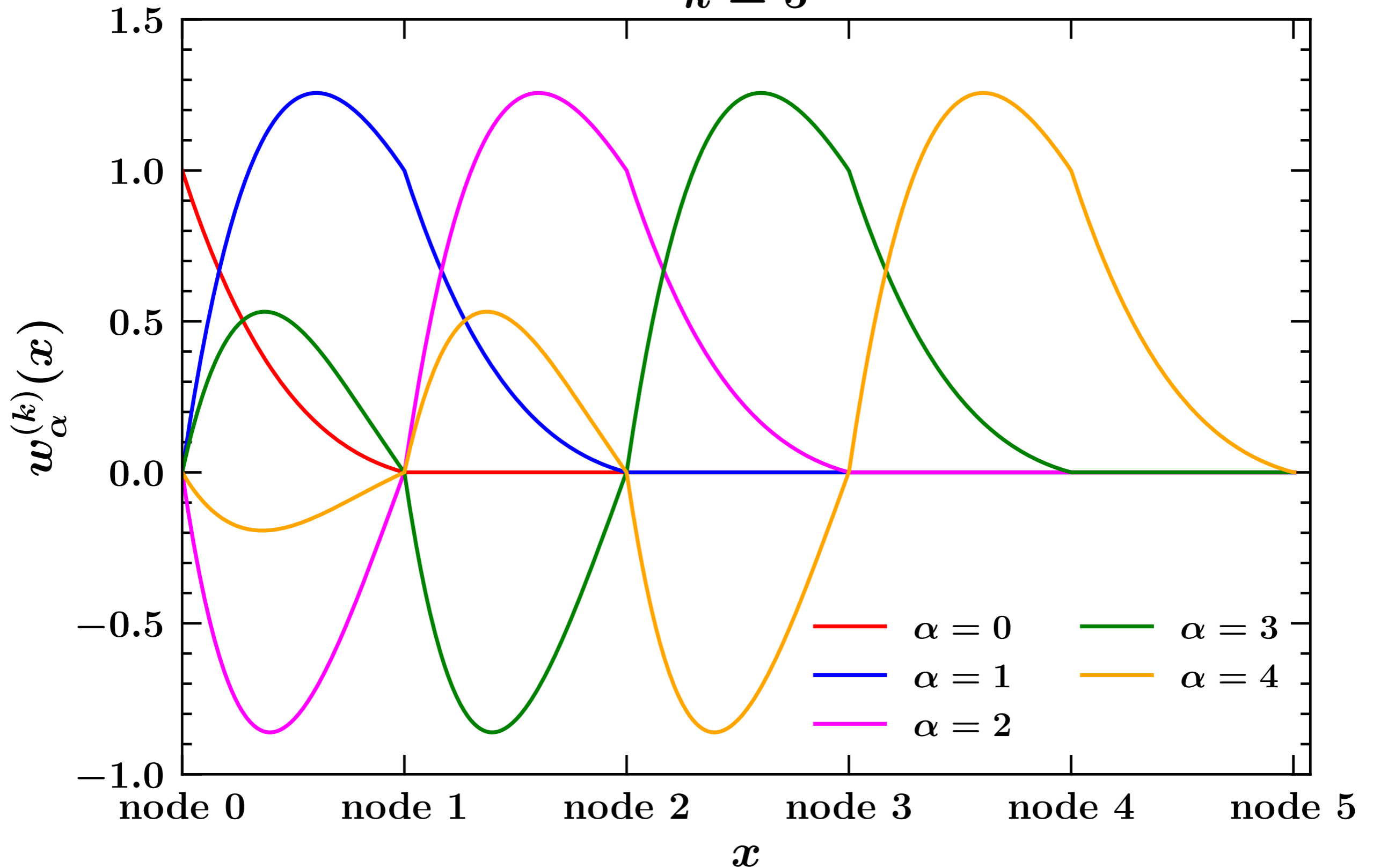
# The interpolating functions

$k = 4$



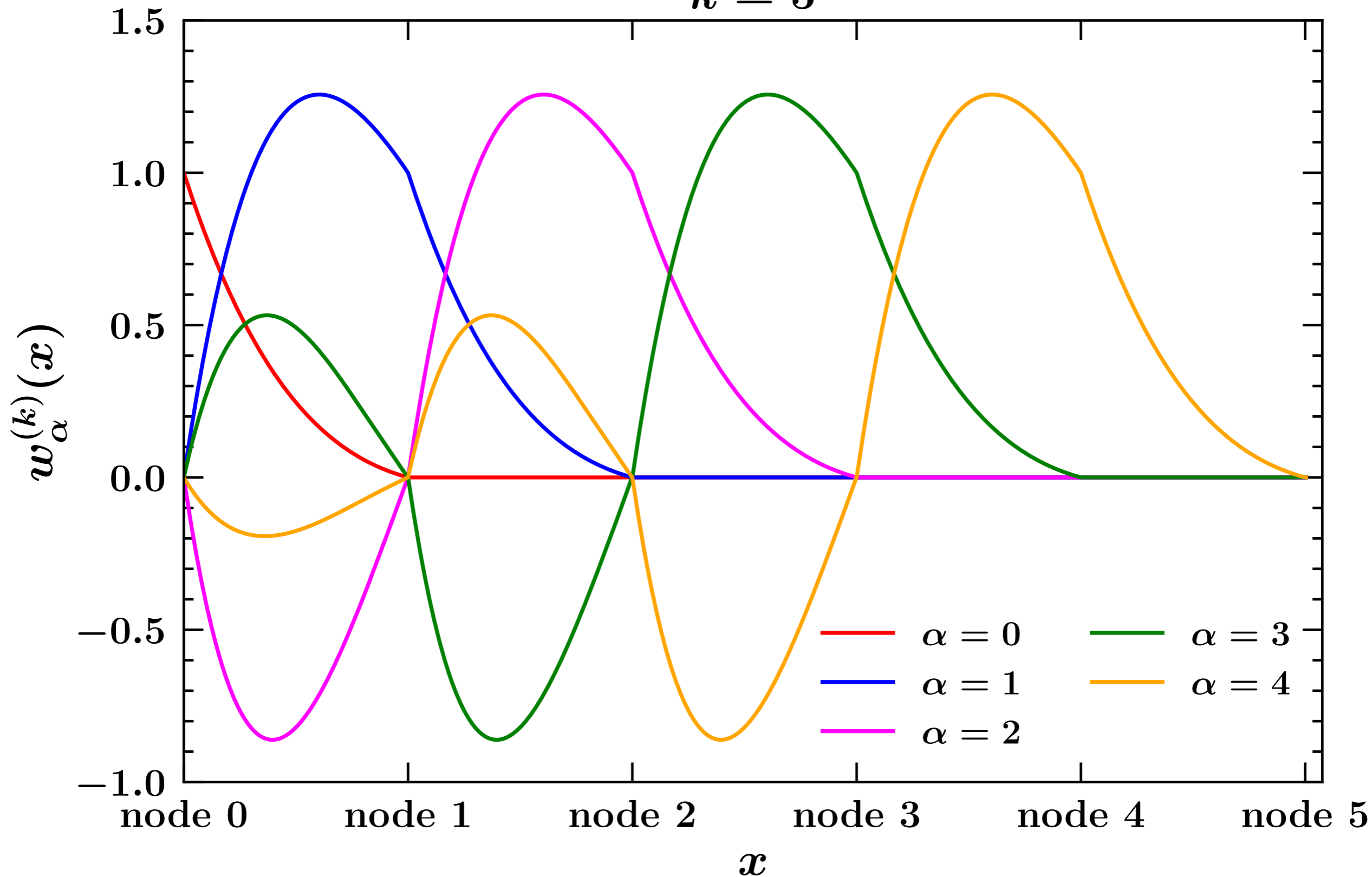
# The interpolating functions

$k = 5$



# The interpolating functions

$k = 5$



At any interpolation degree, the interpolating functions are such that  $w_\alpha^{(k)}(x_\beta) = \delta_{\alpha\beta}$ . 36

# Interpolation test

 Interpolate the function:

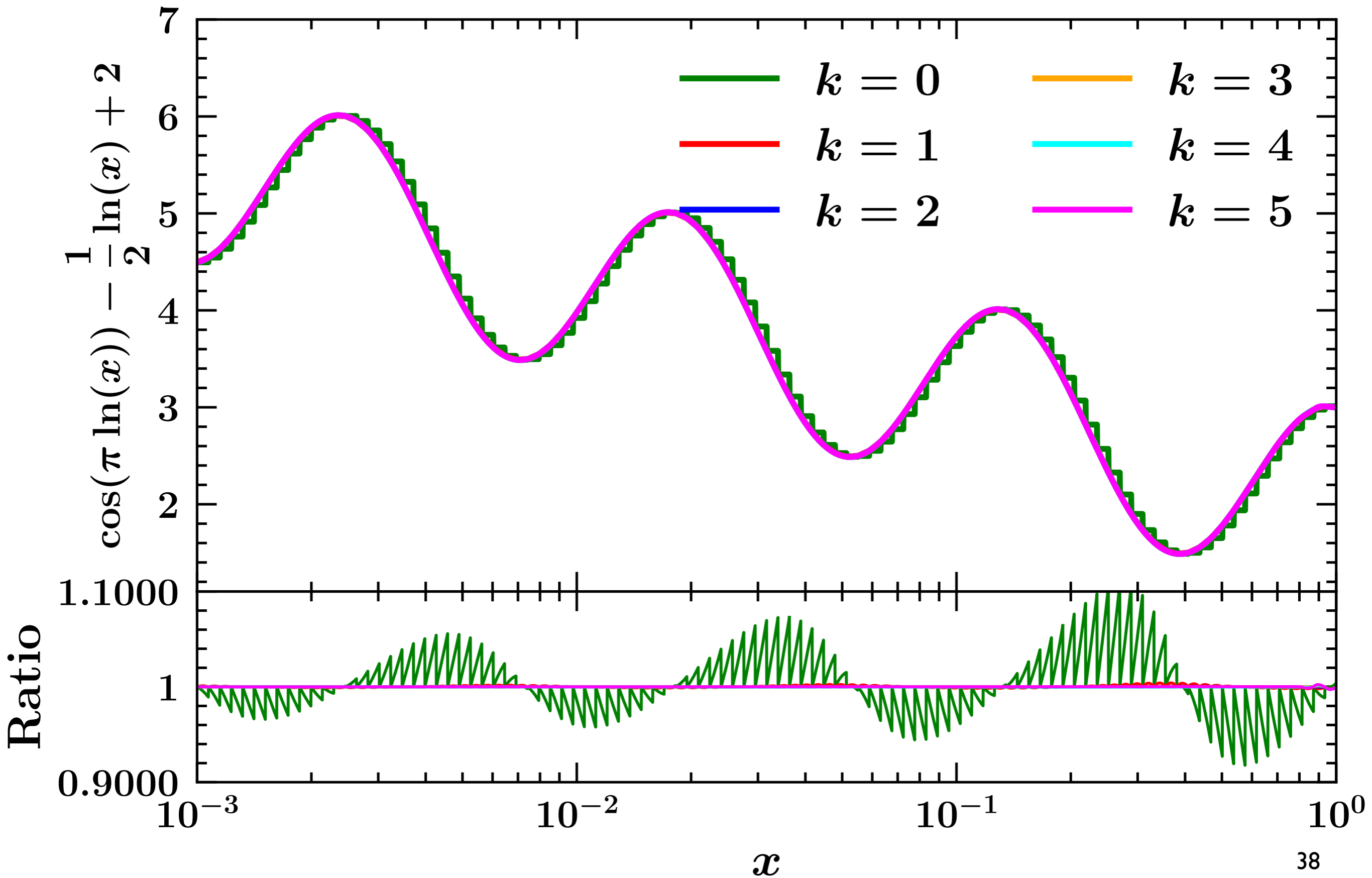
$$f(x) = \cos(\pi \ln(x)) - \frac{1}{2} \ln(x) + 2$$

 on grid with 100 nodes logarithmically distributed between  $10^{-3}$  and 1.

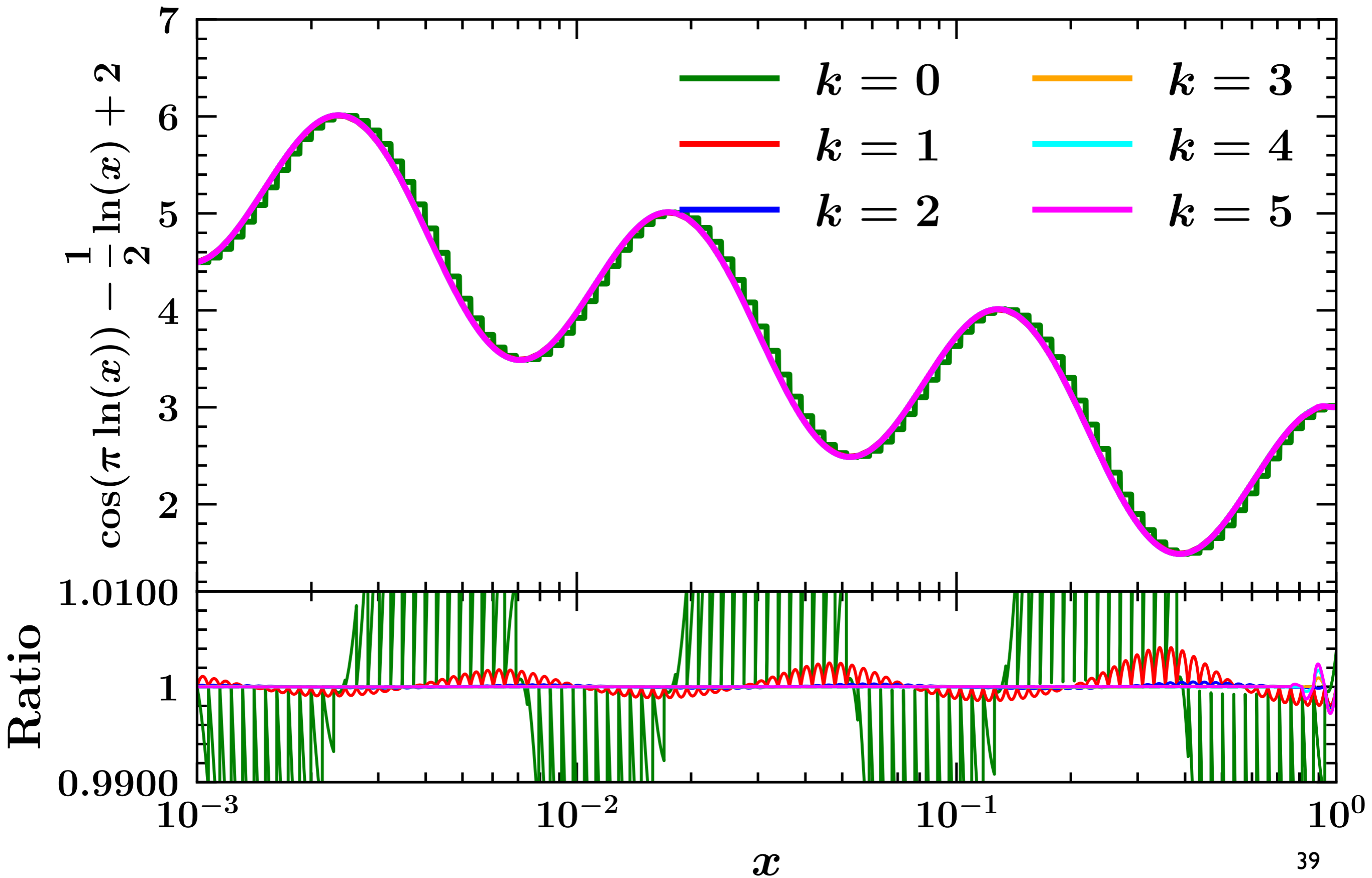
 Test different degrees of the Lagrange interpolants from 0 to 5:

 check the accuracy against the original function.

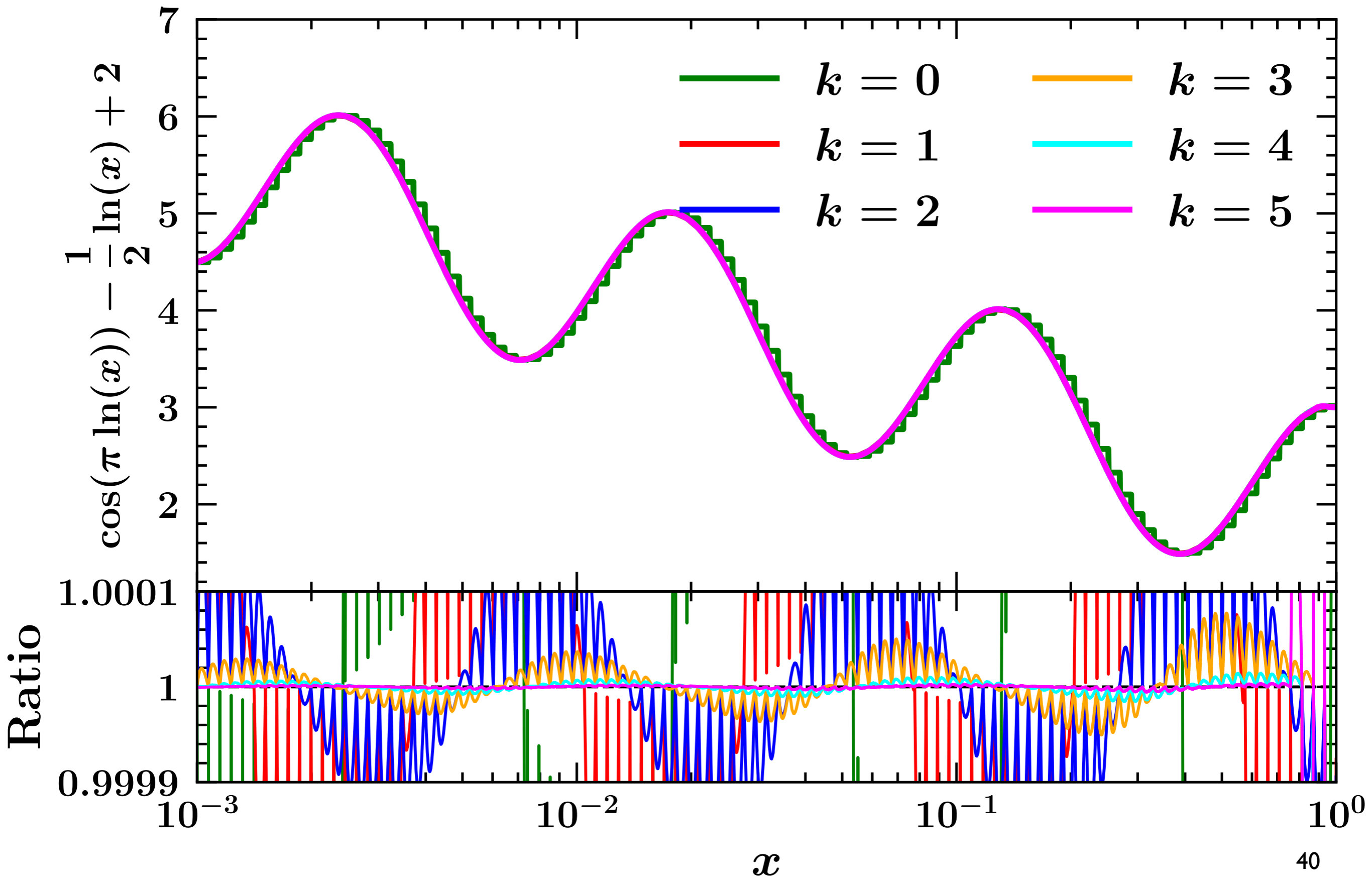
# Interpolation test



# Interpolation test



# Interpolation test





# Perturbative content

## *DGLAP evolution: $x$ -space approach*

- 🍏 The r.h.s. of the DGLAP equations requires computing integrals of the following kind:

$$I(x, \mu) = \int_x^1 \frac{dy}{y} P(y, \alpha_s(\mu)) f\left(\frac{x}{y}, \mu\right)$$

- 🍏 Using the interpolation formula for  $f$  (the PDF):

$$I(x_\beta, \mu) = \sum_{\alpha=0}^{N_x} \underbrace{\left[ \int_{x_\beta}^1 \frac{dy}{y} P(y, \alpha_s(\mu)) w_\alpha^{(k)}\left(\frac{x_\beta}{y}\right) \right]}_{\Gamma_{\beta\alpha}(\mu)} f(x_\alpha, \mu)$$

- 🍏 The  $\Gamma_{\beta\alpha}$  don't depend on  $f$  and thus can be **precomputed** and **stored**.

- 🍏 More compactly:

$$I_\beta(\mu) = \sum_{\alpha=0}^{N_x} \Gamma_{\beta\alpha}(\mu) f_\alpha(\mu) \quad \Rightarrow \quad \mathbf{I}(\mu) = \mathbf{\Gamma}(\mu) \cdot \mathbf{f}(\mu)$$

- 🍏 This allows us to compute  $I$  on each point of the grid.

# Perturbative content

## *DGLAP evolution: $x$ -space approach*

- 🍏 The DGLAP equations reduce to a set of coupled **linear ordinary differential equations** (ODEs) that in vectorial notation read:

$$\frac{d\mathbf{f}(\mu)}{d \ln \mu^2} = \mathbf{\Gamma}(\mu) \cdot \mathbf{f}(\mu) \equiv \mathbf{F}(\mu, \mathbf{f})$$

- 🍏 The functions to be determined are the partonic distribution  $f$  as a function of  $\mu$  on each node of the grid knowing  $\mathbf{f}(\mu_0)$  on the grid.
- 🍏 Many algorithms to solve ODEs exist. A particularly popular choice is the **4th order Runge-Kutta** (RK4):

$$\mathbf{f}_{n+1} = \mathbf{f}_n + \frac{1}{6}(\mathbf{k}_1 + 2\mathbf{k}_2 + 2\mathbf{k}_3 + \mathbf{k}_4) + \mathcal{O}(h^5)$$

$$\mathbf{k}_1 = h\mathbf{F}(\mu_n, \mathbf{f}_n)$$

$$\mathbf{k}_2 = h\mathbf{F}\left(\mu_n + \frac{h}{2}, \mathbf{f}_n + \frac{\mathbf{k}_1}{2}\right)$$

$$\mathbf{k}_3 = h\mathbf{F}\left(\mu_n + \frac{h}{2}, \mathbf{f}_n + \frac{\mathbf{k}_2}{2}\right)$$

$$\mathbf{k}_4 = h\mathbf{F}(\mu_n + h, \mathbf{f}_n + \mathbf{k}_3)$$

- 🍏 Tabulate  $\mathbf{f}$  on a **grid in  $\mu$**  that can successively interpolated.
- 🍏 Final result:  $f(x, \mu)$  is know on a 2D grid in  $x$  and  $\mu$ .

# Perturbative content

## *DGLAP evolution: $x$ -space approach*

🍏 In principle, one needs to compute  $N_x^2$  integrals  $\Gamma_{\beta\alpha}$ .

🍏 However, if one uses a logarithmically distributed grid:

$$x_{\alpha+1} = e^{\delta x} x_{\alpha} \quad \delta x = \text{constant}$$

🍏 and the Lagrange polynomials are expressed in **powers of  $\ln(x)$** :

$$w_{\alpha}^{(k)}(x) = \sum_{i=0, i \leq \alpha}^k \theta(x - x_{\alpha-i}) \theta(x_{\alpha-i+1} - x) \prod_{m=0, m \neq i}^k \frac{\ln x - \ln x_{\alpha-i+m}}{\ln x_{\alpha} - \ln x_{\alpha-i+m}}$$

🍏 one finds:

$$\Gamma_{\beta\alpha} = \begin{cases} \Gamma_{0, \alpha-\beta} & \alpha \geq \beta \\ 0 & \alpha < \beta \end{cases} \quad \Gamma_{\beta\alpha} = \begin{pmatrix} a_0 & a_1 & a_2 & \cdots & a_{N_x} \\ 0 & a_0 & a_1 & \cdots & a_{N_x-1} \\ 0 & 0 & a_0 & \cdots & a_{N_x-2} \\ \vdots & \vdots & \vdots & \ddots & \vdots \\ 0 & 0 & 0 & \cdots & a_0 \end{pmatrix}$$

🍏 The number of integrals reduces to  $N_x$  and so thus the computation time.

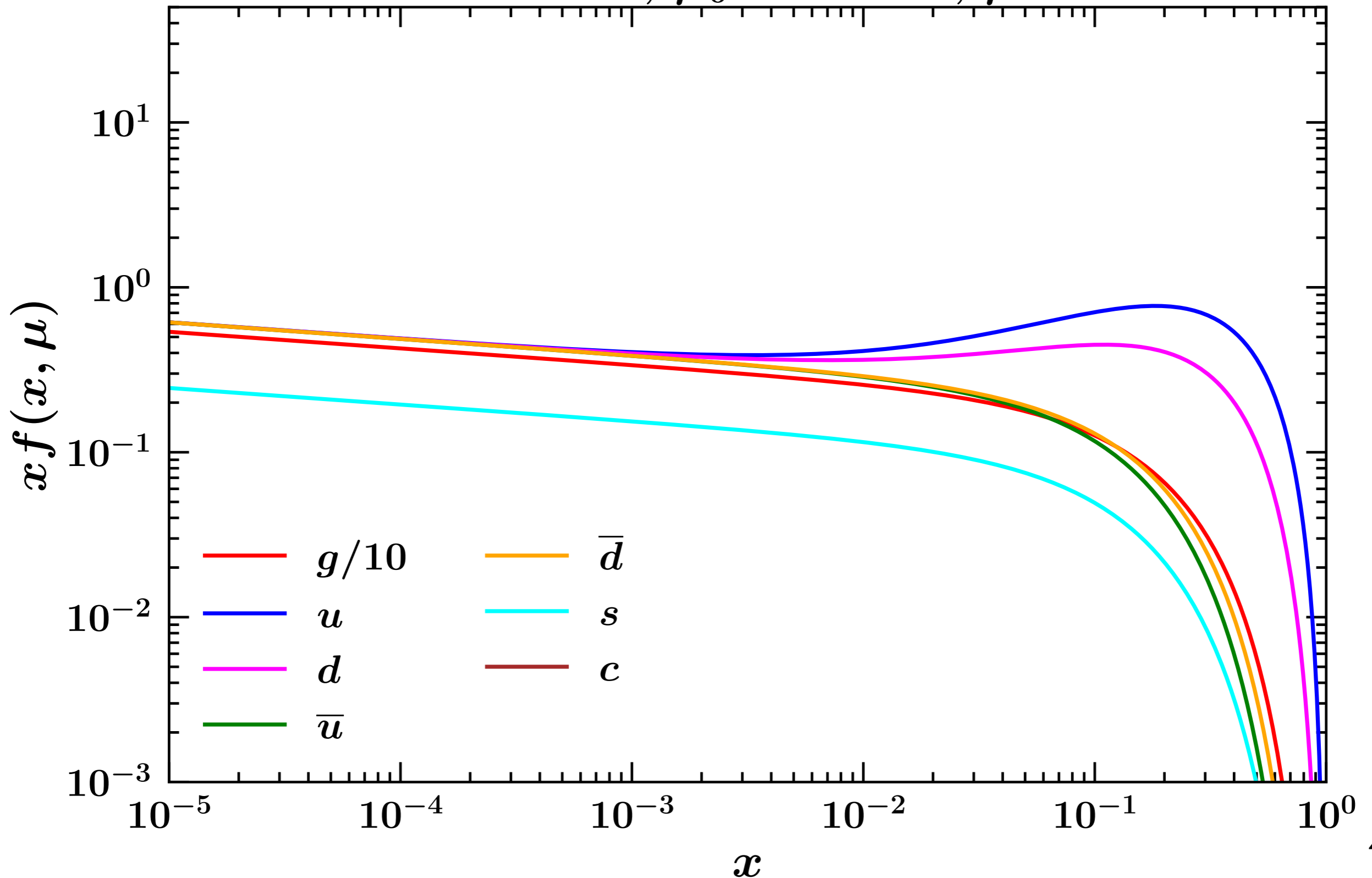
🍏 Problem: a logarithmic grid becomes increasingly sparse at large  $x$ :

🍏 solution: concatenate grids with increasing density as one moves towards large  $x$ .

# Perturbative content

*DGLAP evolution:  $x$ -space approach*

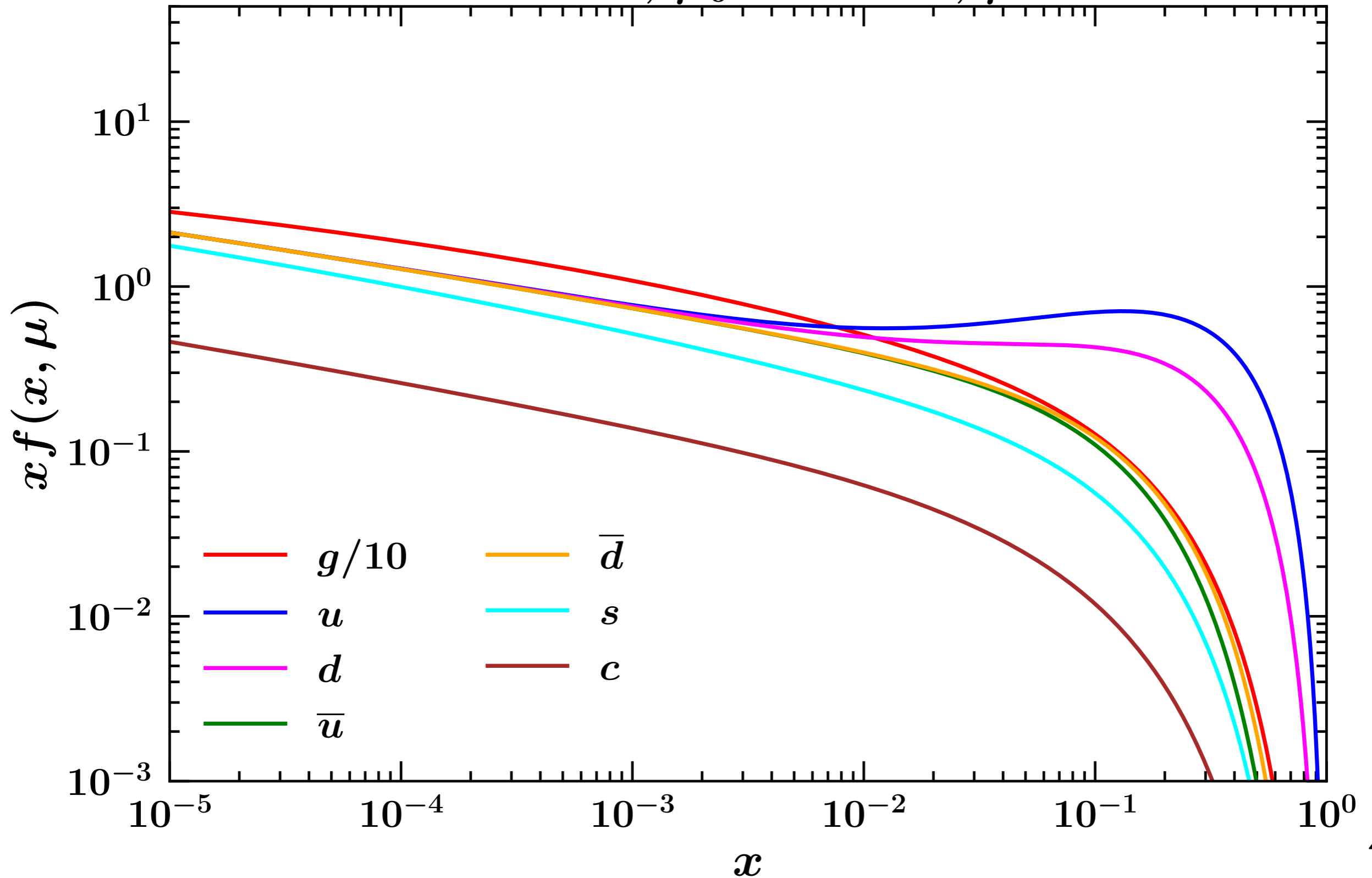
NNLO evolution,  $\mu_0 = 1 \text{ GeV}$ ,  $\mu = 1 \text{ GeV}$



# Perturbative content

*DGLAP evolution:  $x$ -space approach*

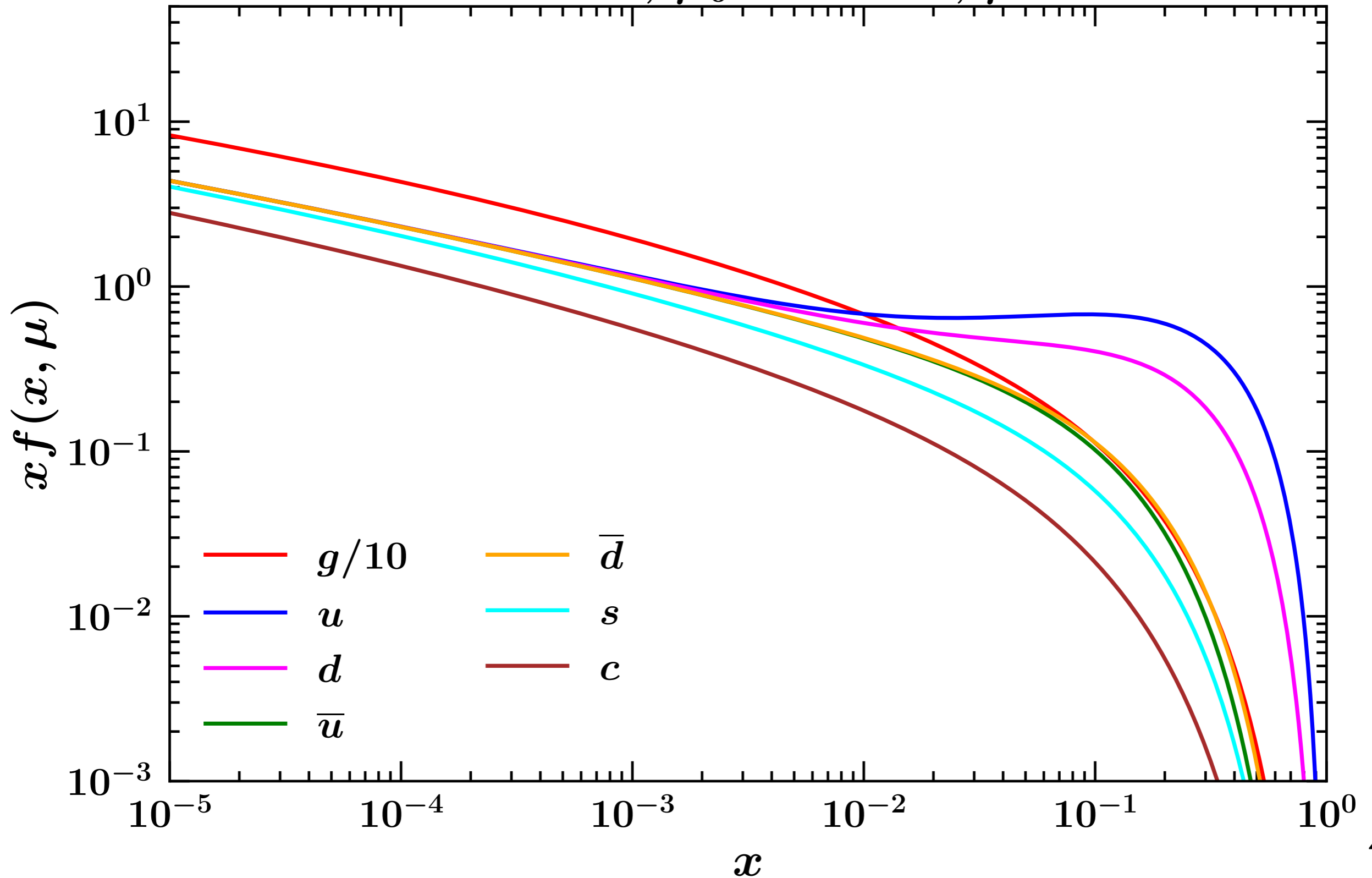
NNLO evolution,  $\mu_0 = 1 \text{ GeV}$ ,  $\mu = 2 \text{ GeV}$



# Perturbative content

*DGLAP evolution:  $x$ -space approach*

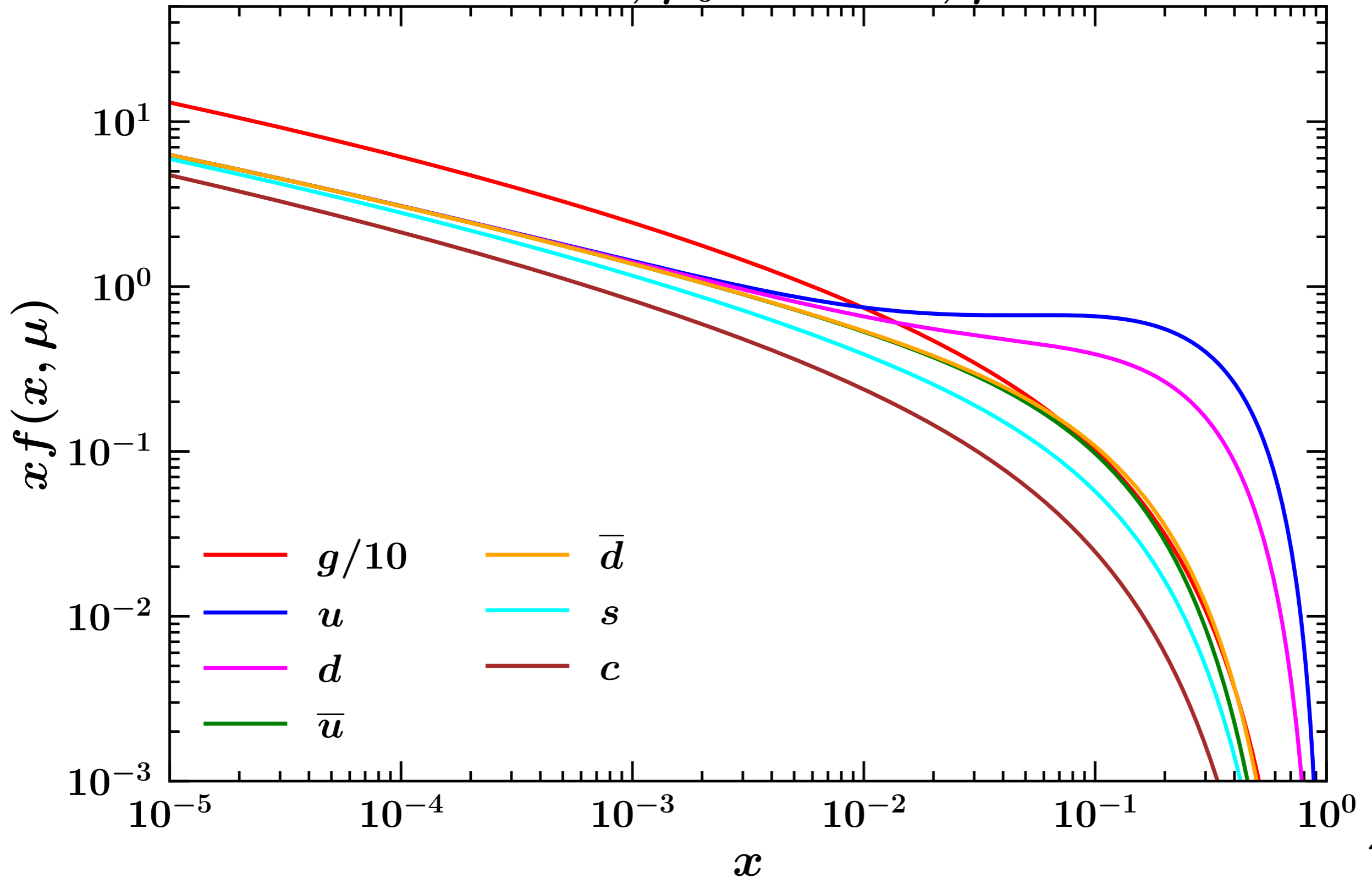
NNLO evolution,  $\mu_0 = 1 \text{ GeV}$ ,  $\mu = 5 \text{ GeV}$



# Perturbative content

*DGLAP evolution:  $x$ -space approach*

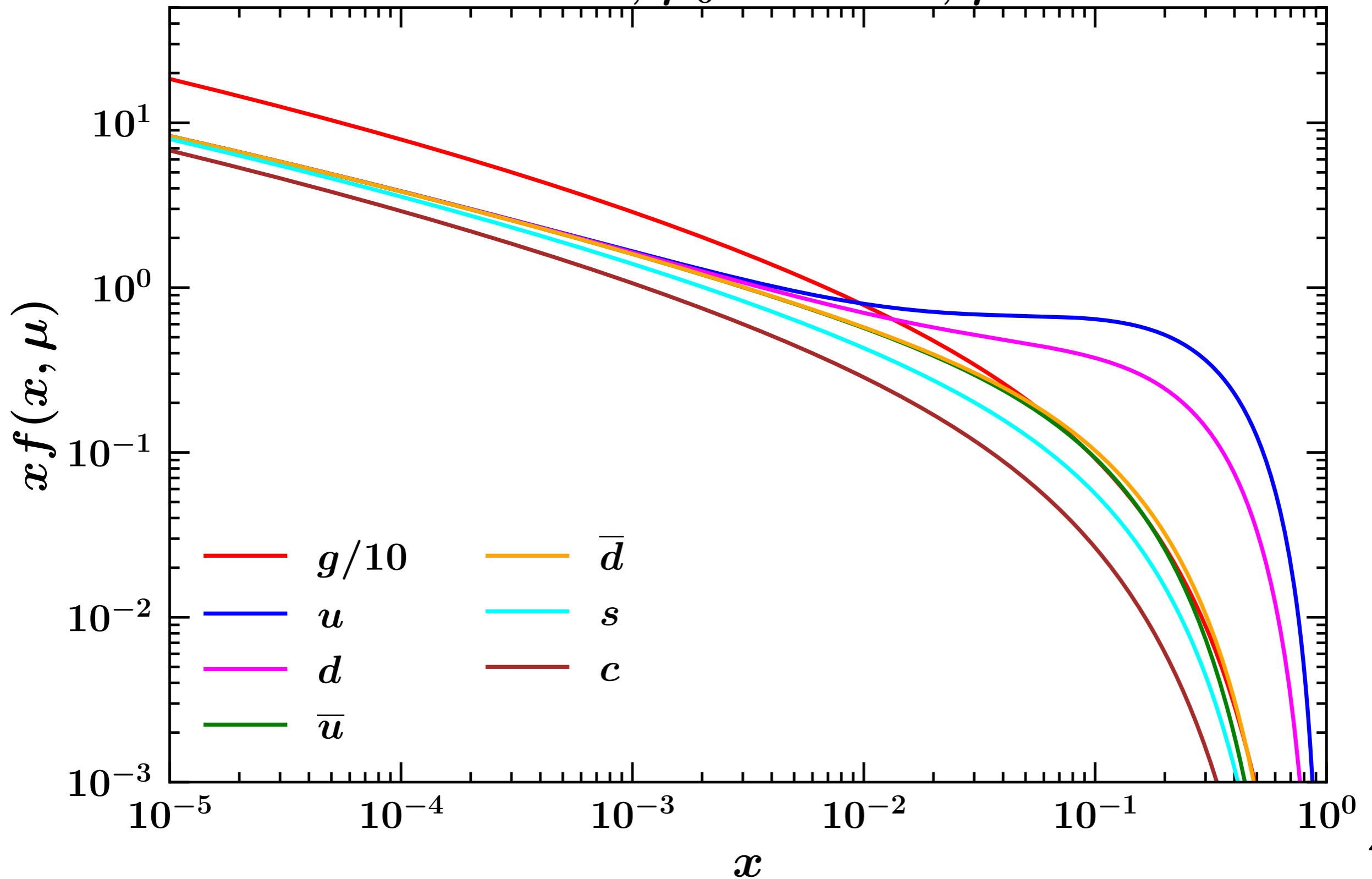
NNLO evolution,  $\mu_0 = 1 \text{ GeV}$ ,  $\mu = 10 \text{ GeV}$



# Perturbative content

*DGLAP evolution:  $x$ -space approach*

NNLO evolution,  $\mu_0 = 1 \text{ GeV}$ ,  $\mu = 20 \text{ GeV}$

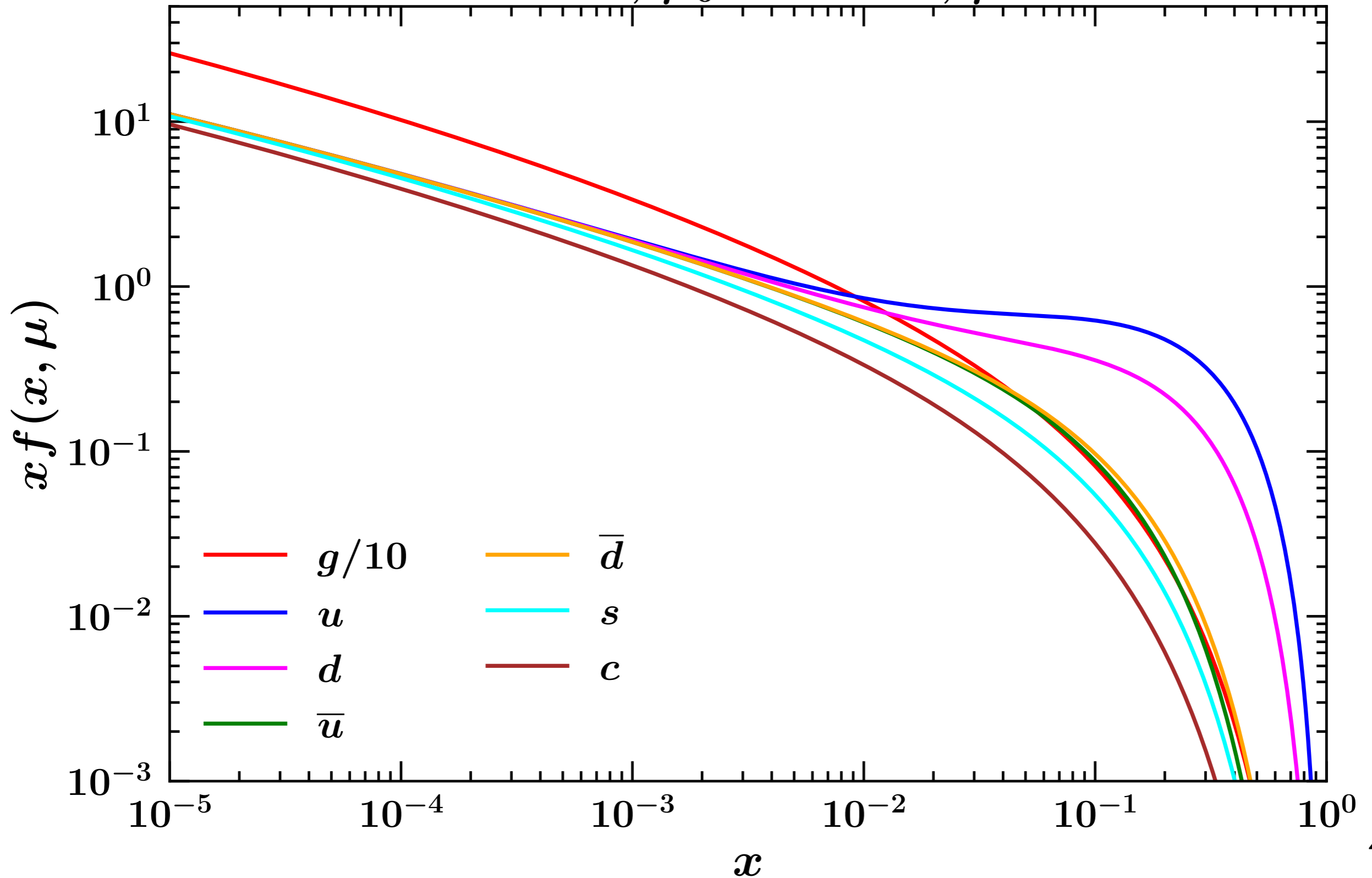




# Perturbative content

*DGLAP evolution:  $x$ -space approach*

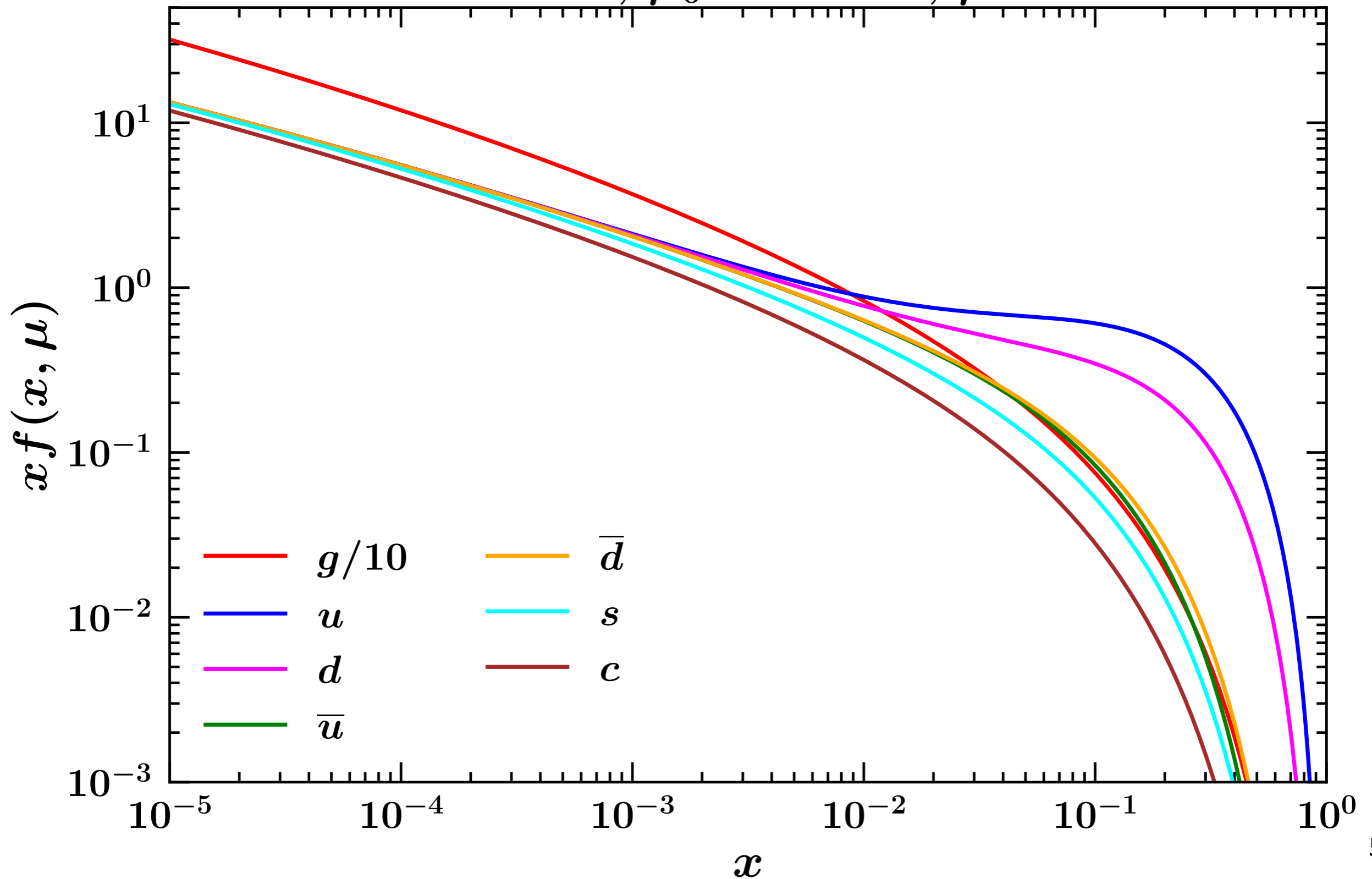
NNLO evolution,  $\mu_0 = 1 \text{ GeV}$ ,  $\mu = 50 \text{ GeV}$



# Perturbative content

*DGLAP evolution:  $x$ -space approach*

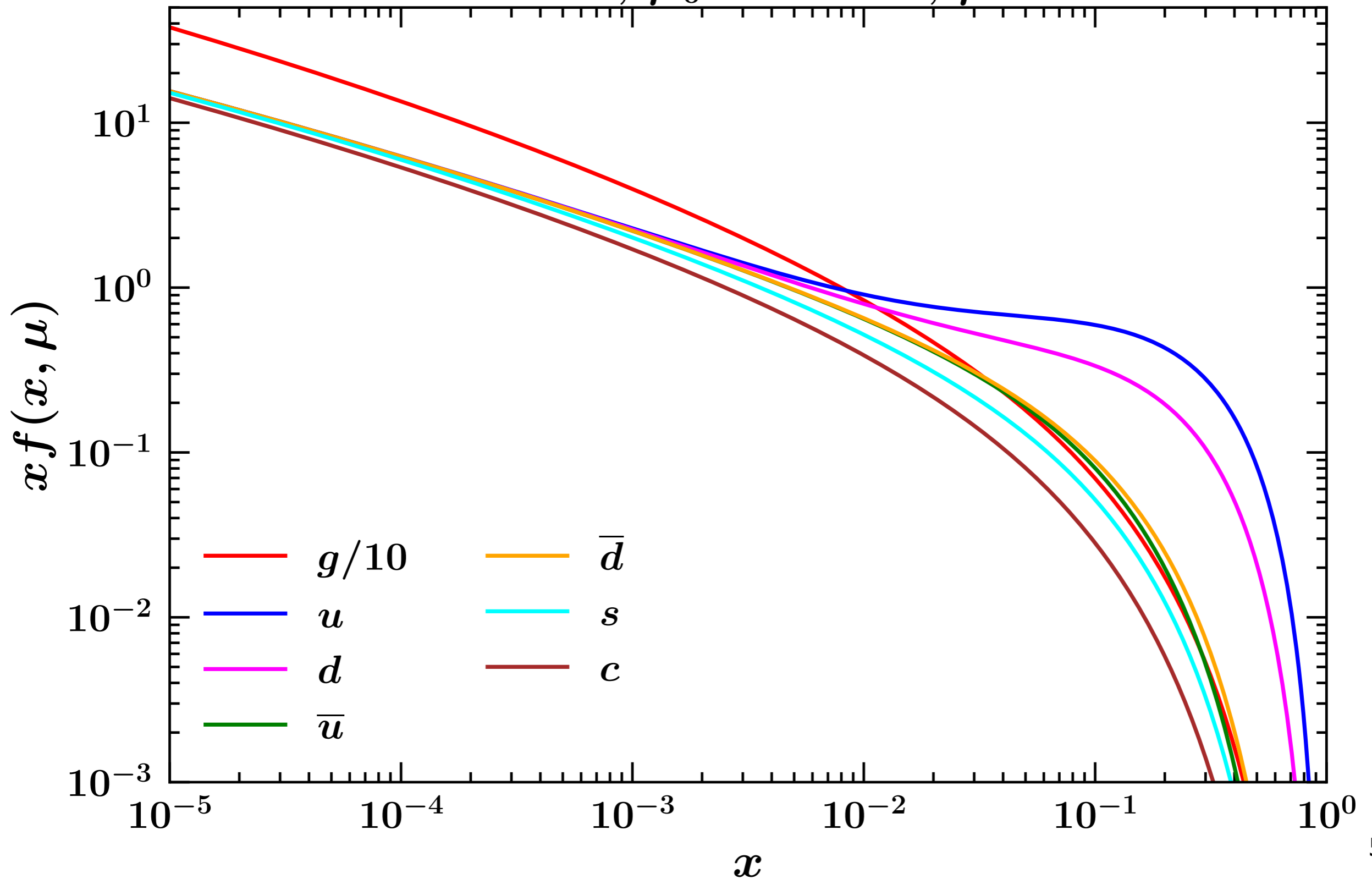
NNLO evolution,  $\mu_0 = 1 \text{ GeV}$ ,  $\mu = 100 \text{ GeV}$



# Perturbative content

*DGLAP evolution:  $x$ -space approach*

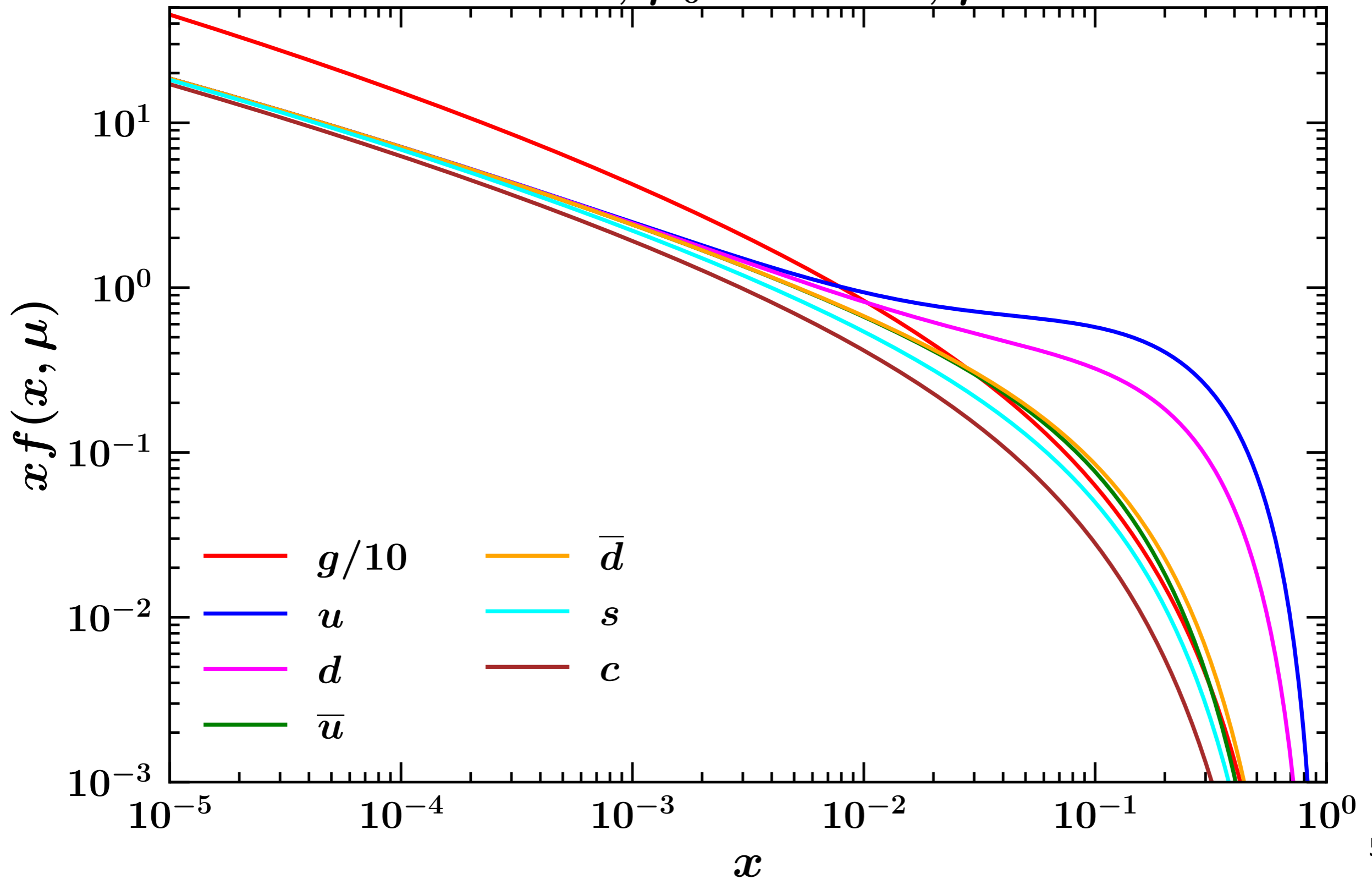
NNLO evolution,  $\mu_0 = 1 \text{ GeV}$ ,  $\mu = 200 \text{ GeV}$



# Perturbative content

*DGLAP evolution:  $x$ -space approach*

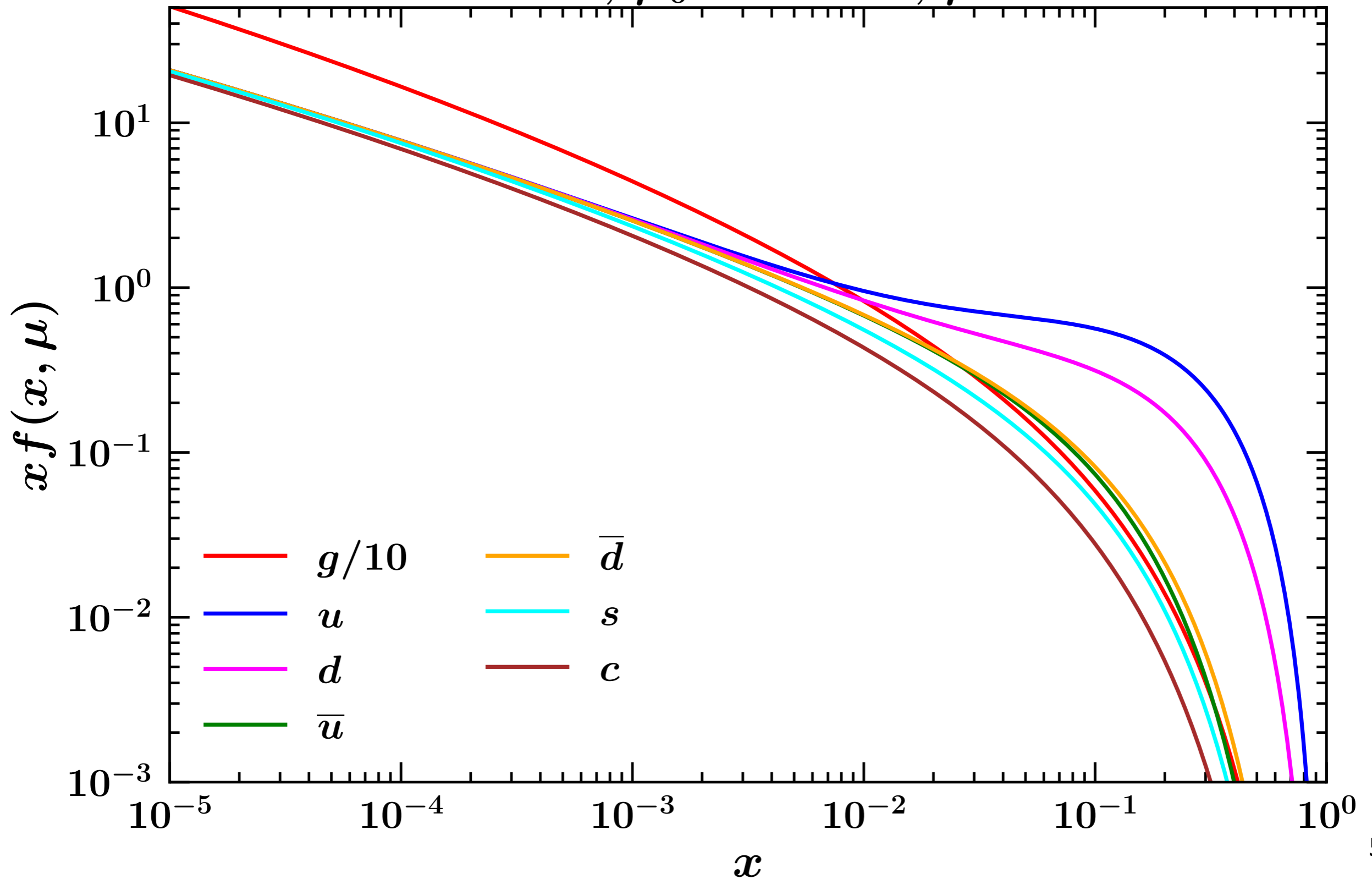
NNLO evolution,  $\mu_0 = 1 \text{ GeV}$ ,  $\mu = 500 \text{ GeV}$



# Perturbative content

*DGLAP evolution:  $x$ -space approach*

NNLO evolution,  $\mu_0 = 1 \text{ GeV}$ ,  $\mu = 1000 \text{ GeV}$

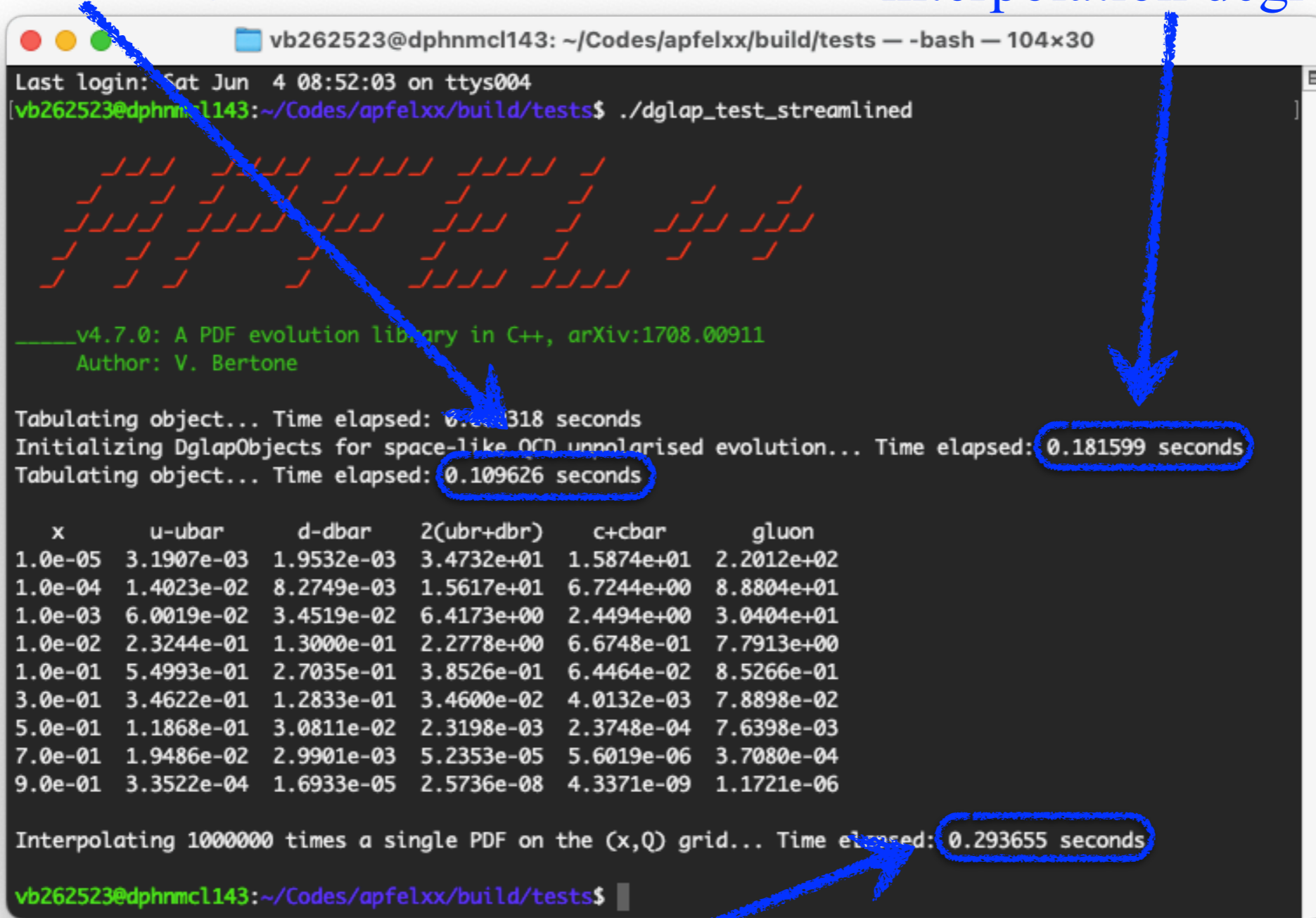


# Perturbative content

## *DGLAP evolution: x-space approach*

Tabulation in  $\mu$   
on a grid with 50 nodes,  
interpolation degree 3

Computation of  $\Gamma_{\beta\alpha}$  on a  
x-space grid with  $\sim 250$  nodes,  
interpolation degree 3



```
vb262523@dphnmcl143: ~/Codes/apfelxx/build/tests -- -bash -- 104x30
Last login: Sat Jun 4 08:52:03 on ttys004
[vb262523@dphnmcl143:~/Codes/apfelxx/build/tests$ ./dglap_test_streamlined

  //  //  //  //  //  //  //  //  //  //  //  //  //  //  //  //  //
 //  //  //  //  //  //  //  //  //  //  //  //  //  //  //  //
//  //  //  //  //  //  //  //  //  //  //  //  //  //  //  //

_____ v4.7.0: A PDF evolution library in C++, arXiv:1708.00911
         Author: V. Bertone

Tabulating object... Time elapsed: 0.0318 seconds
Initializing DglapObjects for space-like QCD unpolarised evolution... Time elapsed: 0.181599 seconds
Tabulating object... Time elapsed: 0.109626 seconds

      x      u-ubar      d-dbar      2(ubr+dbr)      c+cbar      gluon
1.0e-05  3.1907e-03  1.9532e-03  3.4732e+01  1.5874e+01  2.2012e+02
1.0e-04  1.4023e-02  8.2749e-03  1.5617e+01  6.7244e+00  8.8804e+01
1.0e-03  6.0019e-02  3.4519e-02  6.4173e+00  2.4494e+00  3.0404e+01
1.0e-02  2.3244e-01  1.3000e-01  2.2778e+00  6.6748e-01  7.7913e+00
1.0e-01  5.4993e-01  2.7035e-01  3.8526e-01  6.4464e-02  8.5266e-01
3.0e-01  3.4622e-01  1.2833e-01  3.4600e-02  4.0132e-03  7.8898e-02
5.0e-01  1.1868e-01  3.0811e-02  2.3198e-03  2.3748e-04  7.6398e-03
7.0e-01  1.9486e-02  2.9901e-03  5.2353e-05  5.6019e-06  3.7080e-04
9.0e-01  3.3522e-04  1.6933e-05  2.5736e-08  4.3371e-09  1.1721e-06

Interpolating 1000000 times a single PDF on the (x,Q) grid... Time elapsed: 0.293655 seconds
vb262523@dphnmcl143:~/Codes/apfelxx/build/tests$
```

Handwritten blue arrows indicate performance metrics: one points to the terminal title bar, another to the 0.181599 seconds value, and a third to the 0.293655 seconds value. The 0.109626 seconds and 0.181599 seconds values are circled in blue.

Remarkable speed!

# Perturbative content

## *DGLAP evolution: $x$ -space approach*

🍏 “Details” that I didn’t discuss:

🍏 Computing the integrals  $\Gamma_{\beta\alpha}$ :

🍏 integrands are distributions that involve  $\delta$ -functions and  $+$ -distributions.

🍏 Addressing the problem of inaccuracies at large  $x$  caused by a logarithmically-spaced grid.

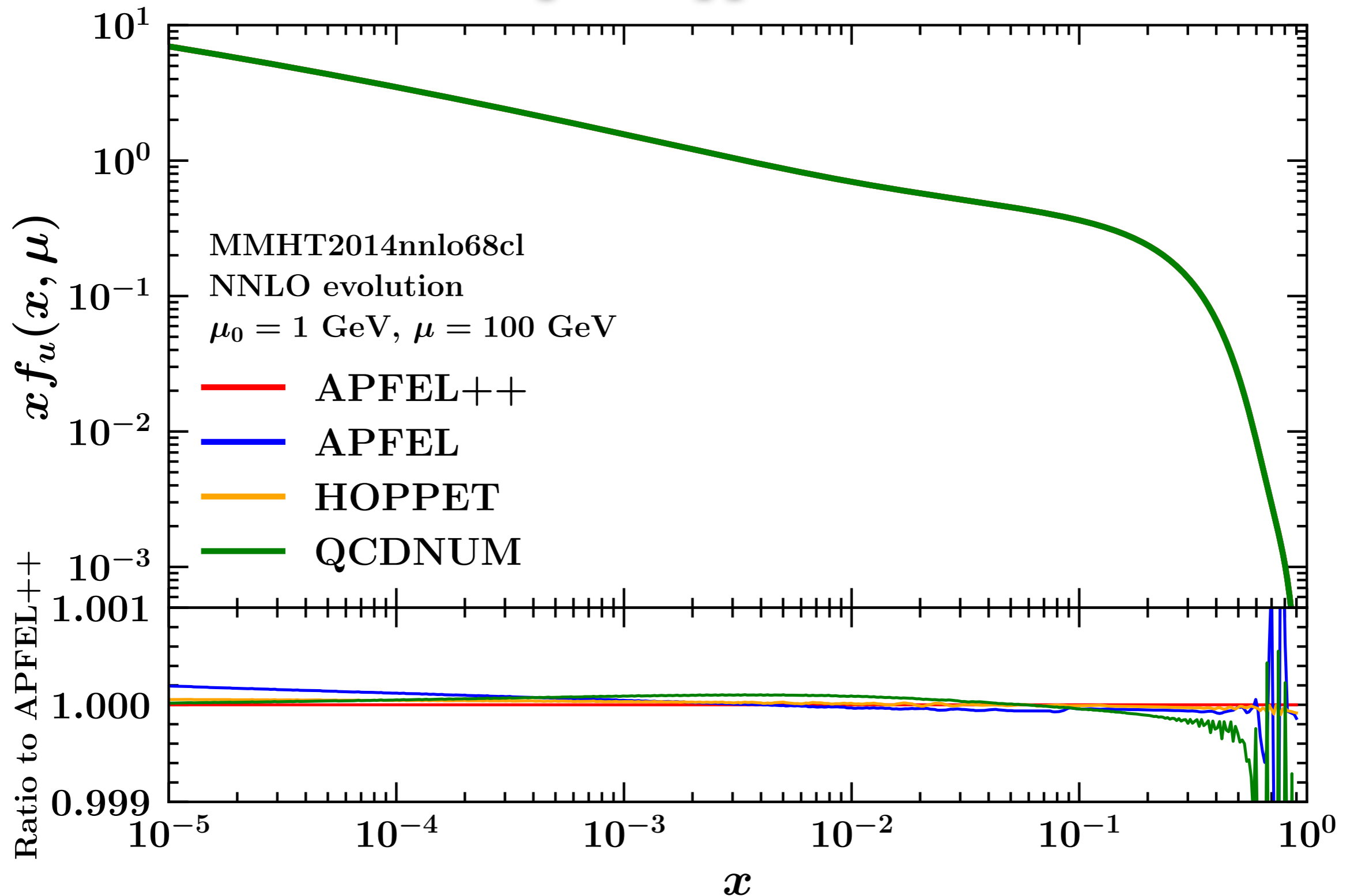
🍏 The flavour dependence of parton distributions.

🍏 The possible presence of heavy-quark thresholds along the evolution.

🍏 ...

# Perturbative content

*DGLAP evolution:  $x$ -space approach*



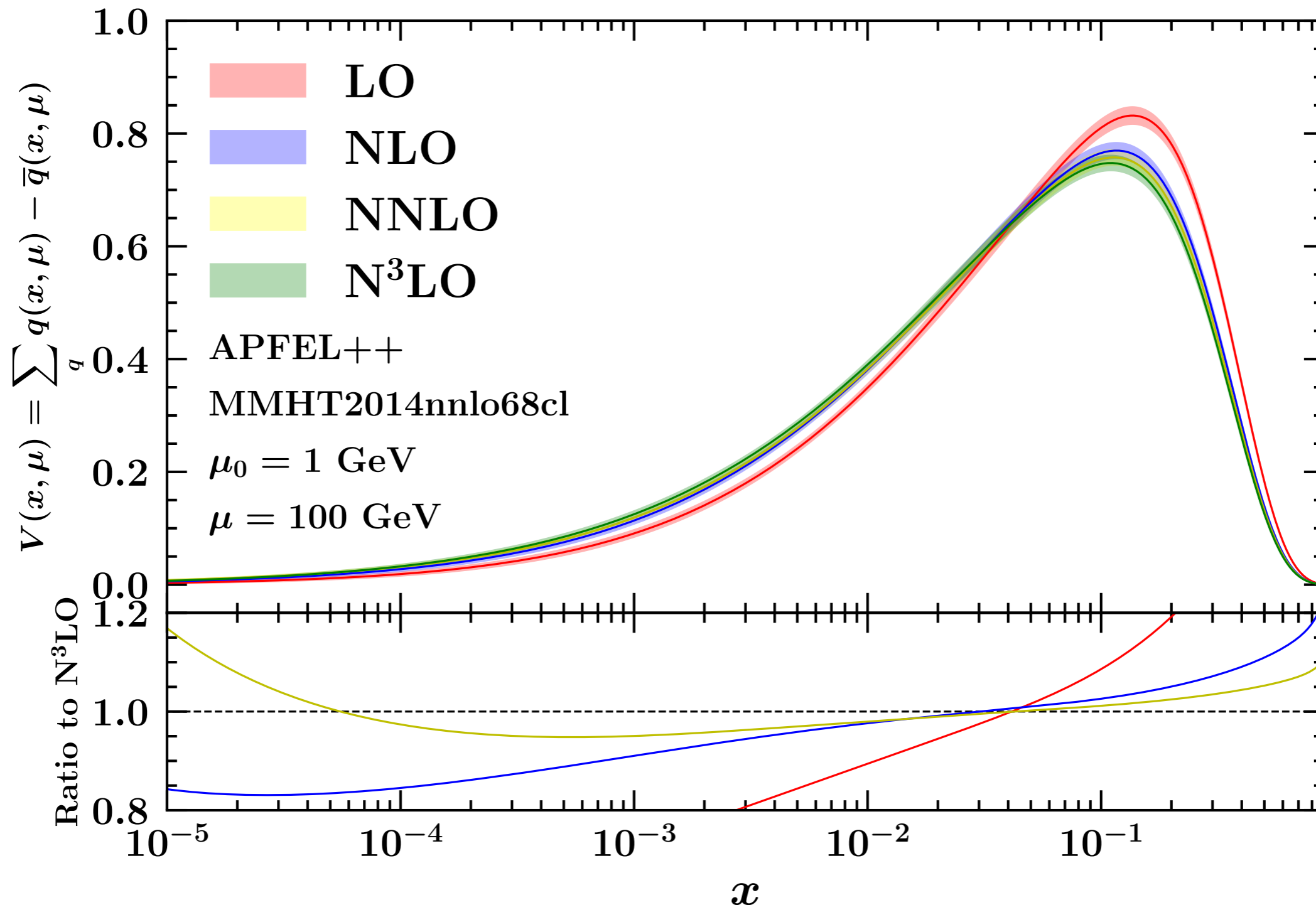
- Independent implementations agree well below the per-mil level! 56



# Perturbative content

## *DGLAP evolution: $x$ -space approach*

- $O(\alpha_s^4)$  **non-singlet** splitting functions in the planar limit recently computed [Moch et al., arXiv:1707.08315] enabling partial N<sup>3</sup>LO evolution. Approximations available for the **Singlet**.



# Perturbative content

## *DGLAP evolution: $\mathcal{N}$ -space approach*

🍏 Mellin transform:

$$f(N) \equiv \mathcal{M}[f(x)](N) = \int_0^1 dx x^{N-1} f(x)$$

🍏 turns a Mellin convolution:

$$[f \otimes g](x) \equiv \int_x^1 \frac{dy}{y} f(y) g\left(\frac{x}{y}\right) = \int_x^1 \frac{dz}{z} f\left(\frac{x}{z}\right) g(z) = \int_0^1 dy \int_0^1 dz \delta(x-yz) f(y) g(z)$$

🍏 into a simple product:

$$[f \otimes g](N) = f(N)g(N)$$

🍏 The DGLAP in Mellin space becomes an ODE:

$$\frac{df(N, \mu)}{d \ln \mu^2} = P(N, \alpha_s(\mu)) f(N, \mu)$$

🍏 A fully analytic solution can be found changing the evolution variable:

$$\frac{d\alpha_s(\mu)}{d \ln \mu^2} = \beta(\alpha_s(\mu)) \quad \Rightarrow \quad \frac{df(N, \mu(\alpha_s))}{d\alpha_s} = \frac{P(N, \alpha_s)}{\beta(\alpha_s)} f(N, \mu(\alpha_s))$$

# Perturbative content

## *DGLAP evolution: $N$ -space approach*

🍏 At LO:

$$P(N, \alpha_s) = \alpha_s P^{(0)}(N) \quad \text{and} \quad \beta(\alpha_s) = \alpha_s^2 \beta_0$$

🍏 so that:

$$\frac{df(N, \mu(\alpha_s))}{d\alpha_s} = \frac{P^{(0)}(N)}{\beta_0} \frac{f(N, \mu(\alpha_s))}{\alpha_s}$$

🍏 The solution is straightforward:

$$f(N, \mu) = \left( \frac{\alpha_s(\mu)}{\alpha_s(\mu_0)} \right)^{P^{(0)}(N)/\beta_0} f(N, \mu_0)$$

🍏 The same analytic approach can be extended beyond LO by making some “perturbatively allowed” approximations.

🍏 This leads to the phenomenon of *perturbative hysteresis*.

[Bertone et al. *Phys.Rev.D* 105 (2022) 9, 096003]

# Perturbative content

## *DGLAP evolution: $\mathcal{N}$ -space approach*

🍏 Also the computation of some observables benefits of this simplification in Mellin space.

🍏 Inclusive DIS is a typical example:

$$F(x, Q) = [C \otimes f](x, Q) \quad \Rightarrow \quad F(N, Q) = C(N, \alpha_s(Q)) f(N, Q)$$

🍏 This reduces the computation of an observable to a simple product that is thus very fast to compute numerically.

# Perturbative content

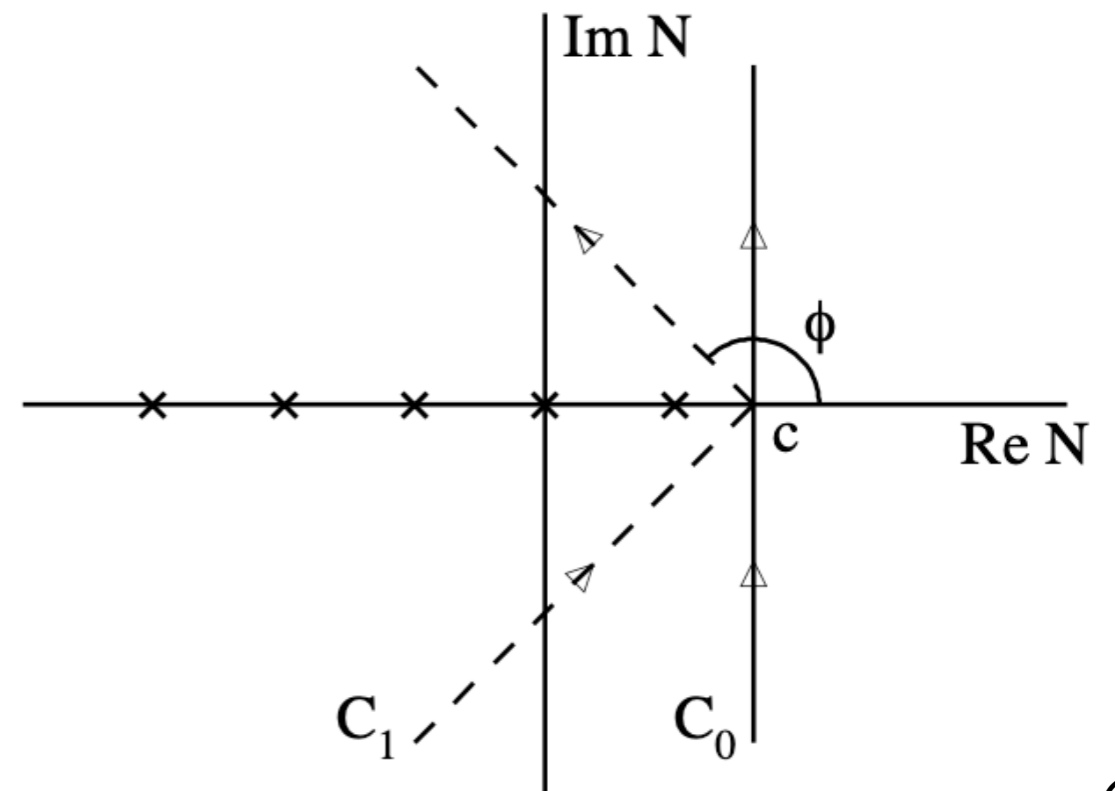
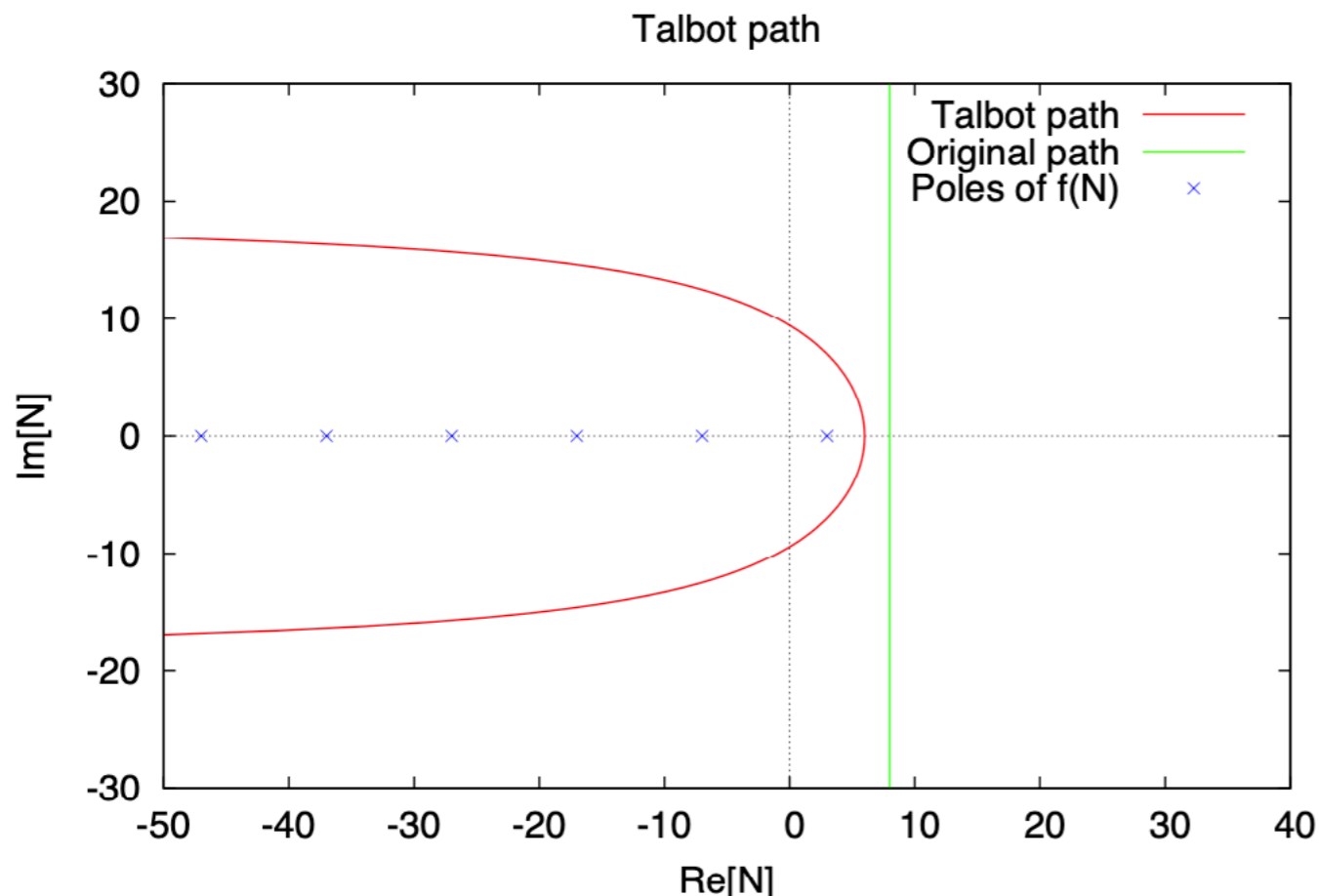
## *DGLAP evolution: $\mathcal{N}$ -space approach*

🍏 Data is however delivered in  $x$  space and it is therefore needed to transform back from  $\mathcal{N}$  to  $x$ -space:

$$f(x) = \frac{1}{2\pi i} \int_{c-i\infty}^{c+i\infty} dN x^{-N} f(N)$$

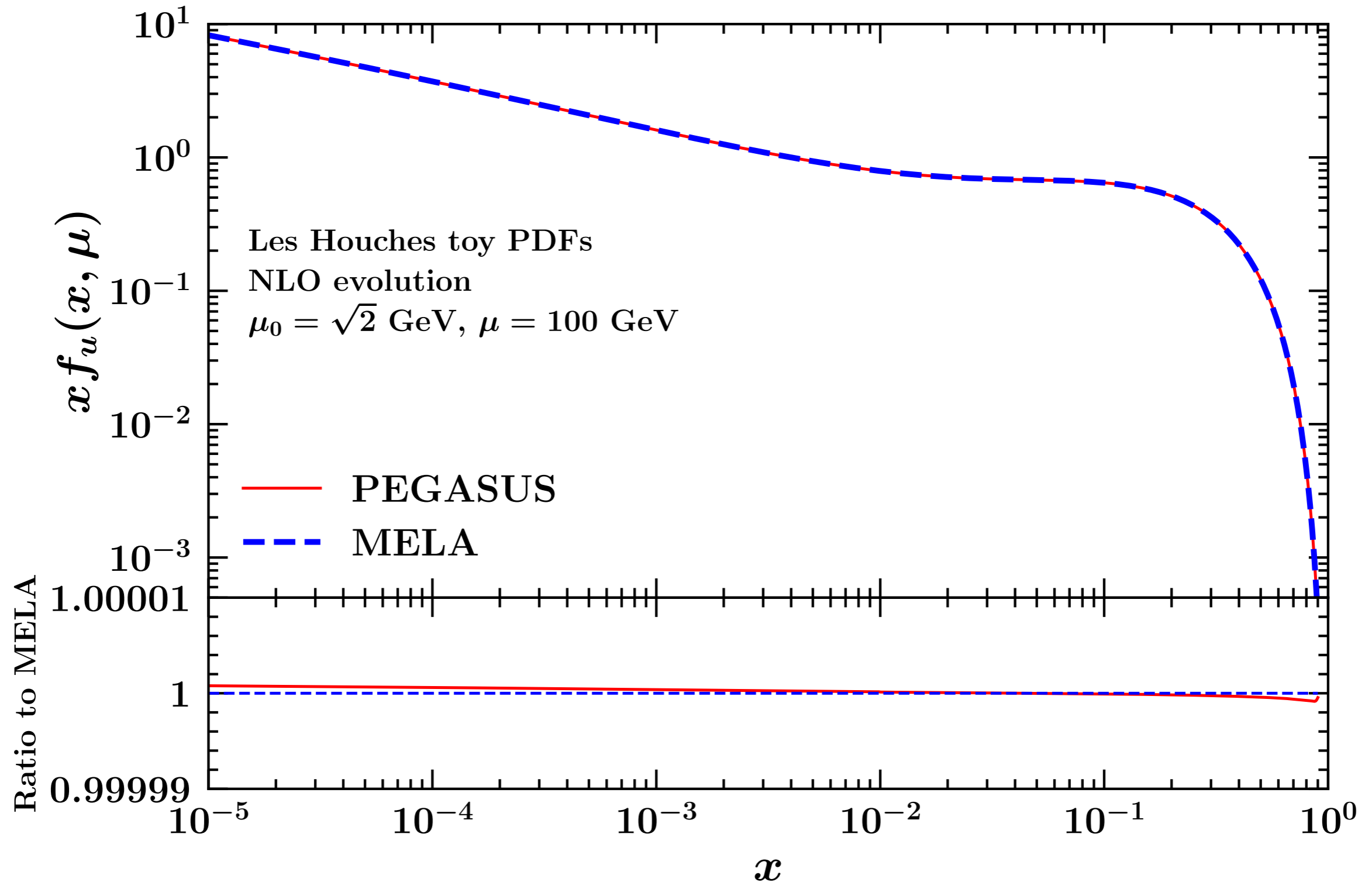
🍏 where  $c$  is a real constant such that the integration contour lies to the right of all the singularities of the integrand:

🍏 the integration contour is typically deformed for numerical implementations.



# Perturbative content

*DGLAP evolution:  $N$ -space approach*



- Independent implementations agree extremely well!

# Perturbative content

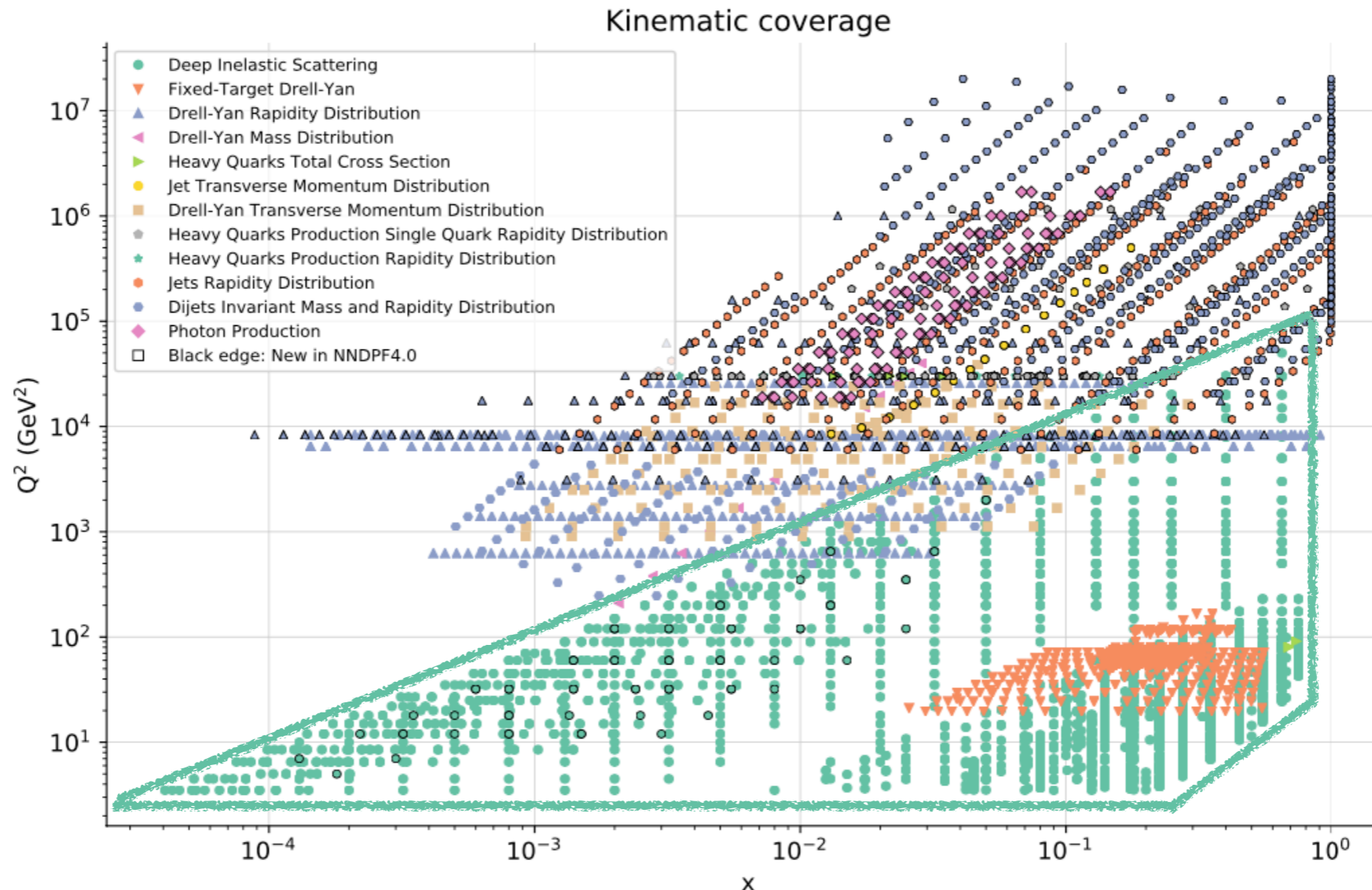
## *DGLAP evolution: $\mathcal{N}$ -space approach*

- 🍏 While being so numerically appealing, the  $\mathcal{N}$ -space approach is affected by a few shortcomings:
  - 🍏 the PDF parameterisation needs to be analytically transformable in Mellin space:
    - 🍏 this drastically restricts the range of possible parameterisations.
  - 🍏 The partonic cross sections need to be analytically known in  $\mathcal{N}$  space:
    - 🍏 this is the case only for a small number of inclusive process and observables (*e.g.* DIS, mass-differential DY, and not much more).
    - 🍏 experimental cuts typically make the computation of analytic Mellin transforms unfeasible.
- 🍏 As of today, no large PDF collaboration uses the  $\mathcal{N}$ -space approach as discussed above:
  - 🍏 NNPDF has adopted in the past and is now planning to adopt again a “hybrid” technology that combines the  $\mathcal{N}$ -space approach with the  $x$ -space one.

# Perturbative content

## *Hard cross sections: inclusive DIS*

- A large part of the dataset of modern PDF fits is still made of DIS data:



- Very broad kinematic coverage:
  - **low values of  $Q$**  comparable with  $m_c$  and  $m_b \rightarrow$  **heavy-quark mass corrections,**
  - **low values of  $x \rightarrow$  small- $x$  resummation corrections.**



# Perturbative content

## *Hard cross sections: inclusive DIS*

- The inclusive DIS cross section is a combination of **structure functions**.
- The inclusion of **heavy-quark** mass corrections in the structure functions needs to be reconciled with the resummation of **collinear logarithms**.
- This is achieved by **matching** different schemes in a General-Mass scheme:
  - the **fixed-flavour (FF)** scheme that includes mass power corrections  $m_h/Q$ , valid for  $m_h \sim Q$ ,
  - the **zero-mass (ZM)** scheme that resums  $\ln(m_h/Q)$ , valid for  $m_h \ll Q$ ,
  - subtraction of the **double counting (DC)** needed.

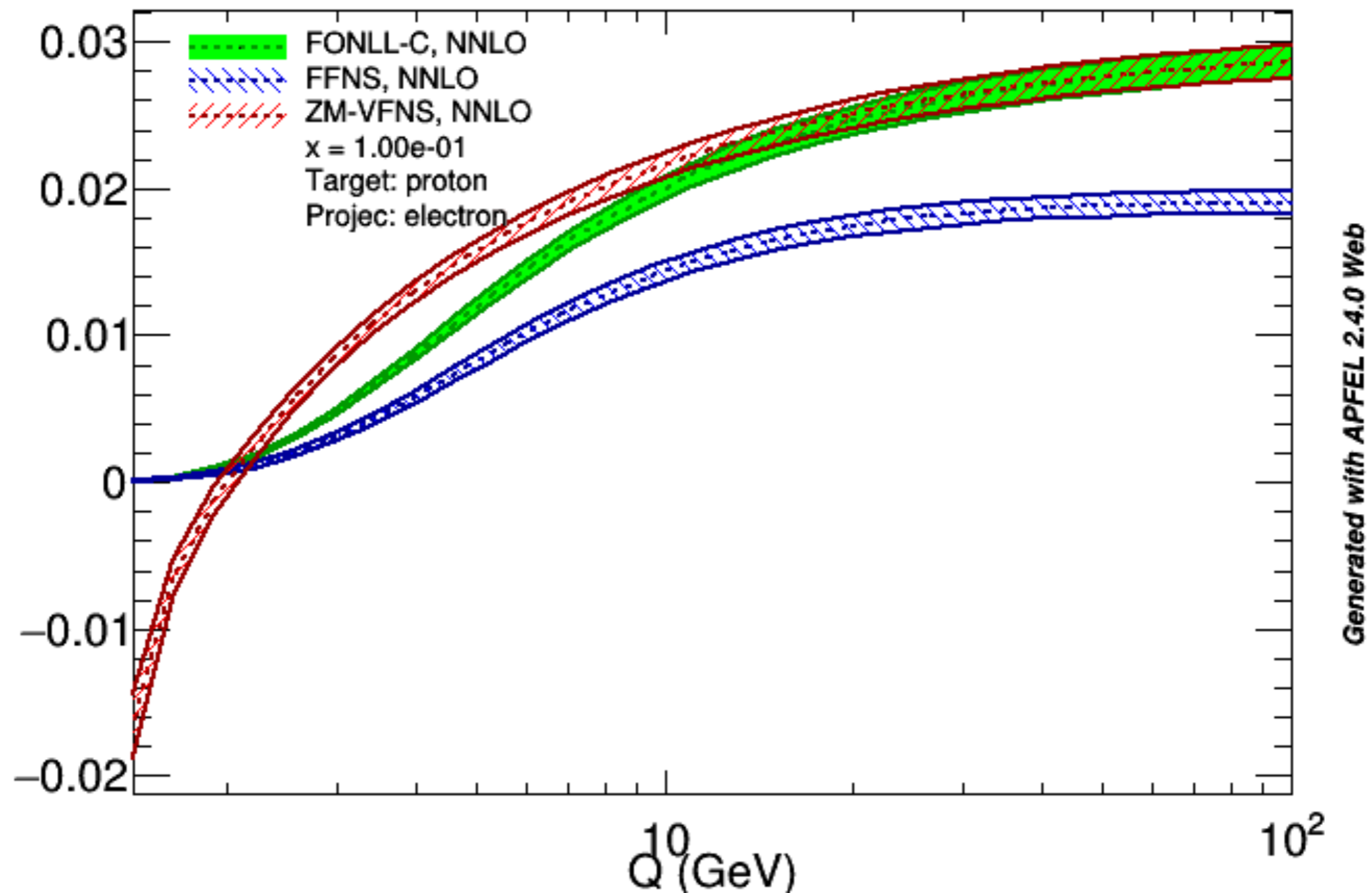
$$F^{\text{GM}}(x, Q) = F^{\text{FF}}(x, Q) + F^{\text{ZM}}(x, Q) - F^{\text{DC}}(x, Q)$$

- Several implementations exist, *e.g.*:
  - ACOT [Phys.Rev., vol. D50, pp. 3102–3118, 1994],
  - FONLL [JHEP, vol. 9805, p. 007, 1998],
  - RT [Phys.Rev., vol. D57, pp. 6871–6898, 1998],
  - BMSN [Eur.Phys.J., vol. C1, pp. 301–320, 1998].
- They all differ by subleading power corrections in the intermediate region. <sup>65</sup>

# Perturbative content

*Hard cross sections: inclusive DIS*

$F_2^C(x, Q)$ , NNPDF2.3 NNLO



- This example makes evident how a GM scheme interpolates between the FF scheme at  $m_h \sim Q$  and the ZM scheme for  $m_h \ll Q$ .

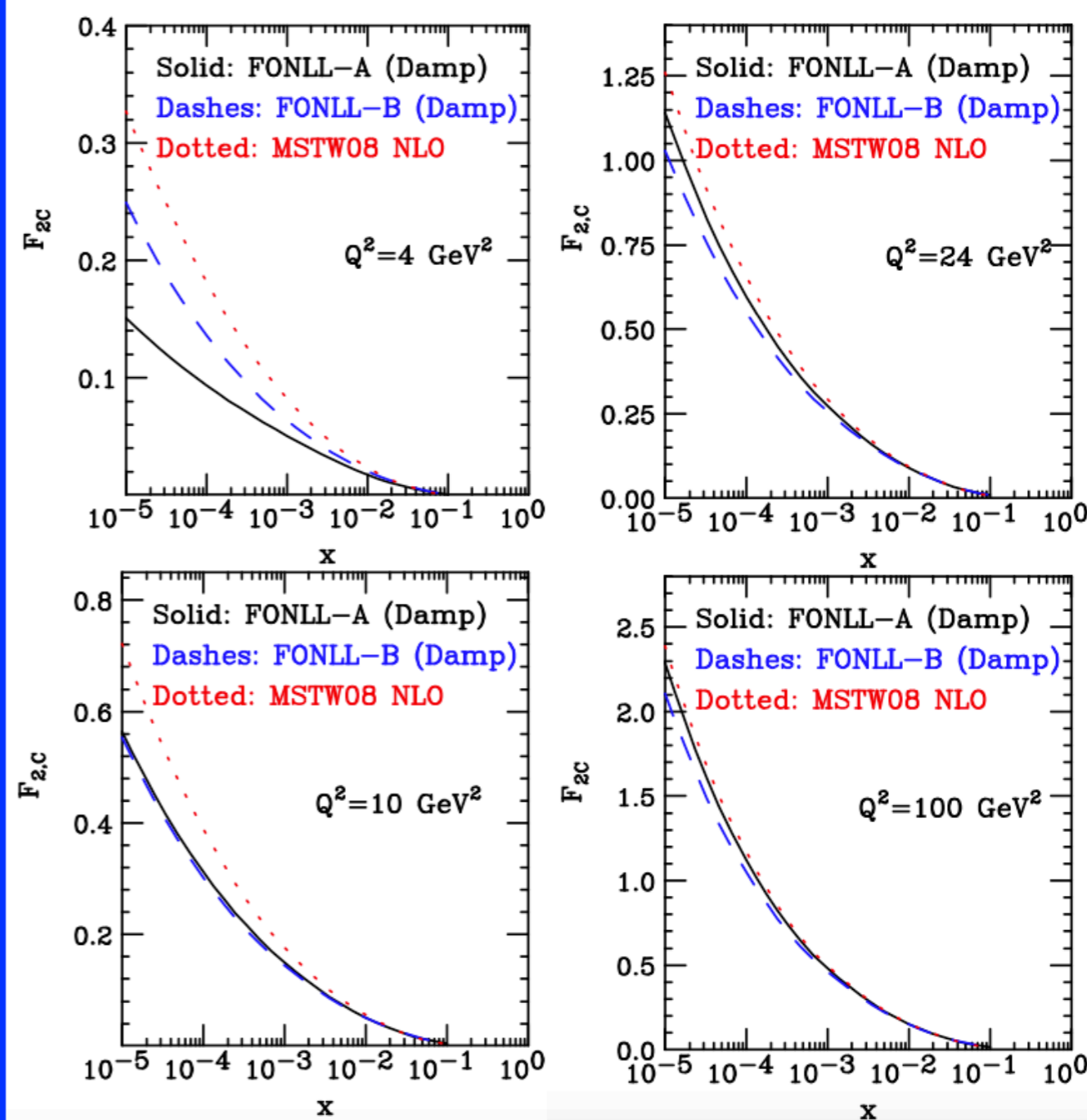
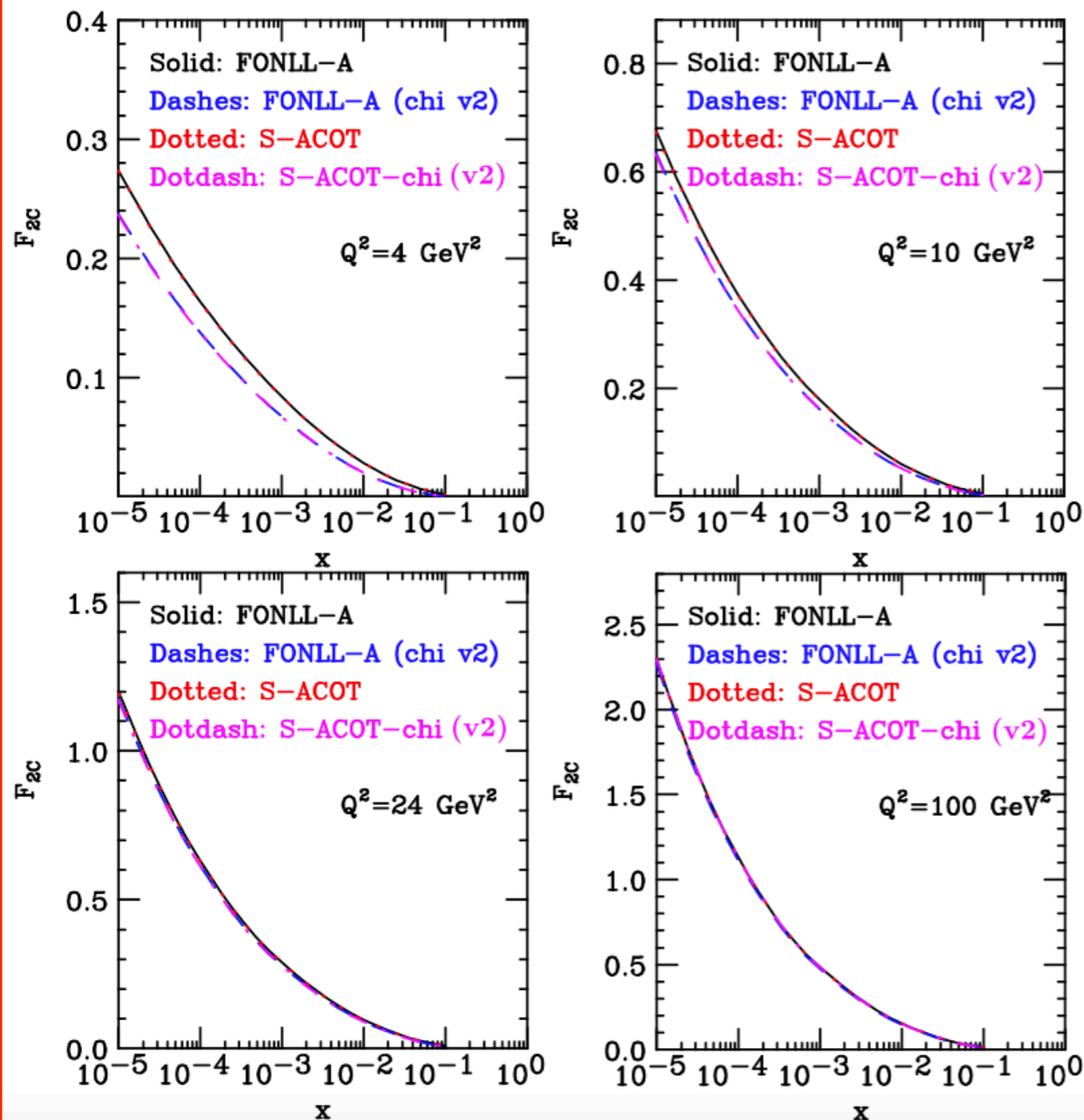
# Perturbative content

## Hard cross sections: inclusive DIS

FONLL vs. ACOT

[arXiv:1003.1241]

FONLL vs. RT (MSTW08)



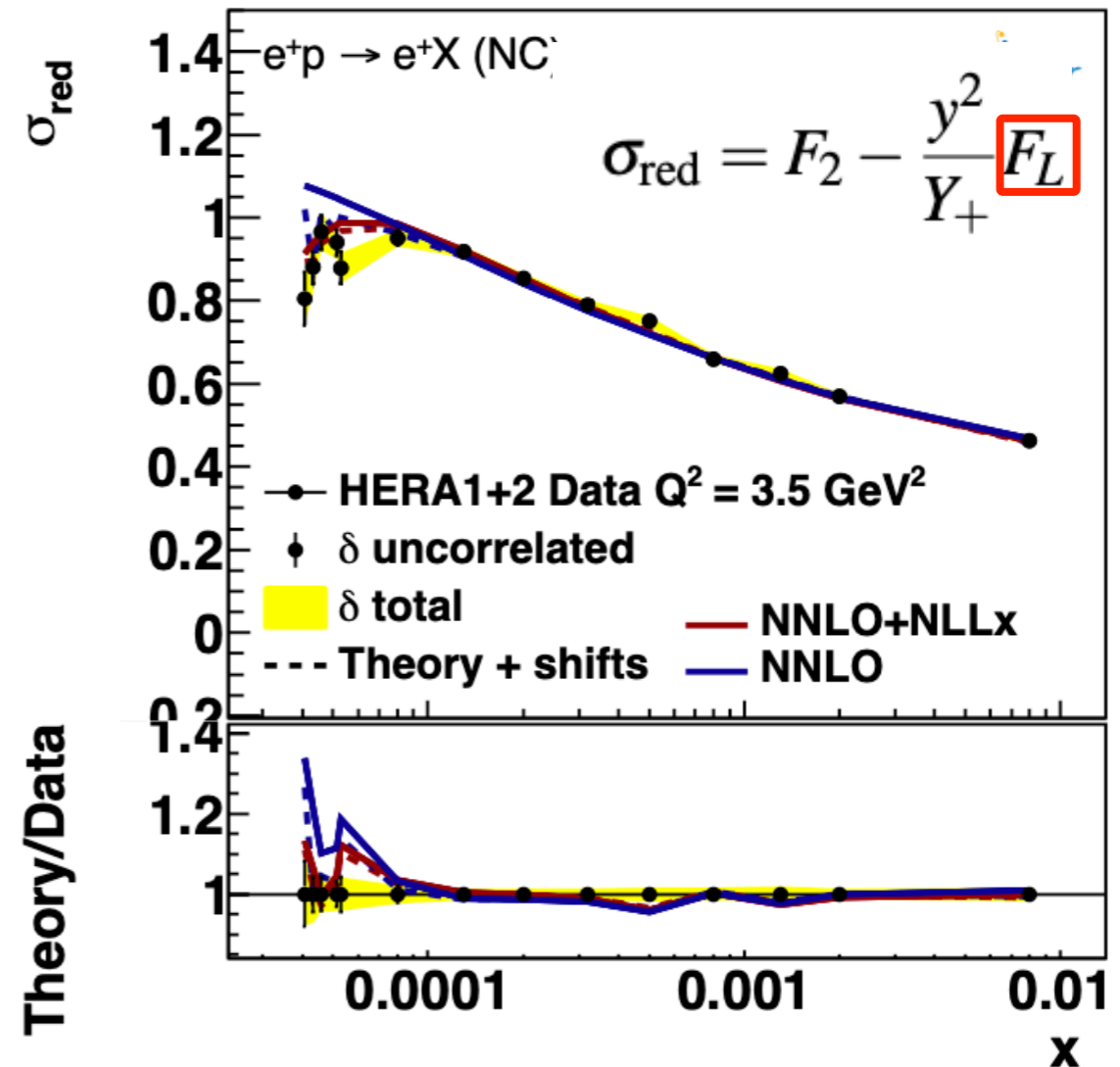
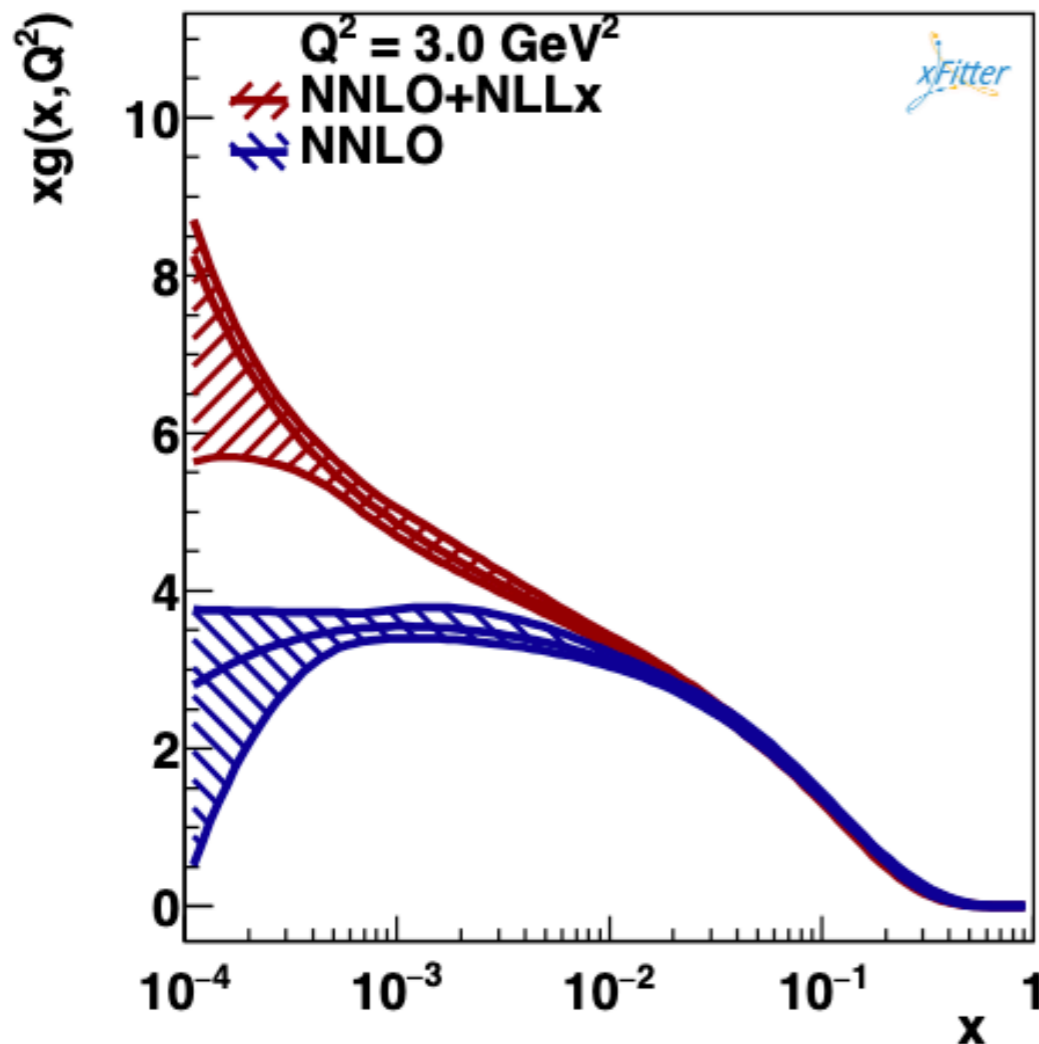
- A direct comparison amongst schemes show that, while for  $m_h \ll Q$  differences are small, they can be sizeable in the intermediated region.

# Perturbative content

## Hard cross sections: inclusive DIS

[NNPDF, *Eur.Phys.J.C* 78 (2018) 4, 321]  
 [xFitter, *Eur.Phys.J.C* 78 (2018) 8, 621]

- The issue of the NLO low- $x$  gluon PDF going negative at low scales is greatly mitigated by including **small- $x$  (BFKL) resummation** effects in PDF fits:
  - relevant for **quarkonium** production at the LHC, [Lansberg, Ozcelik, *Eur.Phys.J.C* 81 (2021) 6, 497]
- Small- $x$  resummation makes the DGLAP evolution **less steep** and thus allows for a larger small- $x$  gluon PDF that behaves as a sea-like distribution.

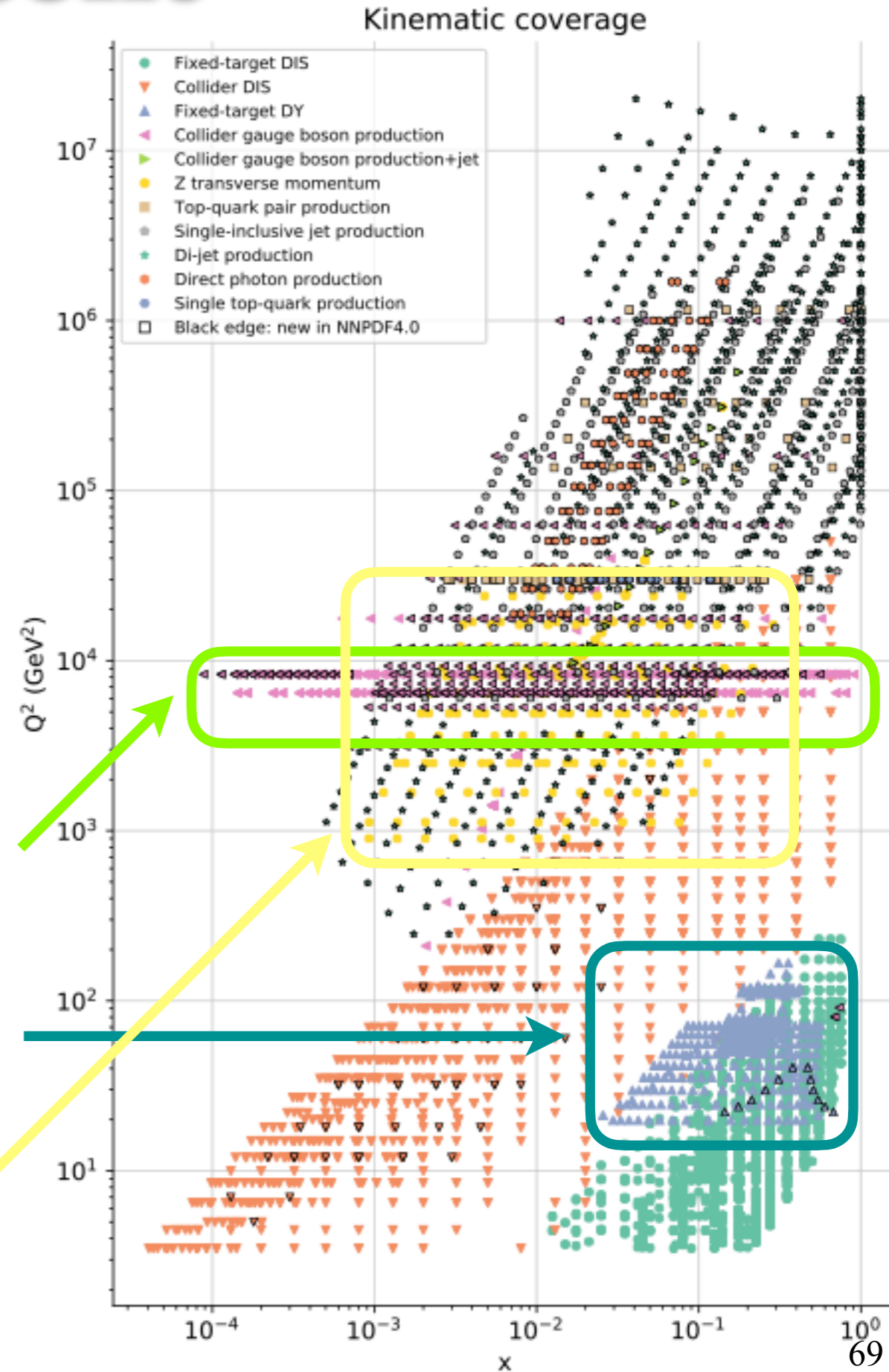


# Perturbative content

## *Hard cross sections: Drell-Yan*

Drell-Yan (both Z and W) is a very important process in **PDF determinations**:

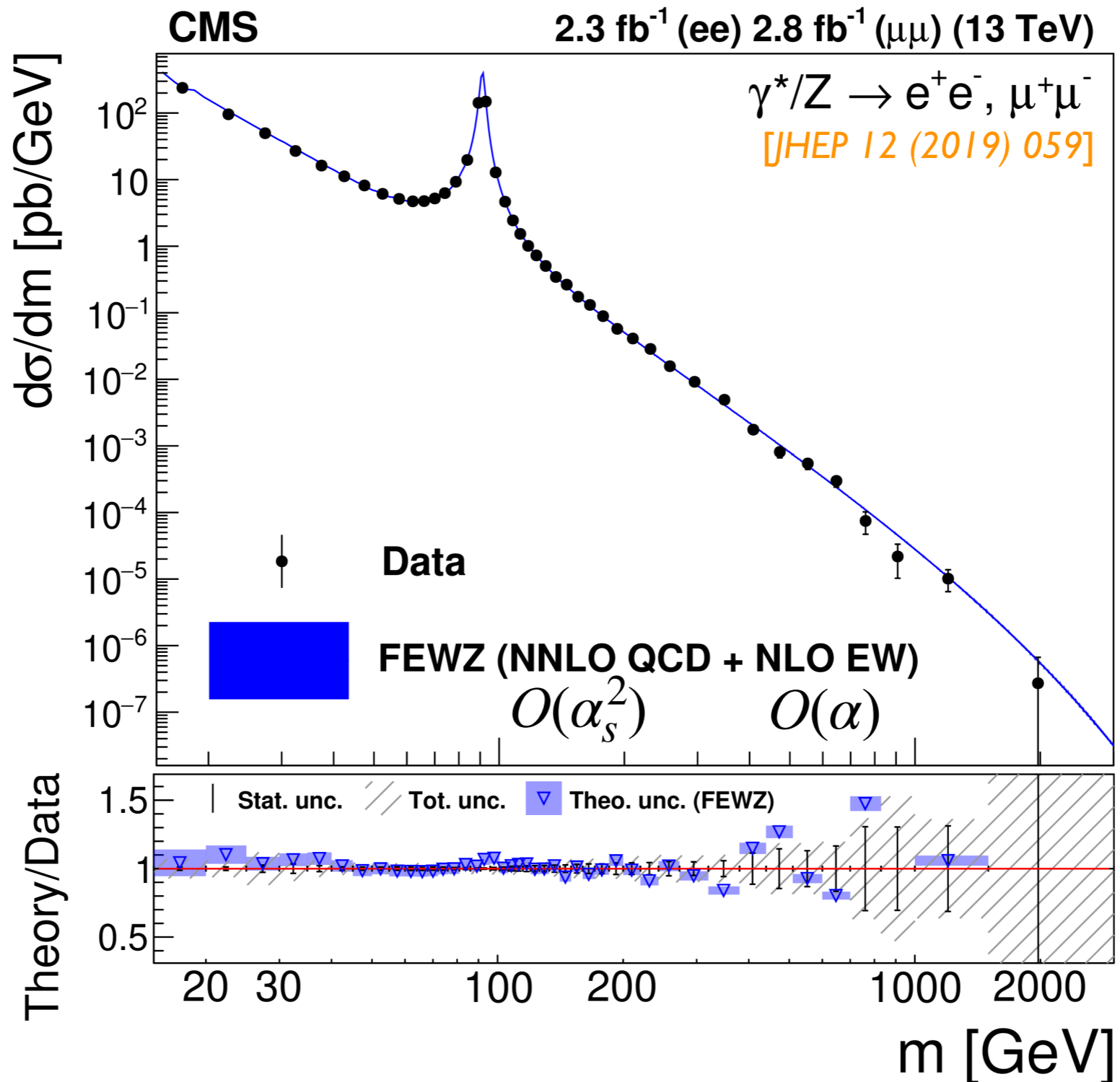
- as opposite to DIS, Drell-Yan gives access to a larger variety of quark PDF combinations:
  - this enables **flavour/antiflavour separation**.
- very wide **kinematic coverage**:
  - collider data, placed at higher energies can reach values of  $x$  as low as  $10^{-4}$ ,
  - fixed-target data is placed at lower scales and probes quark PDFs at higher values of  $x$ .
- $q_T$  distribution gives access to the **gluon PDF**.



# Perturbative content

## Hard cross sections: Drell-Yan

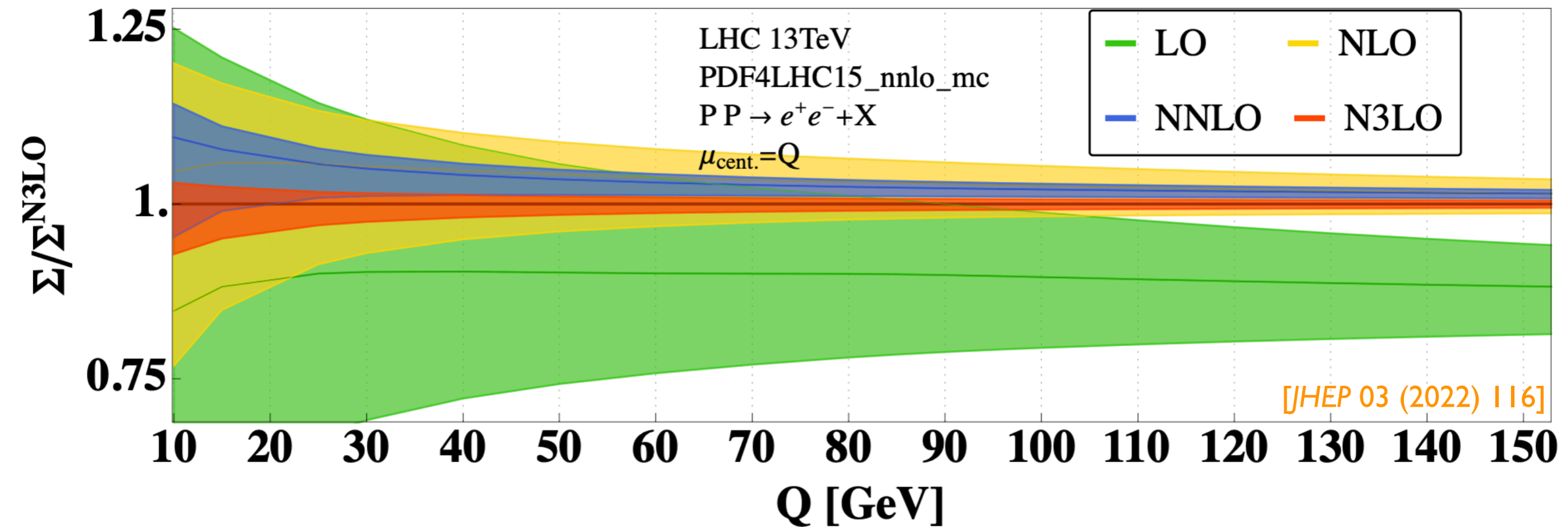
Our current understanding of the **invariant mass spectrum** in Drell-Yan is very good.



# Perturbative content

## *Hard cross sections: Drell-Yan*

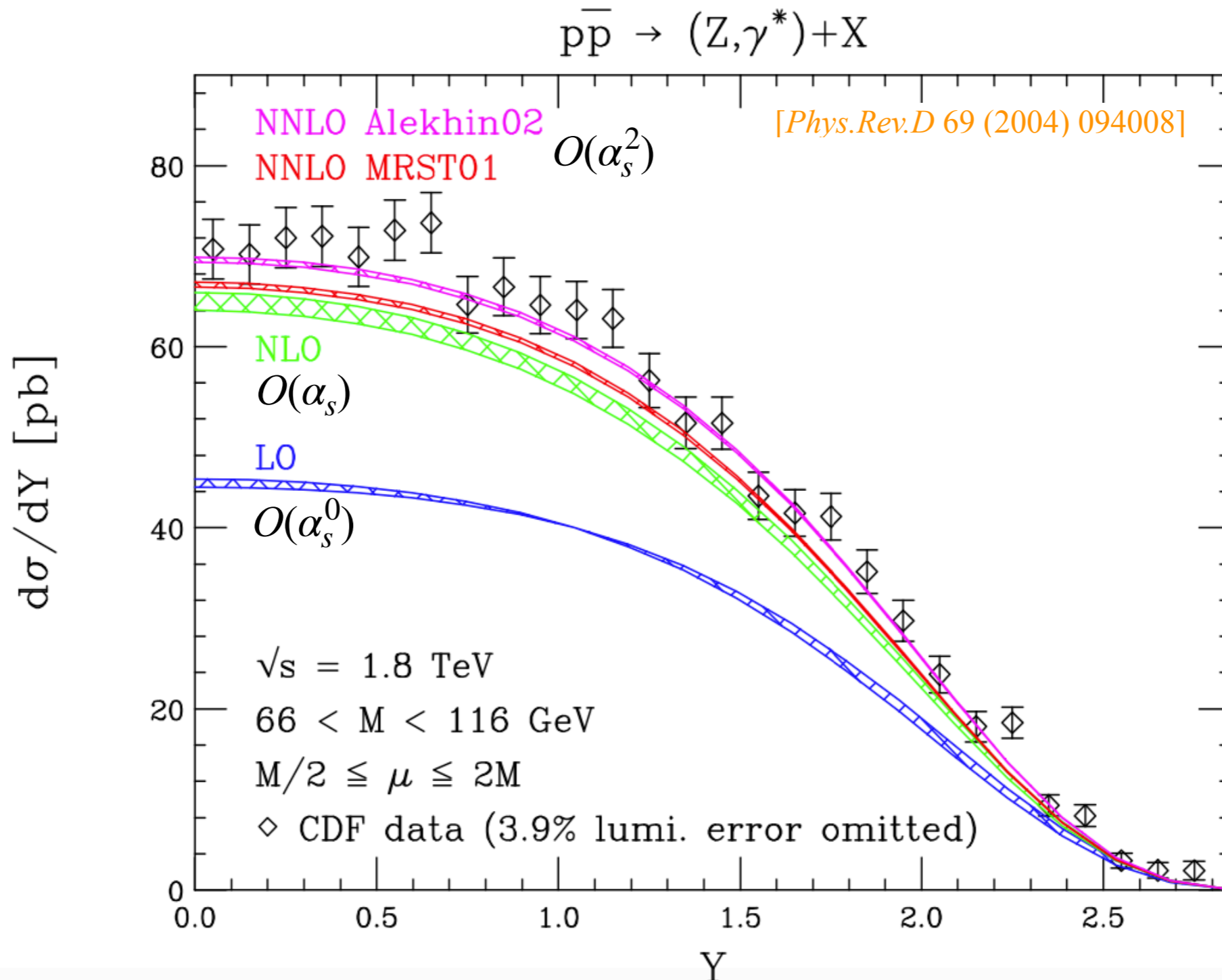
Our current understanding of the **invariant mass spectrum** in Drell-Yan is very good.



# Perturbative content

## Hard cross sections: Drell-Yan

Also the rapidity spectrum is particularly well known.



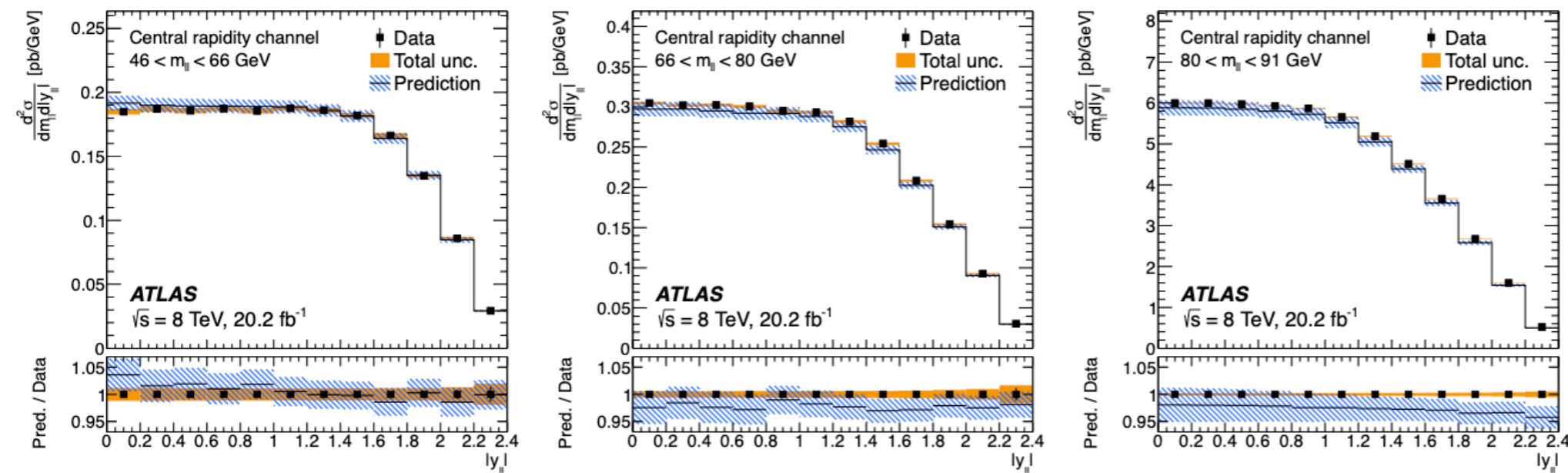
NNLO corrections significantly improve the agreement with data.



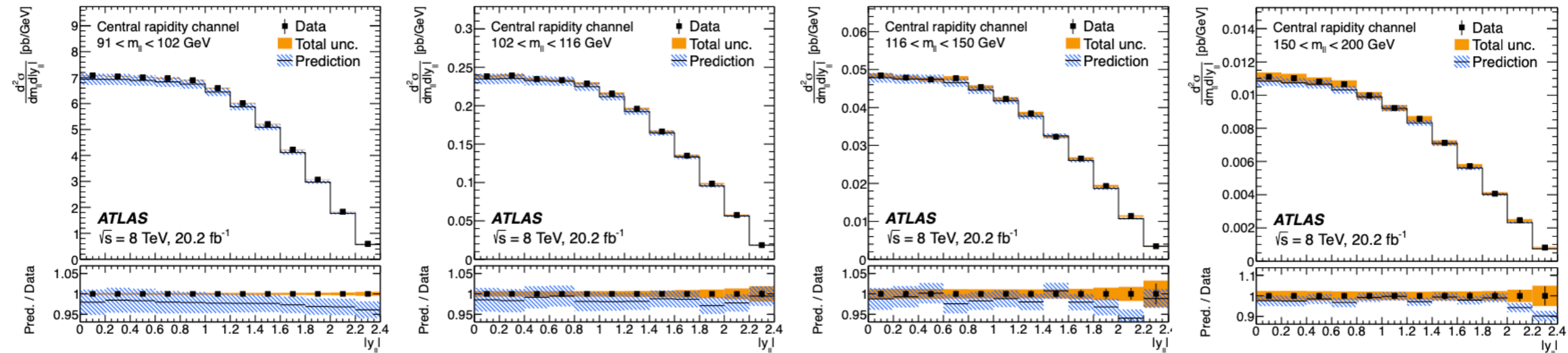
# Perturbative content

## Hard cross sections: Drell-Yan

Also the rapidity spectrum is particularly well known.



[JHEP 12 (2017) 059]

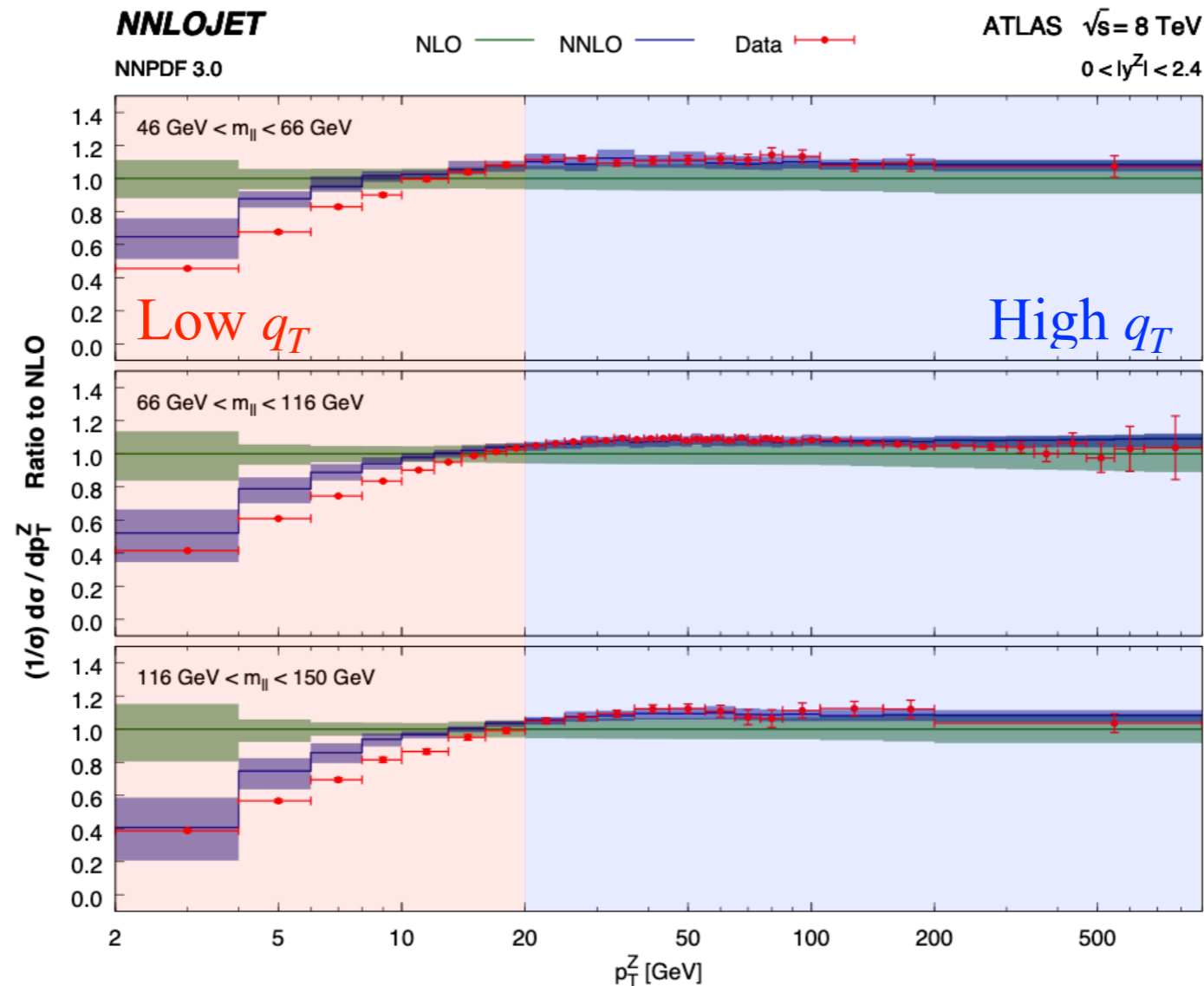


- NNLO + NLO EW predictions.
- Very good data/theory agreement also in lower and higher invariant mass bins.

# Perturbative content

## Hard cross sections: Drell-Yan

The fully differential NNLO (*i.e.*  $O(\alpha_s^3)$ ) corrections to the cross section for  $pp \rightarrow Z+\text{jet}$  was presented in [Phys. Rev. Lett. 117 (2016) 2, 022001] and [Phys.Rev.Lett. 116 (2016) 15, 152001]. These calculations allow us to compute the  $q_T$  spectrum of the  $Z$  to NNLO accuracy.



NNLO corrections improve the agreement with data all across the board:

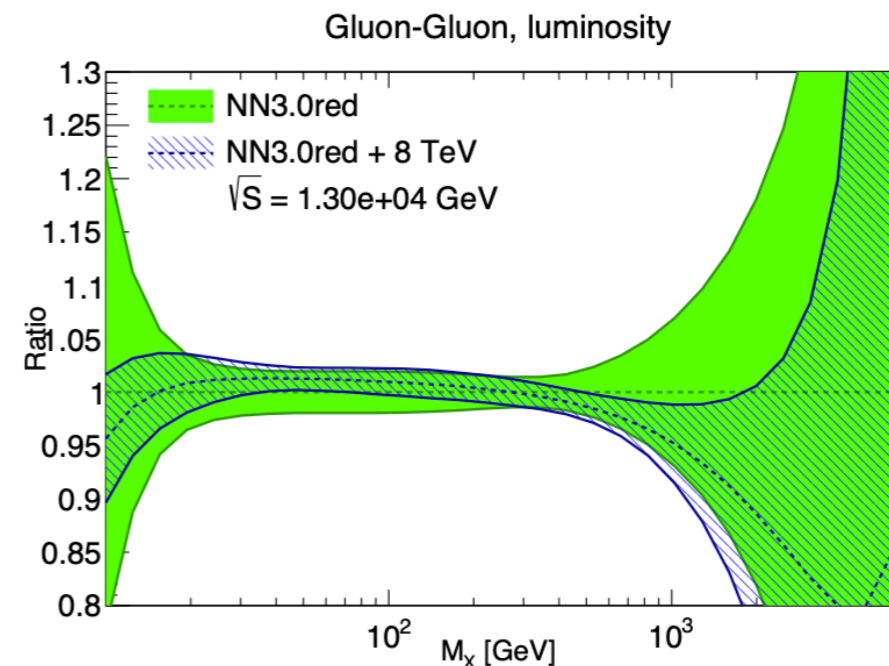
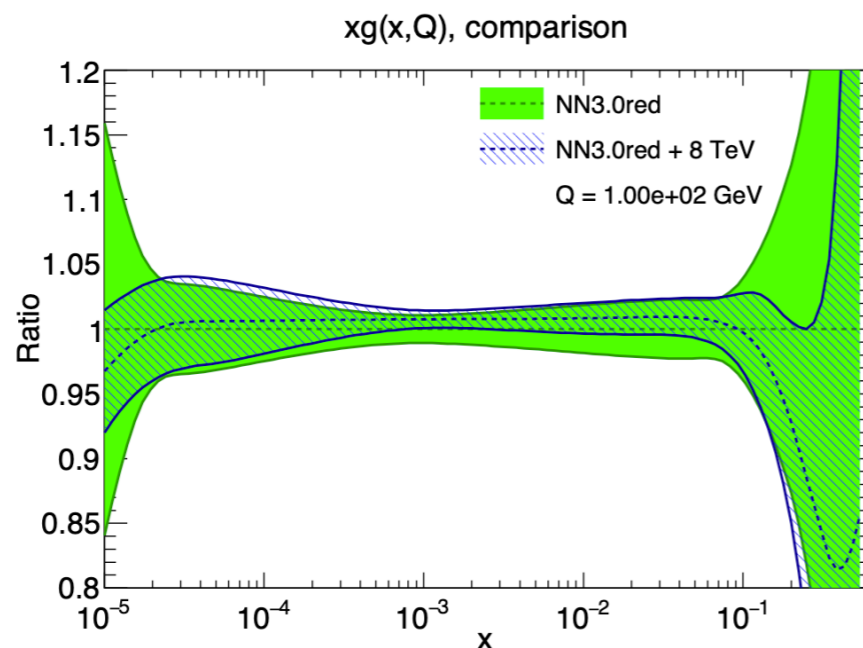
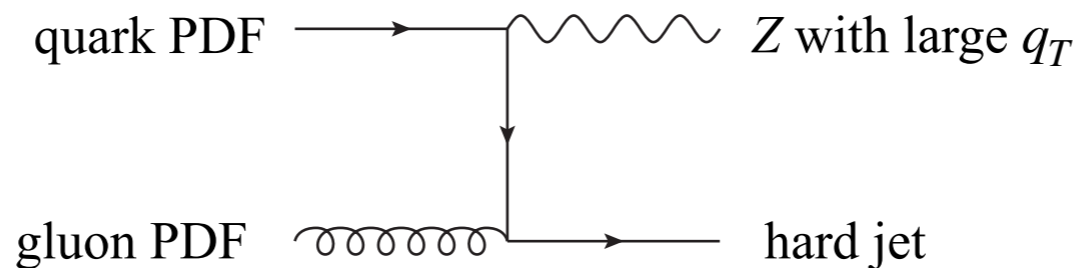
- for  $q_T \sim Q$  the agreement with data is now excellent,
- for  $q_T \ll Q$ , NNLO partly captures the double-log behaviour and provides qualitative improvements in the description of the shape of the data: **resummation still needed.**

# Perturbative content

## Hard cross sections: Drell-Yan

The  $q_T$  of the  $Z$  boson allows us to constraint the collinear gluon PDF:

- as we have seen above, collinear factorisation is reliable for  $q_T \simeq Q$ .
- In order for the  $Z$  to have a large  $q_T$ , it needs an object to recoil against. This is typically a jet. As a consequence, the relevant process is  $pp \rightarrow Z + j + X$ .
- One of the leading-order partonic cross sections contributing to this process is:



The impact on the gluon PDF is **significant**.

# Perturbative content

## Hard cross sections: Drell-Yan

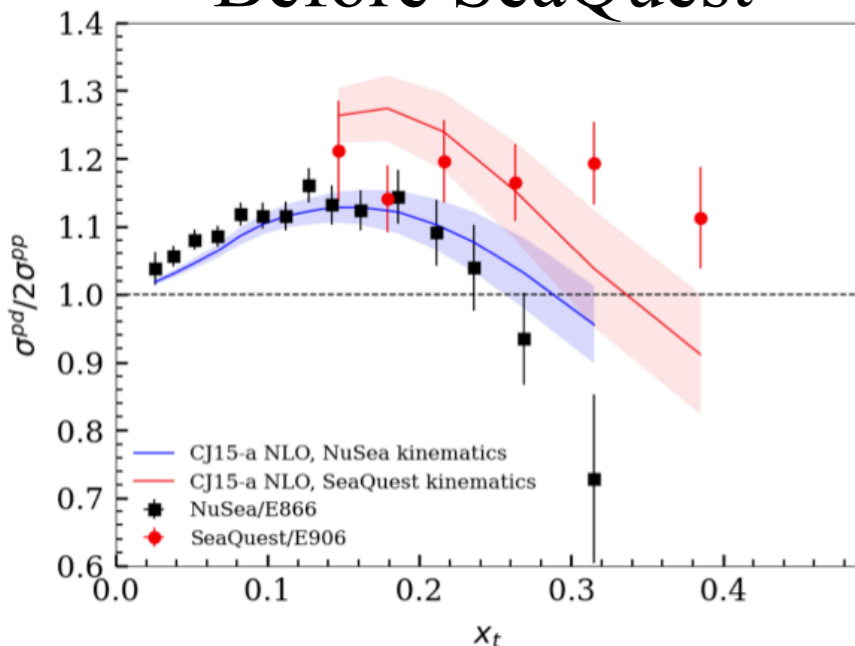
Recently the SeaQuest (E906) experiment at Fermilab has released data for the ratio of cross sections  $\sigma_{pd}/\sigma_{pp}$  [*Nature* 590 (2021) 7847, 561-565].

This ratio is sensitive to the ratio of sea quark PDFs:

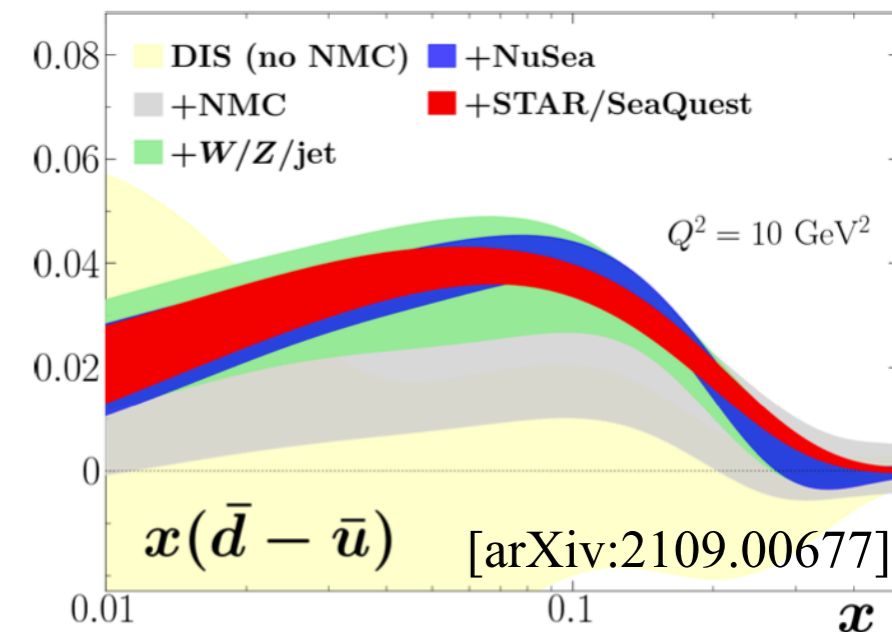
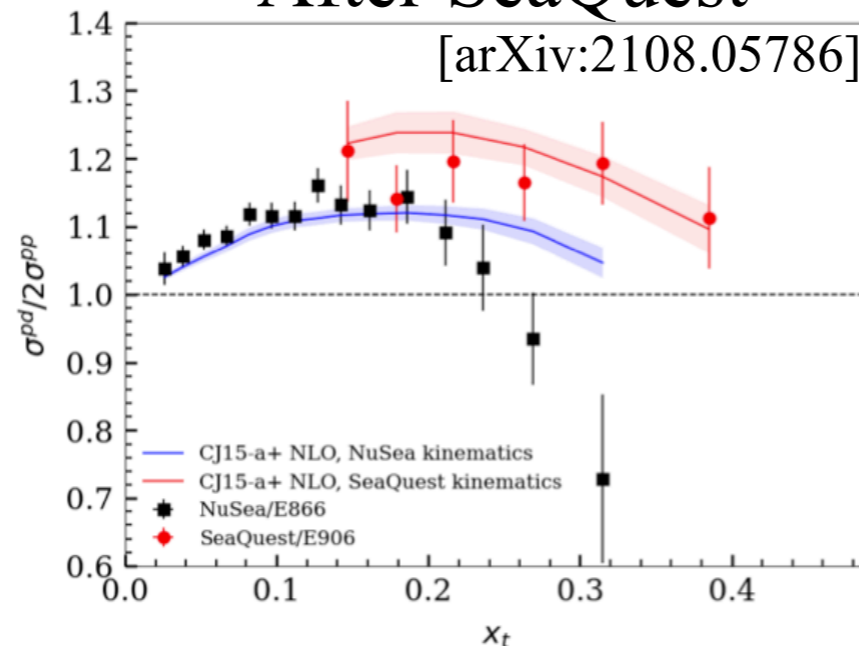
$$\frac{\sigma_{pd}}{\sigma_{pp}} \simeq 1 + \frac{\bar{d}(x)}{\bar{u}(x)}$$

Being a fixed-target experiment, **large values of  $x$**  are probed giving us access to the sea quark PDFs in a region that is presently **poorly known**.

Before SeaQuest



After SeaQuest



Significant impact on the  $\bar{u}$  and  $\bar{d}$  PDFs at large  $x$ .

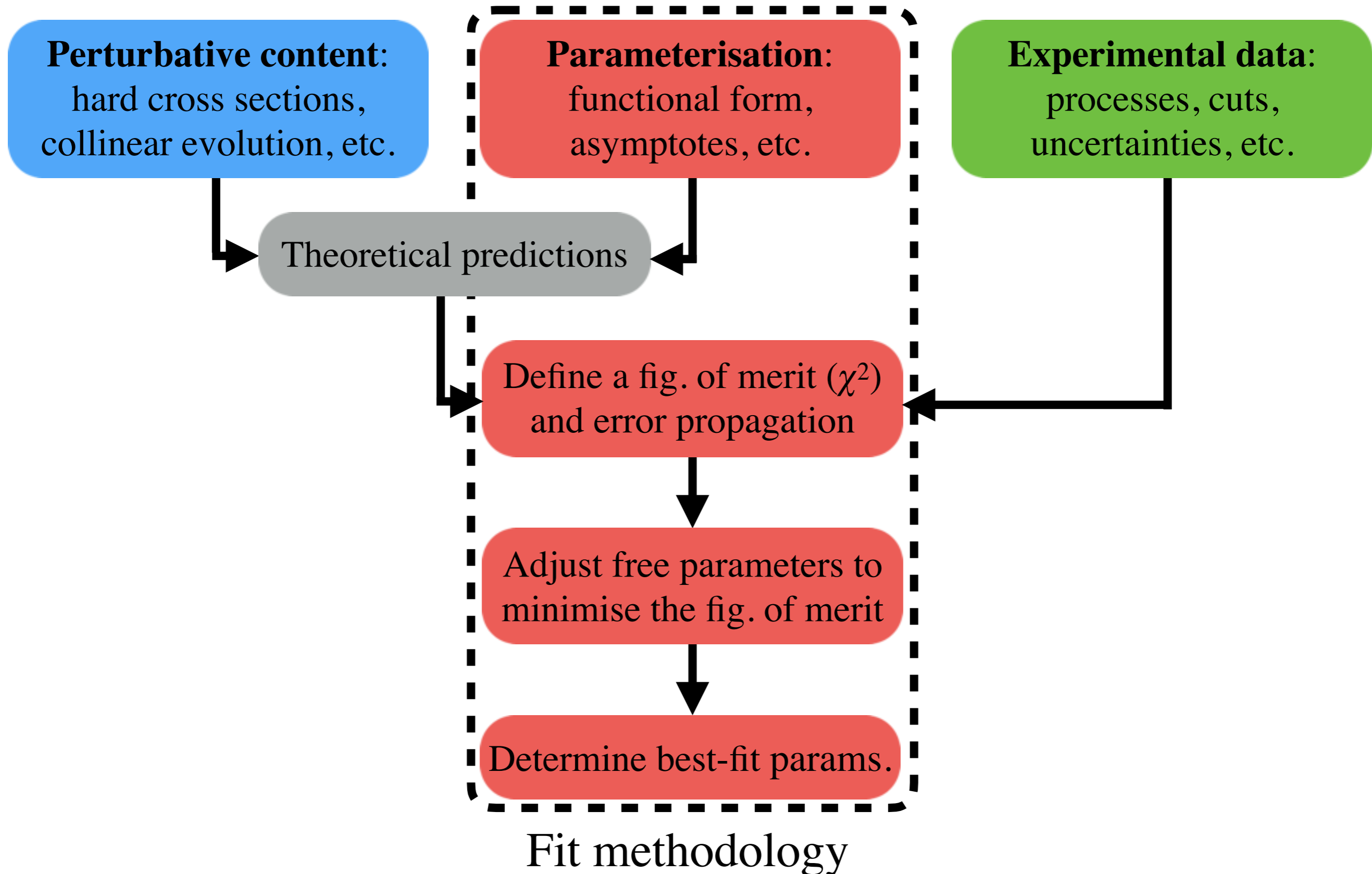
Currently unresolved tension with the older NuSea (E866) data.

# Perturbative content

## *Hard cross sections: fast interfaces*

- Very often, a direct “on-line” computation of physical observables is not a viable option when fitting PDFs:
  - computing a single distribution may take days and this needs to be iterated a large number (thousands) of times during a fit.
- Fast interfaces have been devised to overcome this problem.
- As of today, different interfaces exist:
  - APPLgrid [Carli et al., \[Eur.Phys.J.C 66 \(2010\) 503-524\]](#),
  - FastNLO [FastNLO Collaboration \[DIS 2012, 217-221\]](#),
  - APFELgrid [Bertone, Carrazza, Hartland \[Comput.Phys.Commun. 212 \(2017\) 205-209\]](#),
  - PineAPPL [Carrazza, Nocera, Schwan, Zaro \[JHEP 12 \(2020\) 108\]](#),
  - aMCfast [Bertone, Frederix, Frixione, Rojo, Sutton \[JHEP 08 \(2014\) 166\]](#).
- They are all based on the same idea: interpolating PDFs.

# The general strategy



# Fit methodologies

*Parameterisation: the “standard” approach*

- Distributions are parametrised by means of the functional form:

$$f_i(x) = A_i x^{\alpha_i} (1 - x)^{\beta_i} P_i(x)$$

with:

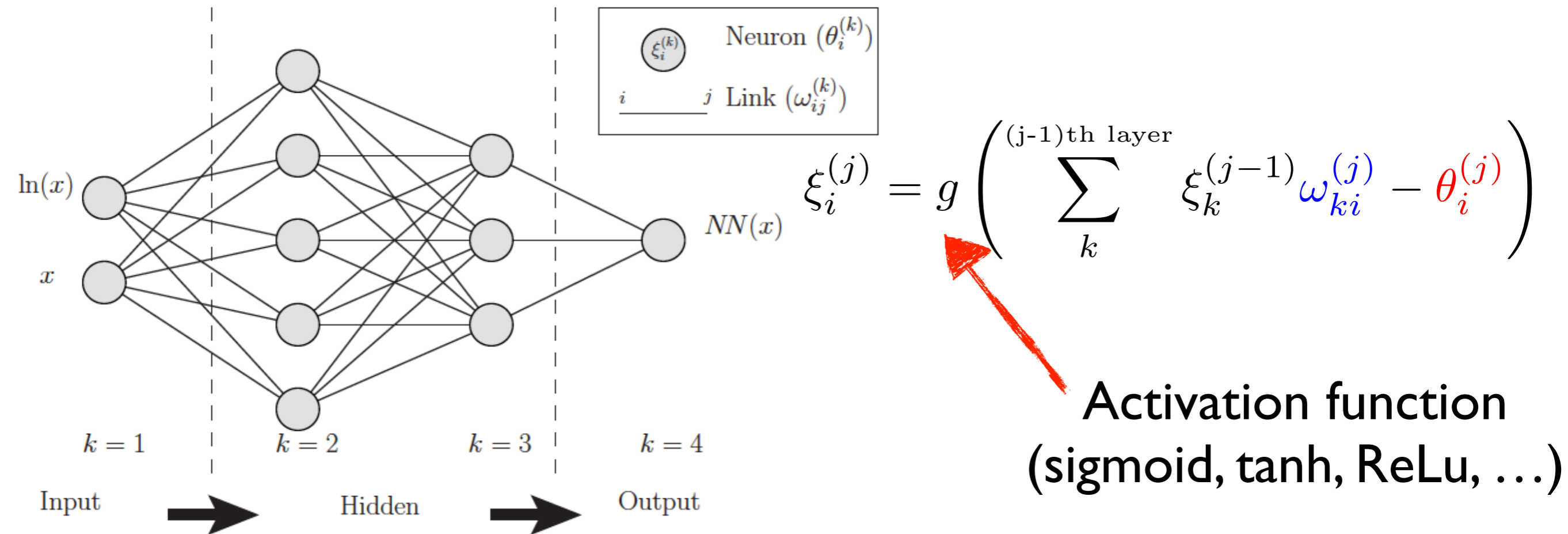
$$P_i(x) = \begin{cases} 1 \\ 1 + \gamma_i x \\ 1 + \gamma_i x + \delta_i \sqrt{x} \\ \dots \end{cases}$$

- **O(3-5) free parameters** for each distribution.
- **Asymptotic behaviour** defined by the exponents  $\alpha_i$  and  $\beta_i$ .
- Typically easy to transform analytically in **Mellin space**.
- **Easy to handle** in a fit thanks to its simplicity.
- Potential **source of bias**.

# Fit methodologies

## Parameterisation: neural networks

- Distributions are parametrised in terms of artificial NNs:



- Each NN has a **large number free parameters**.
- NNs are usually augmented with constraints in the extrap. regions:

$$f_i(x) = A_i x^{\alpha_i} (1 - x)^{\beta_i} NN_i(x) \quad \text{or} \quad f_i(x) = NN_i(x) - NN_i(1)$$

- NNs are **flexible** and thus limit biases but are **harder to handle**



# Fit methodologies

## *Figure of merit: the $\chi^2$ definition*

- A crucial aspect in the determination of PDFs is the definition of the **figure of merit** to be minimised/maximised.

- A popular choice is the  $\chi^2$  but **many variants** are possible:

- No correlation, no normalisation unc.: 
$$\chi^2 = \sum_{i=1}^{N_{\text{dat}}} \frac{(T_i - D_i)^2}{\sigma_i^2}$$

- No correlation, with normalisation unc.: 
$$\chi^2 = \sum_{j=1}^{N_{\text{exp}}} \left[ \left( \frac{1 - \mathcal{N}_j}{\delta \mathcal{N}_j} \right)^2 + \sum_{i=1}^{N_{\text{dat}}^j} \frac{(\mathcal{N}_j T_i - D_i)^2}{\sigma_i^2} \right]$$

- Nuisance parameters: 
$$\chi^2 = \sum_i \frac{\left[ T_i \left( 1 - \sum_j \gamma_j^i b_j \right) - D_i \right]^2}{\delta_{i,\text{unc}}^2 T_i^2 + \delta_{i,\text{stat}}^2 D_i T_i} + \sum_j b_j^2$$

- Covariance matrix: 
$$\chi^2 = \sum_{ij} (T_i - D_i) V_{ij}^{-1} (T_j - D_j)$$

- Due to the **D'Agostini bias**, a sound treatment of normalisation uncertainties requires particular care (*e.g.* the  $t_0$  prescription).

# Fit methodologies

## *D'Agostini bias*

🍏 A set of **two** experimental data points  $\mathbf{x}_i$  (with  $i = 1, 2$ ) with their own **uncorrelated** uncertainties  $\sigma_i$  measuring the **same** quantity.

Therefore, they can be fitted with a **single constant**  $\mu$ .

🍏 Two cases considered:

1. the **offset** case: a fully correlated (additive) uncertainty  $\sigma_c$  is included.

Notice that  $\sigma_c$  is the same for both  $\mathbf{x}_1$  and  $\mathbf{x}_2$ . The covariance matrix reads:  $V_{ij} = \delta_{ij}\sigma_i^2 + \sigma_c^2$ .

2. the **normalisation** case: a fully correlated uncertainty whose absolute value is proportional to  $\mathbf{x}_i$  through the constant factor  $\delta_f$ . (normalisation uncertainty). The covariance matrix reads:

$$V_{ij} = \delta_{ij}\sigma_i^2 + \delta_f^2 x_i x_j.$$

🍏 The  $\chi^2$ , defined as: 
$$\chi^2 = \sum_{i,j=1}^2 (\mu - x_i) V_{ij}^{-1} (\mu - x_j)$$

can be minimised analytically requiring 
$$\left. \frac{d\chi^2}{d\mu} \right|_{\mu=\bar{\mu}} = 0$$

# Fit methodologies

## *D'Agostini bias*

- 🍏 In case 1) (offset) the best-fit value is:

$$\bar{\mu} = \frac{\sigma_2^2 x_1 + \sigma_1^2 x_2}{\sigma_1^2 + \sigma_2^2} = \frac{\frac{x_1}{\sigma_1^2} + \frac{x_2}{\sigma_2^2}}{\frac{1}{\sigma_1^2} + \frac{1}{\sigma_2^2}}$$

- 🍏 As expected,  $\bar{\mu}$  is a weighted average of the measurements where the weights are the inverse of the uncorrelated uncertainties.
- 🍏 In case 2) (normalisation) the best-fit value is:

$$\bar{\mu} = \frac{\sigma_2^2 x_1 + \sigma_1^2 x_2}{\sigma_1^2 + \sigma_2^2 + (\delta_f x_1 - \delta_f x_2)^2} = \frac{\frac{x_1}{\sigma_1^2} + \frac{x_2}{\sigma_2^2}}{\frac{1}{\sigma_1^2} + \frac{1}{\sigma_2^2} + \left( \frac{\delta_f x_1 - \delta_f x_2}{\sigma_1 \sigma_2} \right)^2}$$

- 🍏 The term in the red box is the origin of the D'Agostini bias:
  - 🍏 if the normalisation uncertainty is large, the best-fit value  $\bar{\mu}$  is systematically below both measurements  $x_1$  and  $x_2$ .

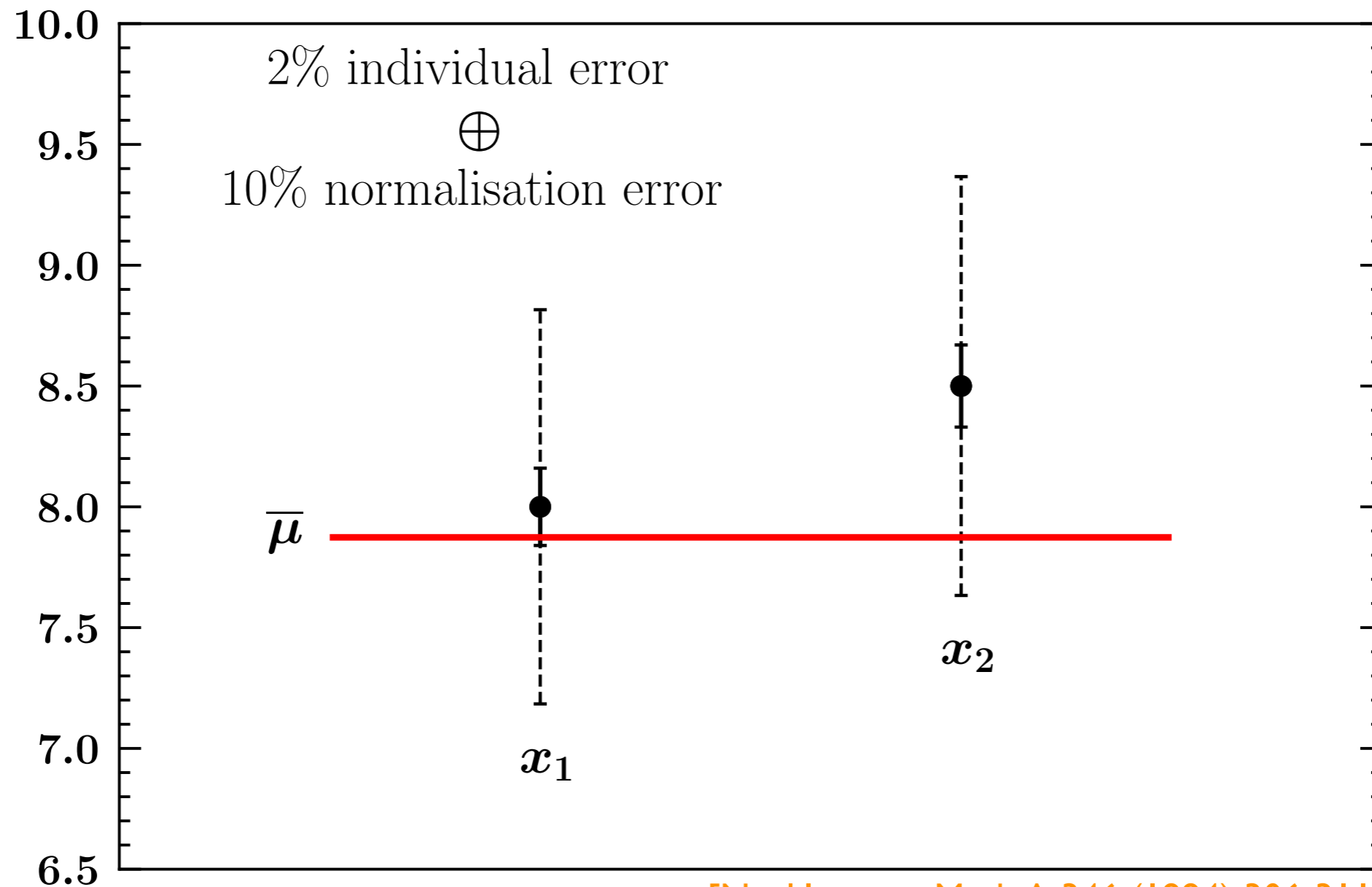
# Fit methodologies

## *D'Agostini bias*

🍏 Let us take the following numerical example:

$x_1 = 8.0 \pm 2\%$ ,  $x_2 = 8.5 \pm 2\%$ , 10% normalisation uncertainty

$$\bar{\mu} = 7.87$$



# Fit methodologies

## *The $t_0$ method*

- 🍏 The  $t_0$  prescription prescribes to replace the normalisation uncertainties  $\delta_f x_i$  with  $\delta_f t_0$  where  $t_0$  is a “**guess**” for  $\mu$ :

$$V_{ij} = \delta_{ij} \sigma_i^2 + \delta_f^2 t_0^2$$

- 🍏 This just modifies the normalisation uncertainties in such a way that they become equal in absolute value (like in the offset case) and thus solving the problem.

$$\bar{\mu}_0 = \frac{\frac{x_1}{\sigma_1^2} + \frac{x_2}{\sigma_2^2}}{\frac{1}{\sigma_1^2} + \frac{1}{\sigma_2^2}}$$

- 🍏 In this simple case the value of  $t_0$  is irrelevant in that it drops.
- 🍏 In more complicated cases (more data with a more complicated physical law), the value(s) of the  $t_0$  are iterated until convergence is reached.

# Fit methodologies

## *Error propagation*

- A faithful determination implies a solid estimate of the **uncertainty** on PDFs propagating from the **experimental** dataset.

1. **Hessian** method: the  $\chi^2$  is **expanded** around its minimum  $\mathbf{a}_0$ :

$$\chi^2(\{\mathbf{a}\}) \simeq \chi^2(\{\mathbf{a}_0\}) + \underbrace{\frac{1}{2} \frac{\partial^2 \chi^2}{\partial a_i \partial a_j} \Big|_{\mathbf{a}_0}}_{H_{ij}} (a_i - a_{0i})(a_j - a_{0j})$$

The Hessian matrix  $H_{ij}$  is **diagonalised** and an uncertainty along each eigenvector is defined as  $\Delta\chi^2 = 1$  (often a larger **tolerance** is introduced).

2. **Monte Carlo** sampling: artificial **replicas** of the dataset generated as:

$$D_i^{(k)} = D_i + r_i^{(k)} \sigma_i, \quad \begin{array}{l} k = 1, \dots, N_{\text{rep}} \\ i = 1, \dots, N_{\text{dat}} \end{array}$$

$r_i^{(k)}$  is a *normally distributed* and *univariate* random number. A fit is performed to each replica to produce  $N_{\text{rep}}$  sets of distributions  $\{f_k\}$ , such that:

$$\langle \mathcal{O} \rangle = \frac{1}{N_{\text{rep}}} \sum_{k=1}^{N_{\text{rep}}} \mathcal{O}[f_k] \quad \text{and} \quad \sigma_{\mathcal{O}} = \sqrt{\langle \mathcal{O}^2 \rangle - \langle \mathcal{O} \rangle^2}$$

# Fit methodologies

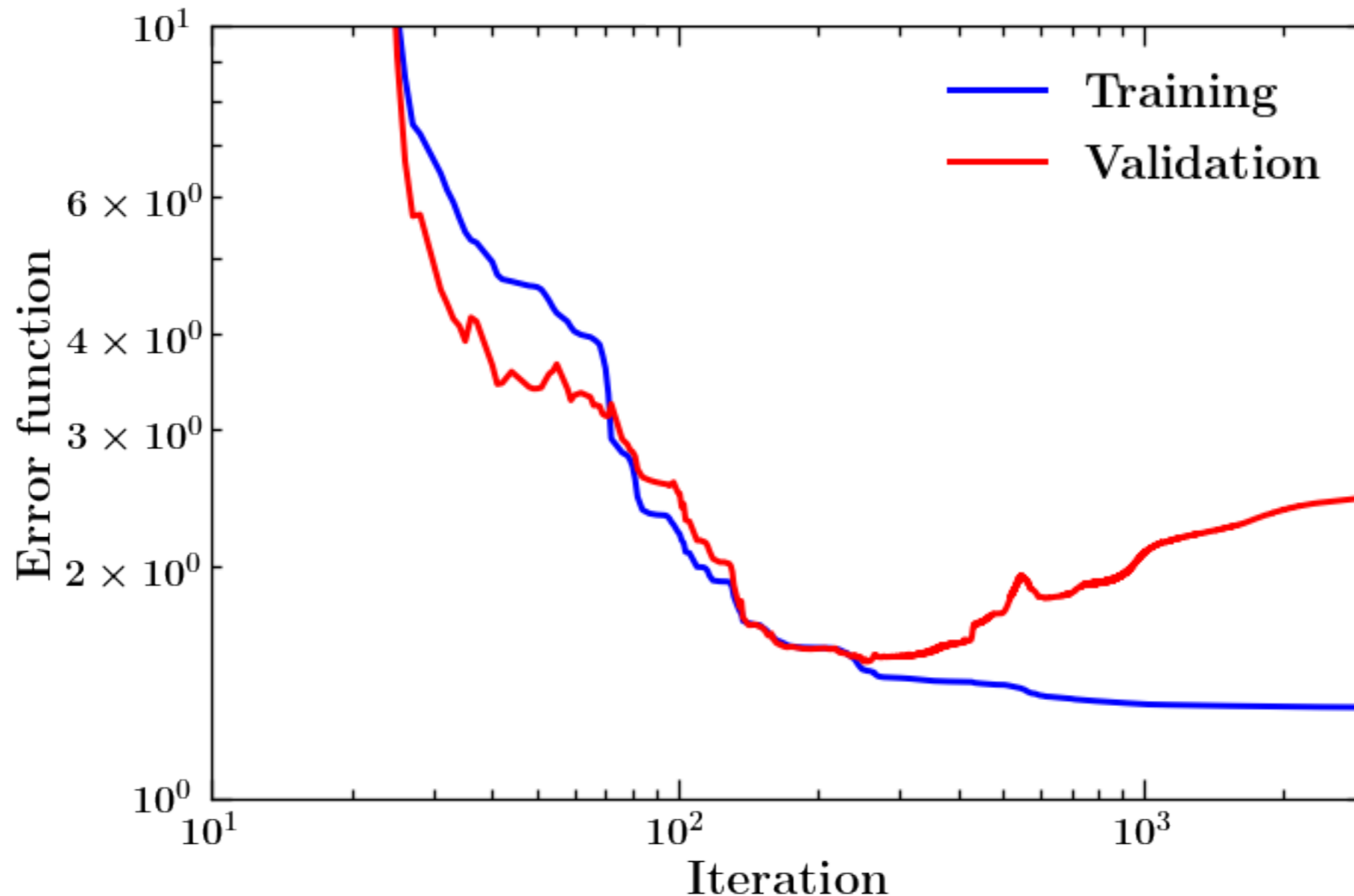
## *Minimisation and stopping*

- Simple parameterisations (**O(20) free parameters**) are usually fitted using **MINUIT** (or similar):
  - the absolute minimum of the  $\chi^2$  is found *deterministically* by computing (numerically or analytically) the first derivative and moving **downhill**.
- A NN parameterisation (**O(200) free parameters**) generates a complex parameter space impossible to explore with MINUIT:
  - a **genetic algorithm** is often used to explore the parameter space,
  - this avoids getting trapped into **local minima** of the  $\chi^2$ .
  - Algorithms inspired by **machine-learning** techniques are being explored,
  - **gradient-descent** based algorithms are recently also being used.
- The extreme flexibility of NNs may cause **overfitting**, *i.e.* statistical fluctuations of the data sample may be unwillingly fitted:
  - the **cross-validation** method allows one to overcome this problem.

# Fit methodologies

## *Cross validation*

- Split the dataset into **training** and **validation** subsets.
- Minimise the training  $\chi^2$  while monitoring the validation  $\chi^2$ .
- Stop the fit when the validation  $\chi^2$  reaches its absolute minimum.





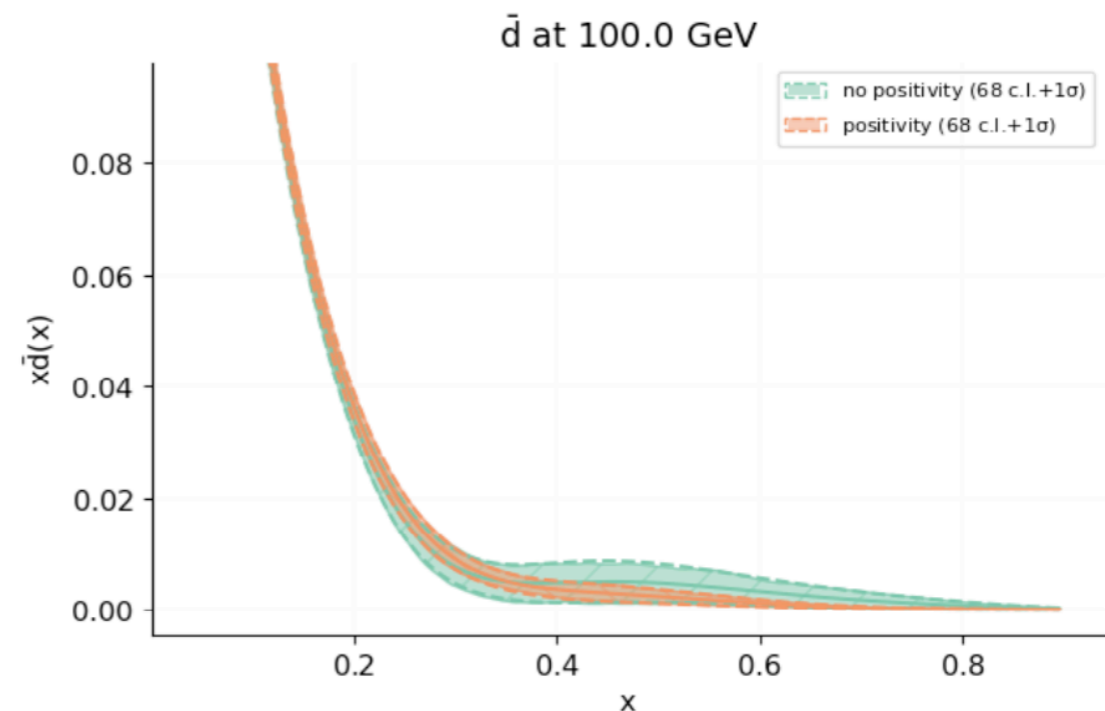
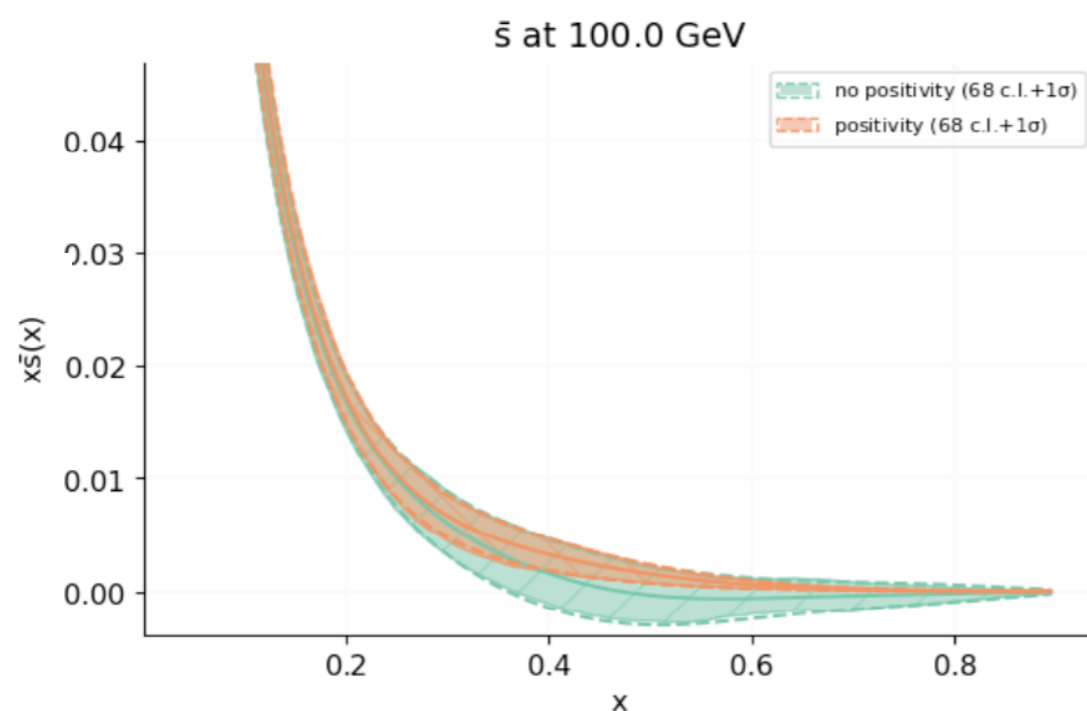
# Main PDF collaborations

## *Unpolarised proton PDFs*

- **CTEQ** collaboration:
  - standard parameterisation (**Bernstein** polynomials),
  - **Hessian** method (with dynamical tolerance) for error propagation.
- **NNPDF** collaboration:
  - neural network parameterisation (feed forward NN with preprocessing),
  - **Monte Carlo** method for error propagation.
- **MSHT** collaboration:
  - standard parameterisation (**Chebyshev** polynomials),
  - **Hessian** method (with dynamical tolerance) for error propagation.
- Other collaborations exist (e.g. ABMP, HERAPDF, CJ, JAM, etc.) but they are typically less inclusive in terms of data.

# Positivity and PDFs

- PDFs have to such to guarantee the **positivity of cross sections**:
  - cross sections can be interpreted as probabilities  $\implies$  must be **positive**.
- Possible ways to enforce positivity are:
  1. determine PDFs enforcing that a **specific set of observables** is positive:  
[NNPDF, *JHEP* 04 (2015) 040]
    - does not guarantee *all* possible observables to be positive.
    - allows PDFs to be negative (sometimes unwanted, *e.g.* MC generators).
  2. Assume **PDFs** to be **positive definite** from the start:  
[CTEQ, *Phys.Rev.D* 103 (2021) 1, 014013]
    - does it really guarantee positivity of the observables?
- Positivity has a strong impact of PDFs:



# Positivity and PDFs

- Recently it has been proposed that **PDFs** in  $\overline{\text{MS}}$  **are positive**:

[Candido, Forte, Hekhorn, *JHEP* 11 (2020) 129]

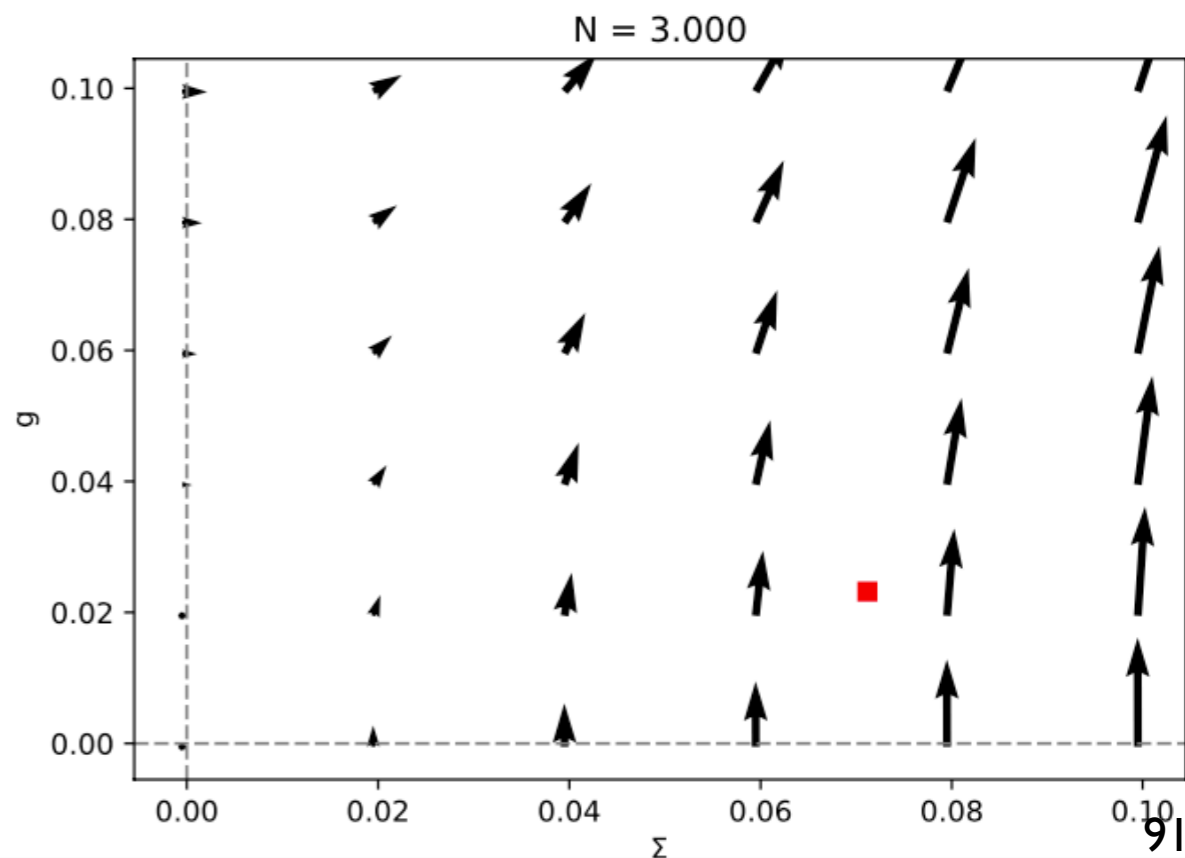
It is common lore that Parton Distribution Functions (PDFs) in the  $\overline{\text{MS}}$  factorization scheme can become negative beyond leading order due to the collinear subtraction which is needed in order to define partonic cross sections. We show that this is in fact not the case and next-to-leading order (NLO)  $\overline{\text{MS}}$  PDFs are actually positive in the perturbative regime. In order to prove this, we modify the subtraction prescription, and perform the collinear subtraction in such a way that partonic cross sections remain positive. This defines a **factorization scheme in which PDFs are positive**. We then show that **positivity of the PDFs is preserved when transforming from this scheme to  $\overline{\text{MS}}$** , provided only the strong coupling is in the perturbative regime, such that the NLO scheme change is smaller than the LO term.

- Define an *ad hoc* factorisation scheme (for DIS) in which PDFs are positive (POS scheme).
- Find the transformation that gives  $\overline{\text{MS}}$  PDFs in terms of the POS ones:

$$f^{\overline{\text{MS}}}(Q^2) = \left[ \mathbb{I} + \frac{\alpha_s}{2\pi} K^{\text{POS}} \otimes \right]^{-1} f^{\text{POS}}(Q^2)$$

- The authors find that this transformation tends to make PDFs more positive.
- If POS PDFs are positive (by definition)  $\implies$   $\overline{\text{MS}}$  are to be even more positive.

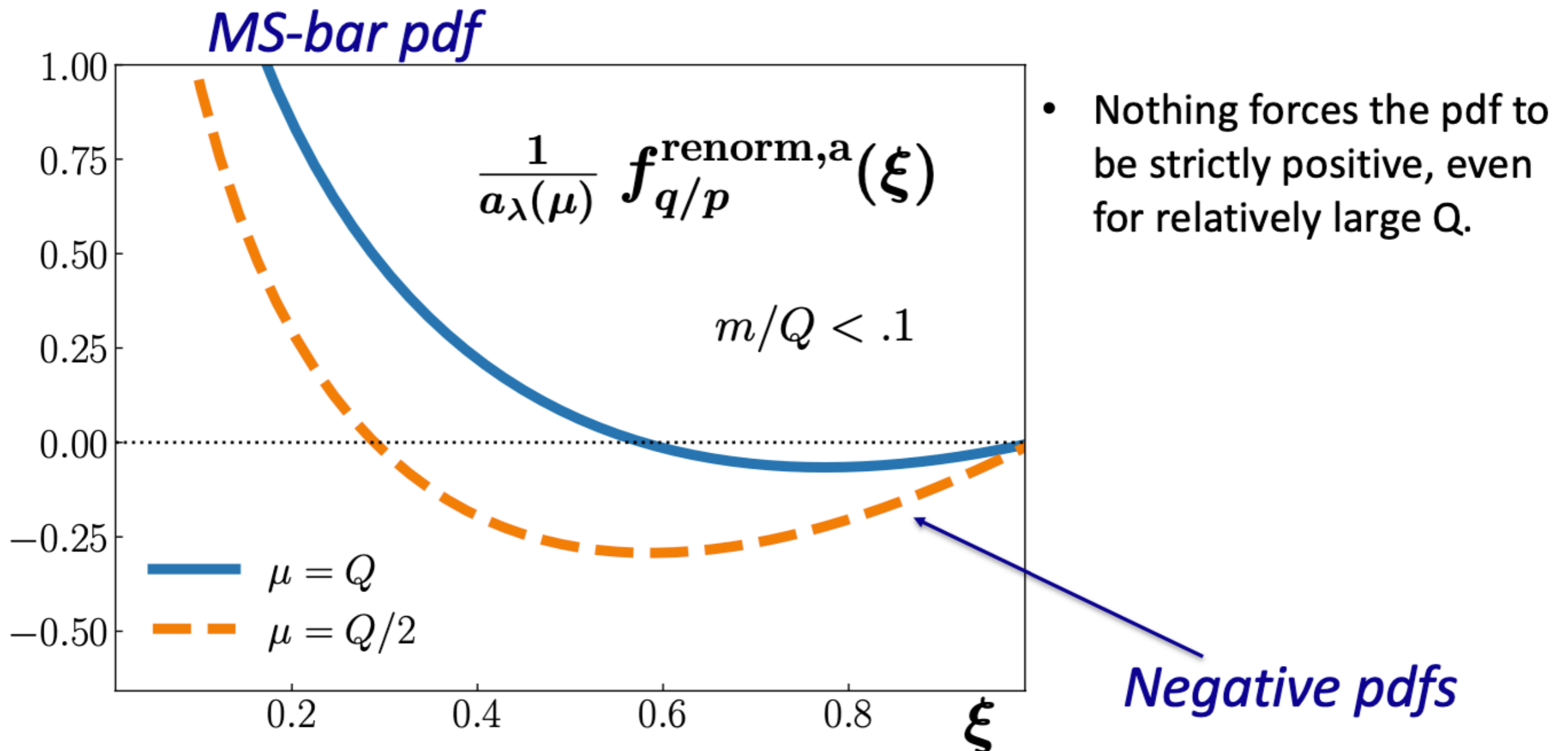
POS scheme with NNPDF31\_nlo\_as\_0118 at  $Q^2 = 100.0 \text{ GeV}^2$



# Positivity and PDFs

- More recently though Collins, Rogers, and Sato have found an opposite result:
  - by direct computation of the PDF using its operator definition focusing on the removal of the **UV divergence**.

[Rogers, talk at QCD Evolution 2021]



- The question remains open: are  $\overline{\text{MS}}$  PDFs allowed to go negative?

# Parton luminosities

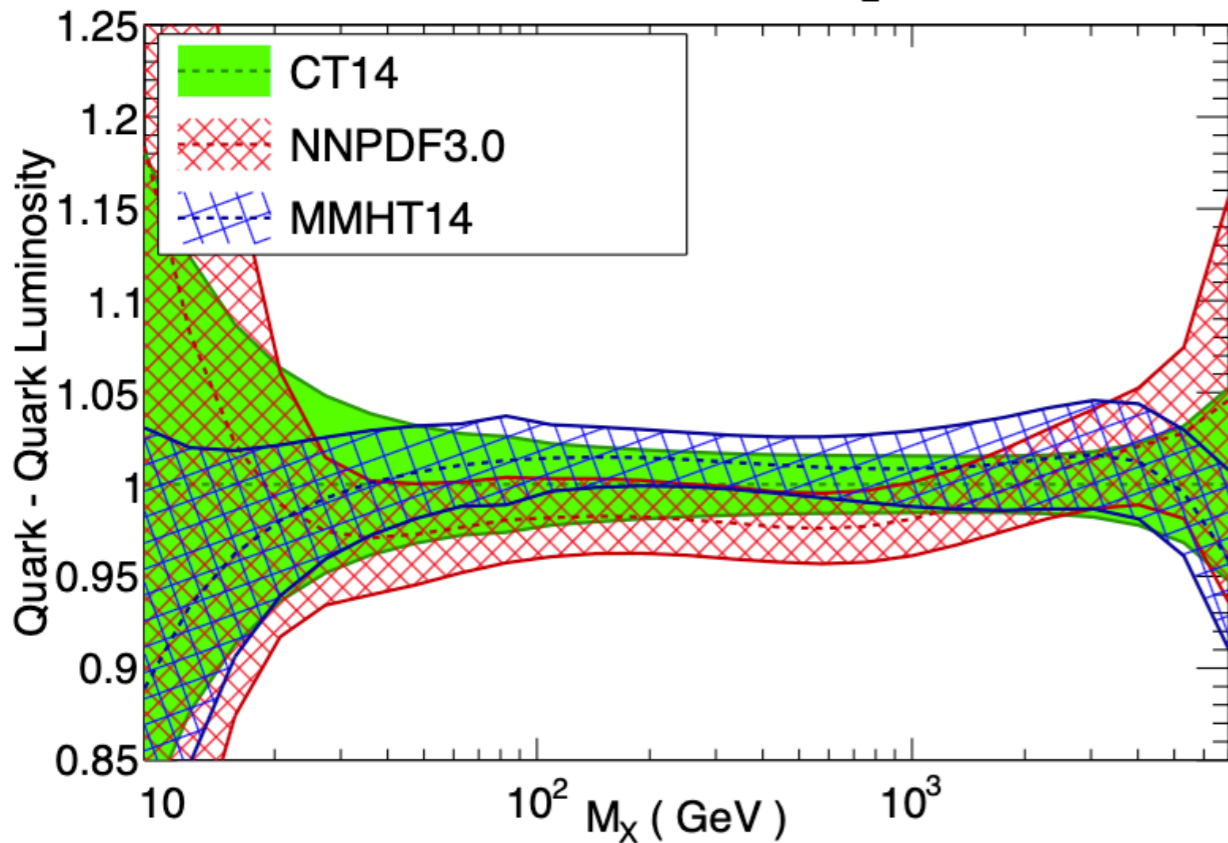
- Interesting quantities are the so-called **parton luminosities**:

$$\mathcal{L}_{ij} = \frac{1}{s} \int_{M_X^2/s}^1 \frac{dy}{y} f_i(y, M_X) f_j \left( \frac{M_X^2}{ys}, M_X \right)$$

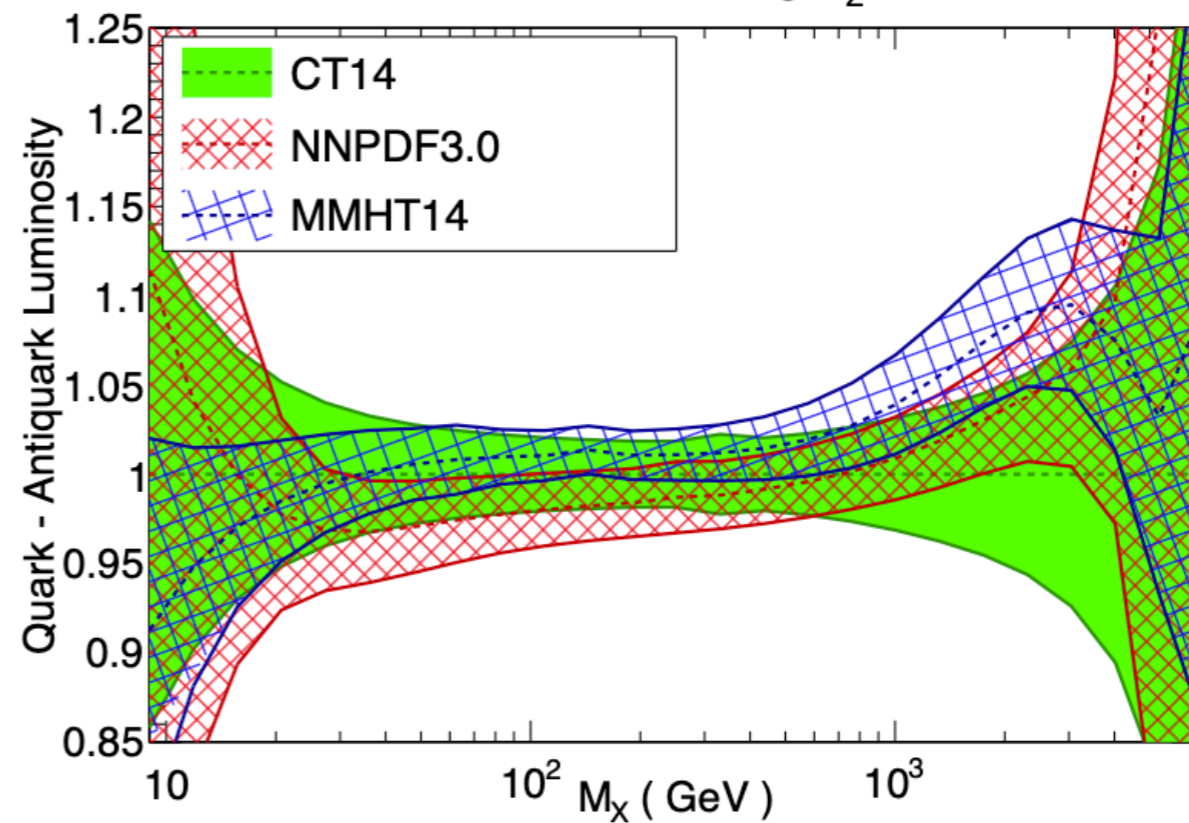
- Relevant for invariant mass distributions of the final state in  $pp$  collision processes, *e.g.*:
  - **Drell-Yan** mostly sensitive to  $\mathcal{L}_{q\bar{q}}$ ,
  - **Higgs** and  $t\bar{t}$  production in gluon fusion mostly sensitive to  $\mathcal{L}_{gg}$ ,
  - **$W$  + charm** mostly sensitive to  $\mathcal{L}_{sg}$ ,
  - ...

# A snapshot back in 2015

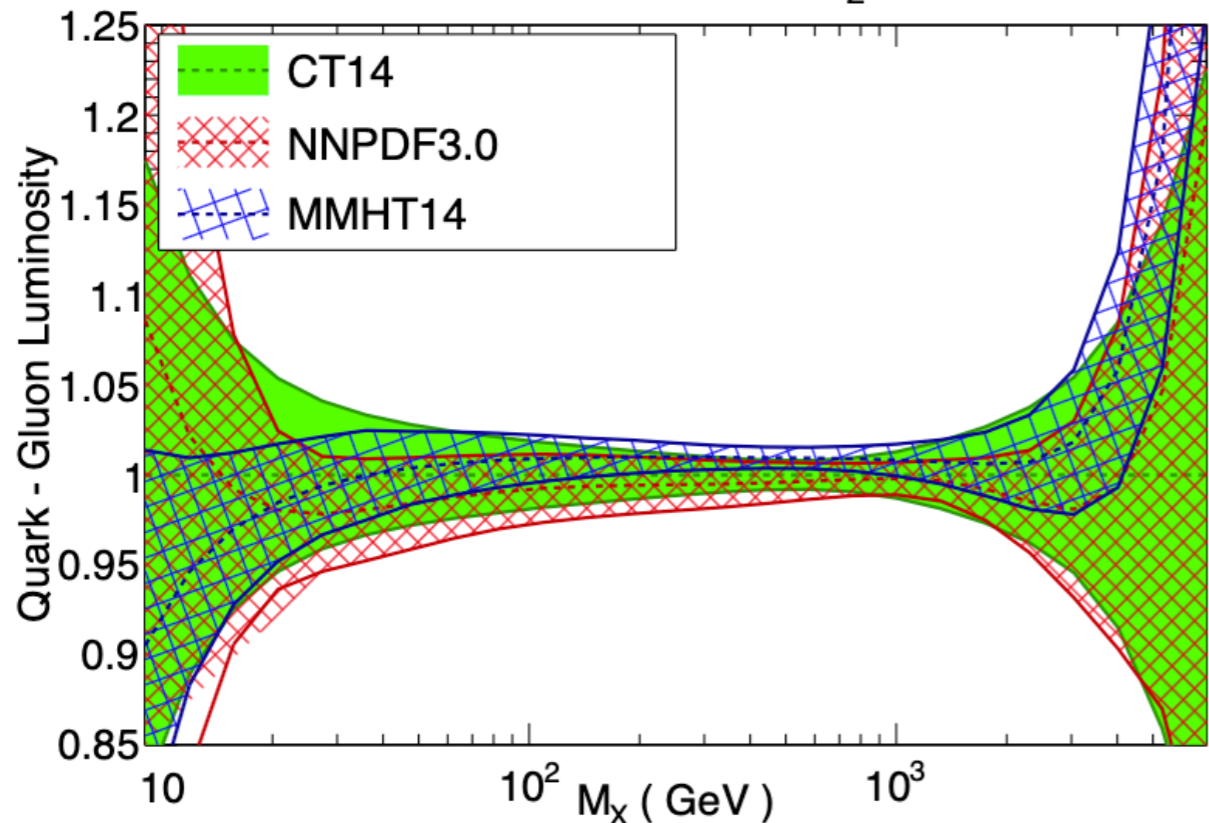
LHC 13 TeV, NNLO,  $\alpha_s(M_Z)=0.118$



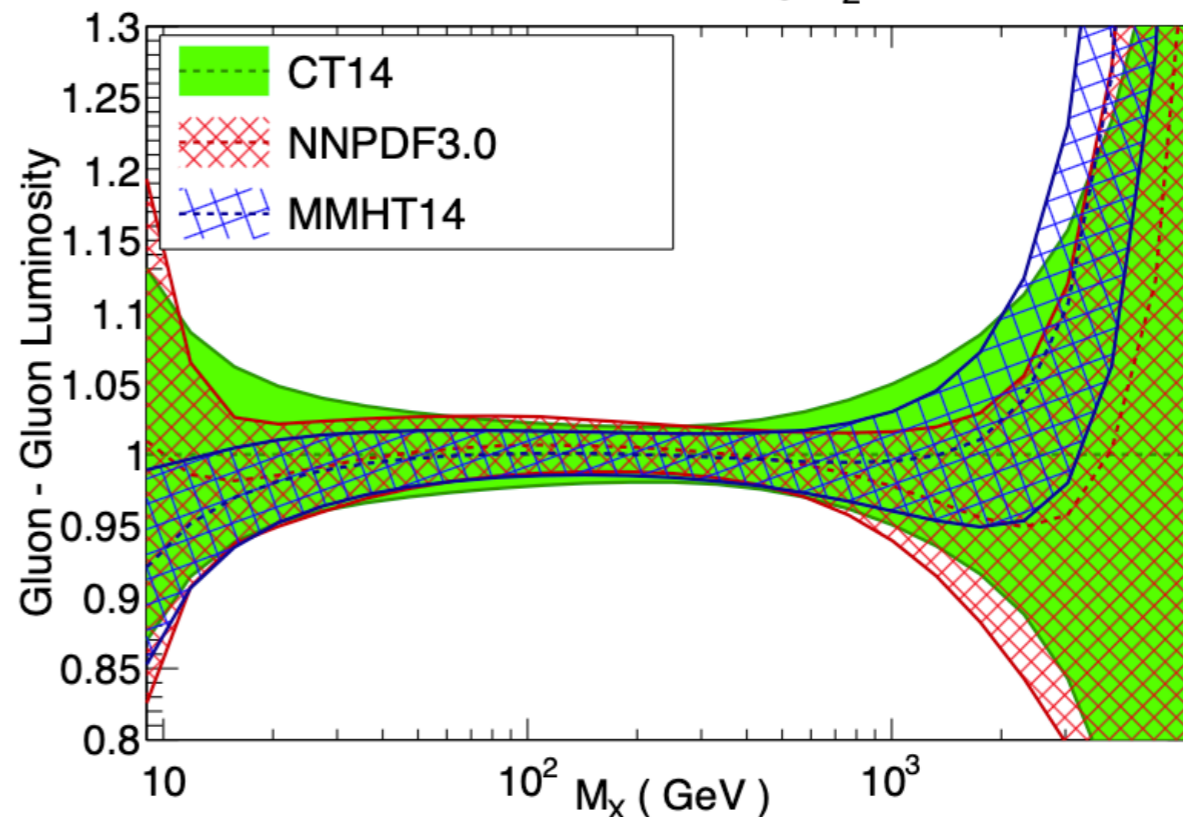
LHC 13 TeV, NNLO,  $\alpha_s(M_Z)=0.118$



LHC 13 TeV, NNLO,  $\alpha_s(M_Z)=0.118$

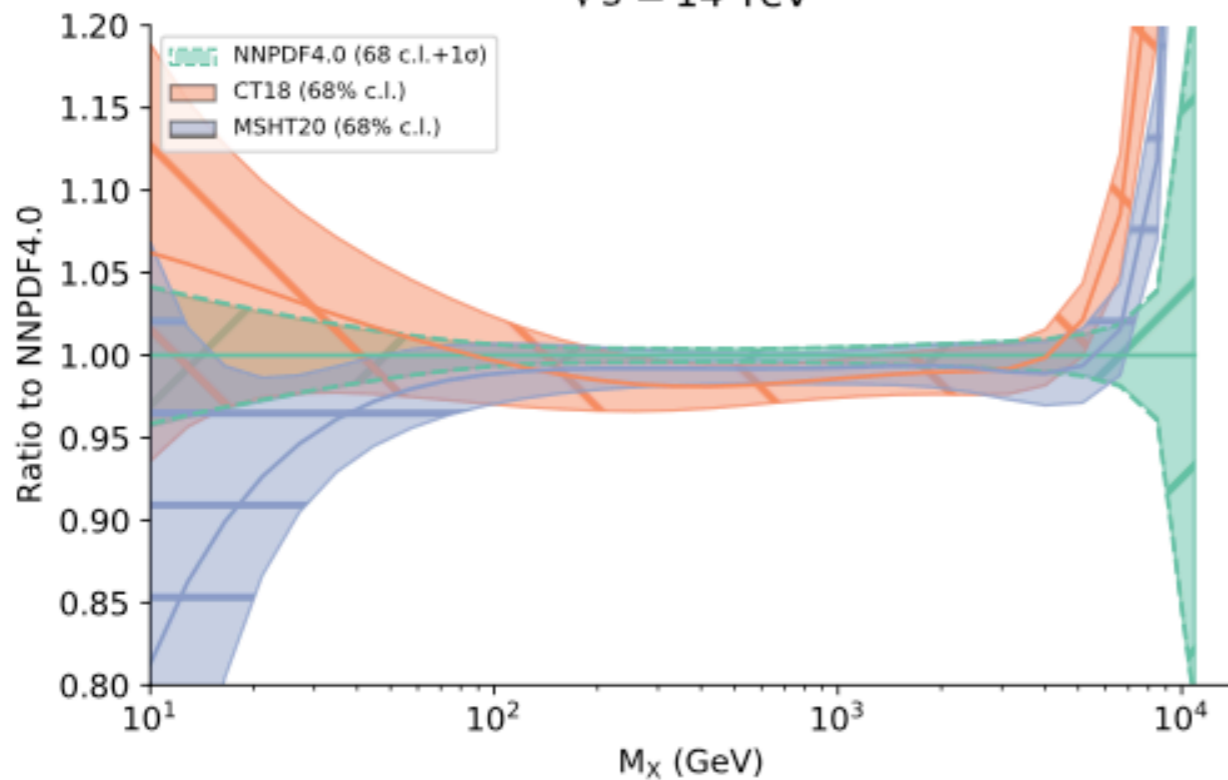


LHC 13 TeV, NNLO,  $\alpha_s(M_Z)=0.118$

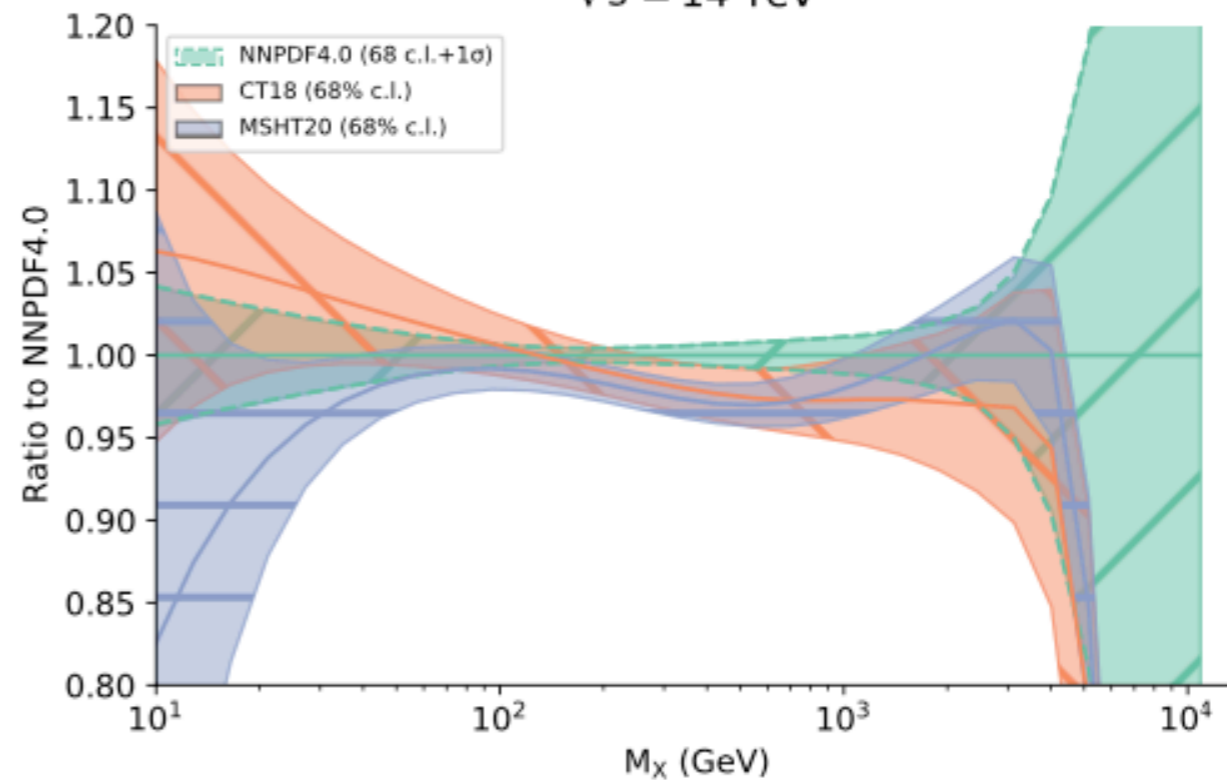


# A snapshot today

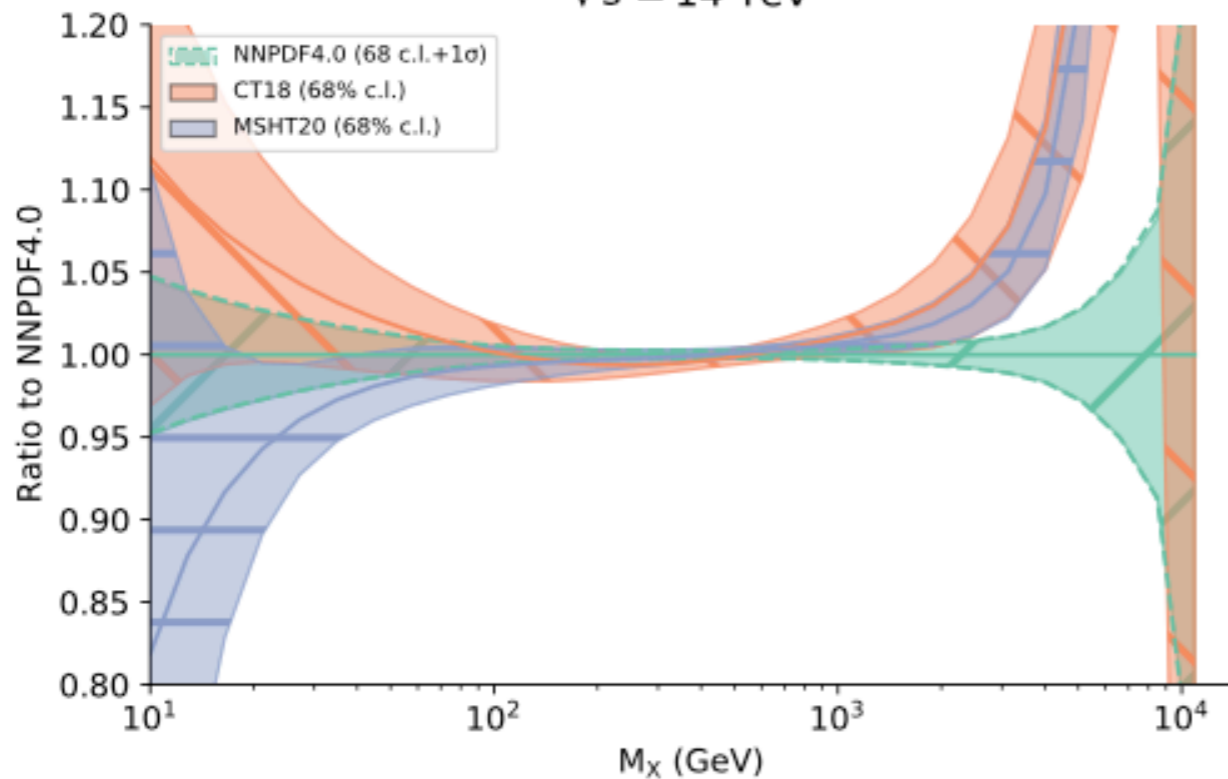
qq luminosity  
 $\sqrt{s} = 14$  TeV



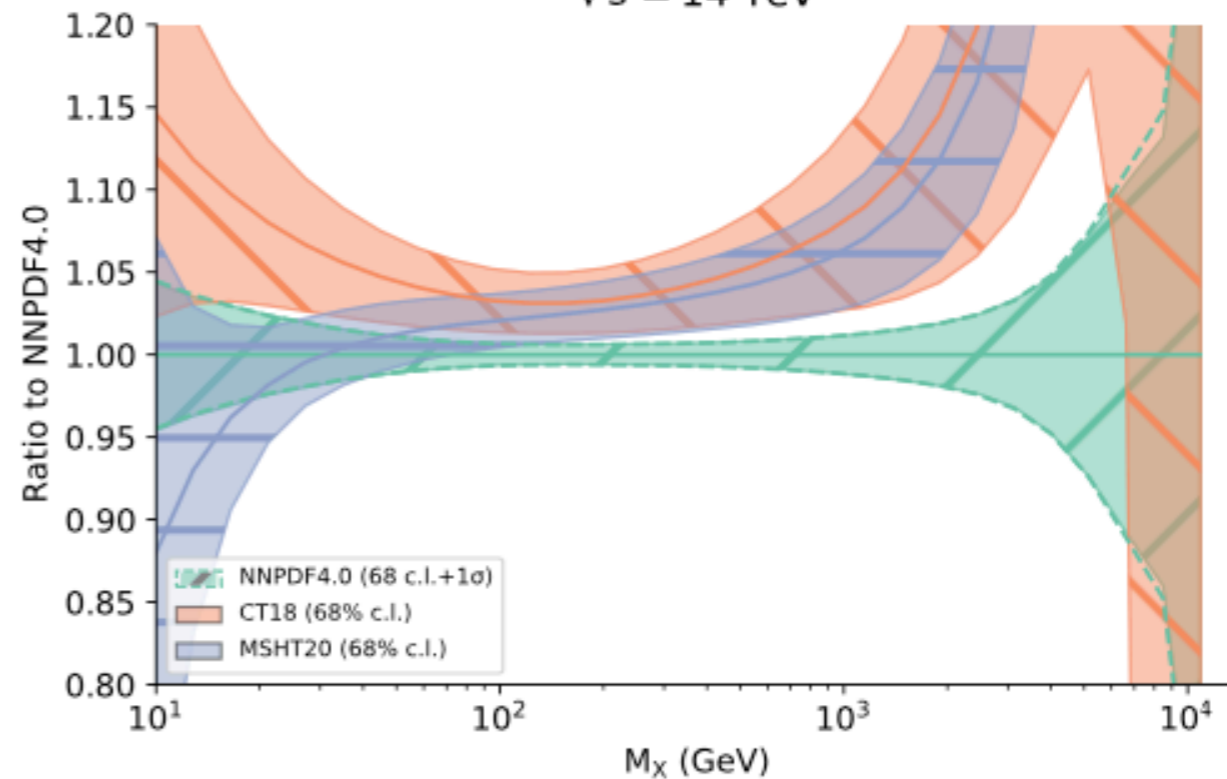
q $\bar{q}$  luminosity  
 $\sqrt{s} = 14$  TeV



gg luminosity  
 $\sqrt{s} = 14$  TeV



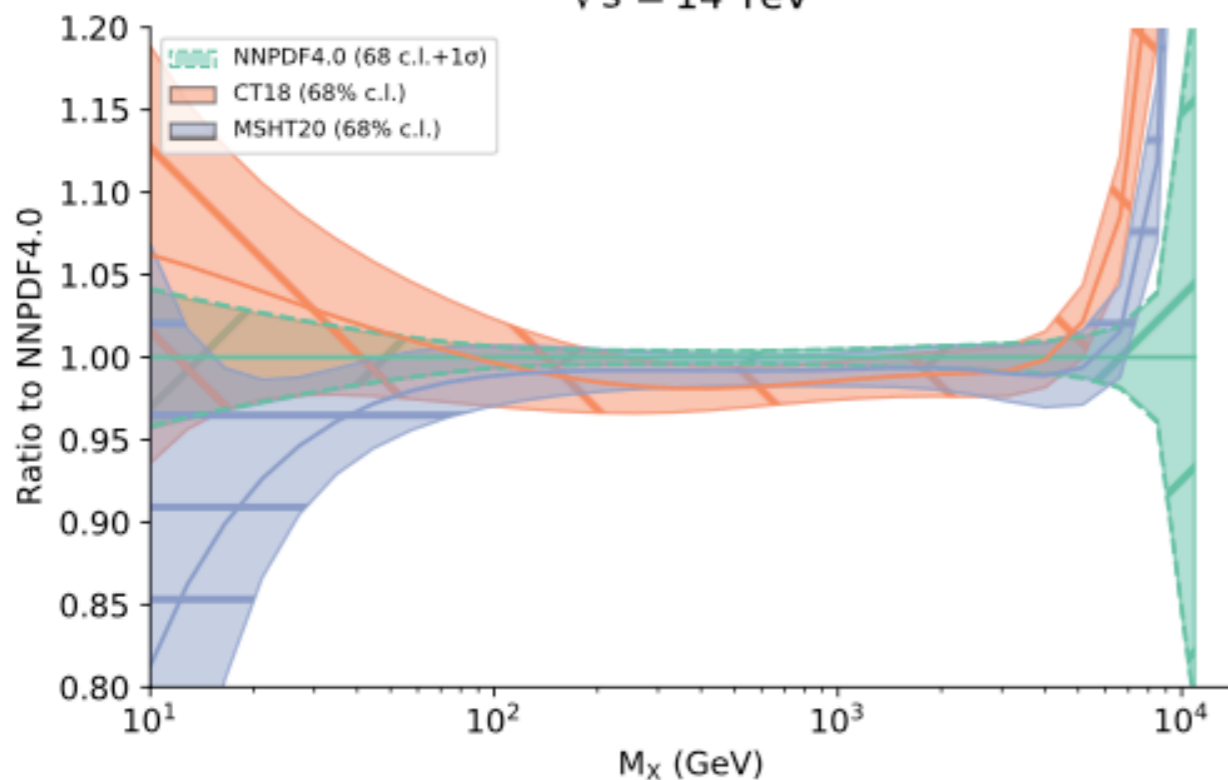
gg luminosity  
 $\sqrt{s} = 14$  TeV



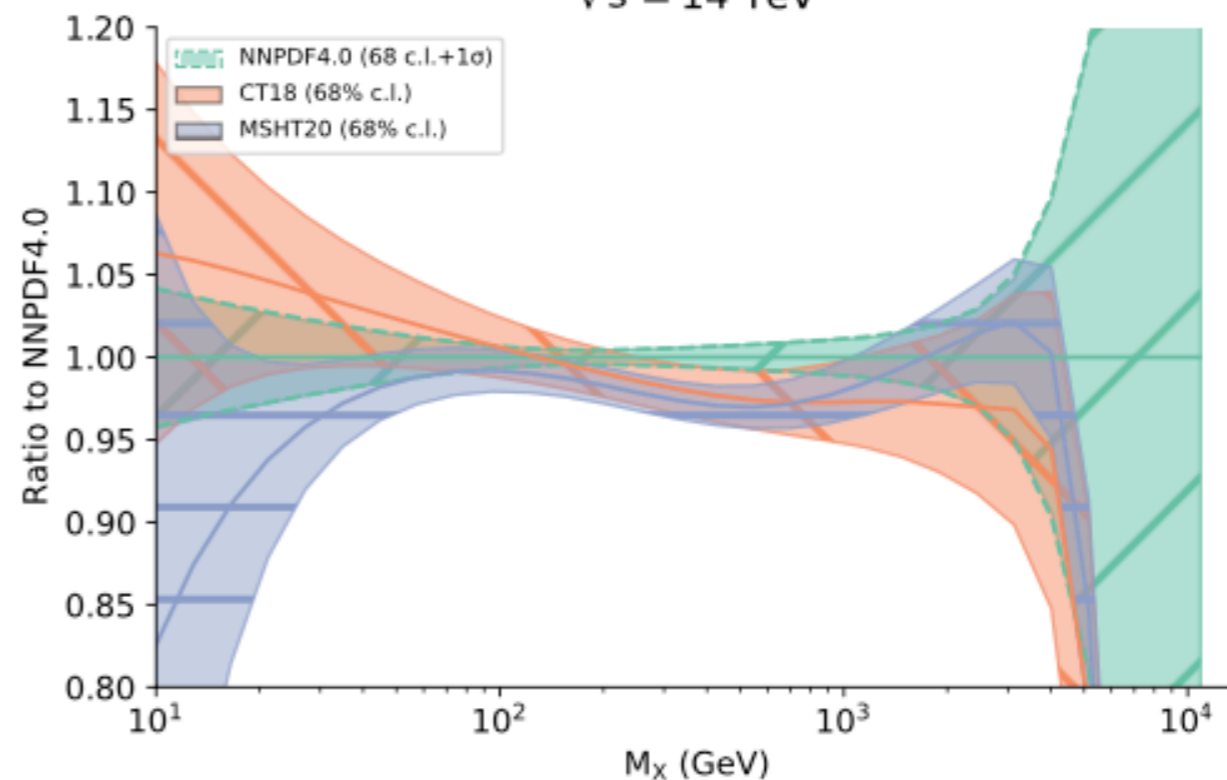
[E. Nocera's talk at DIS2021]

# A snapshot today

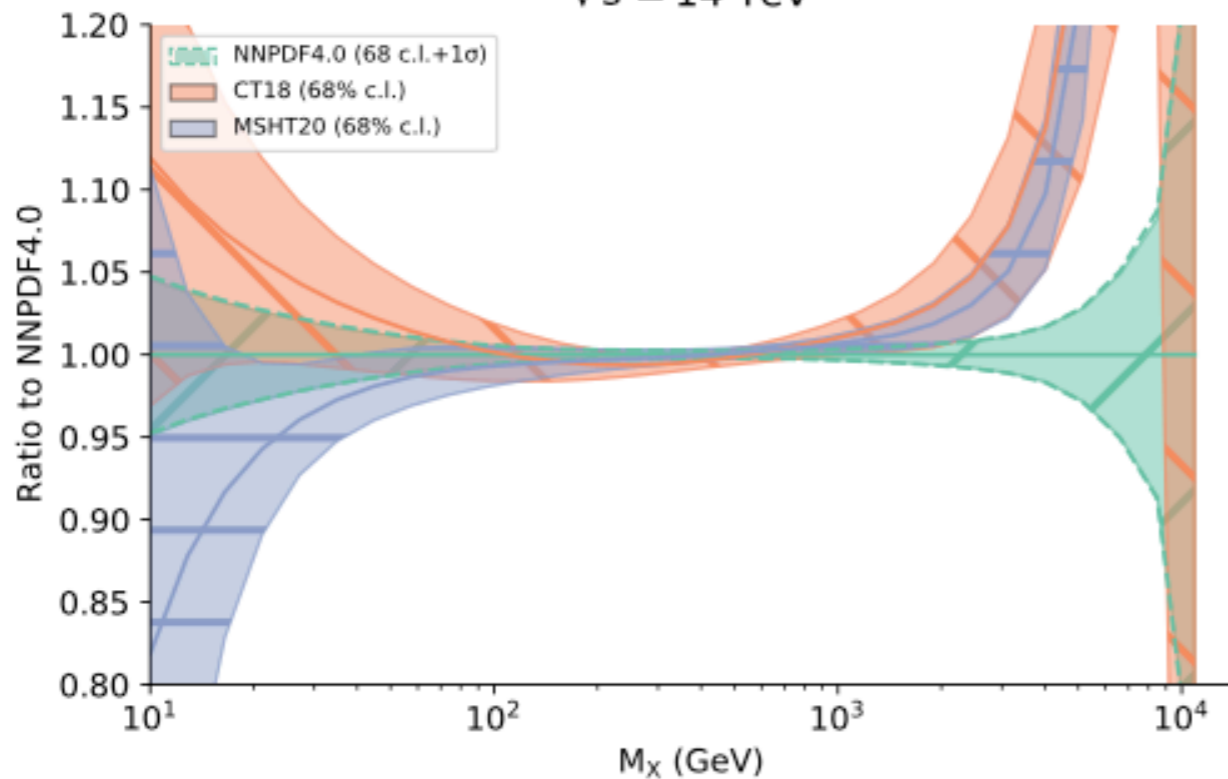
qq luminosity  
 $\sqrt{s} = 14$  TeV



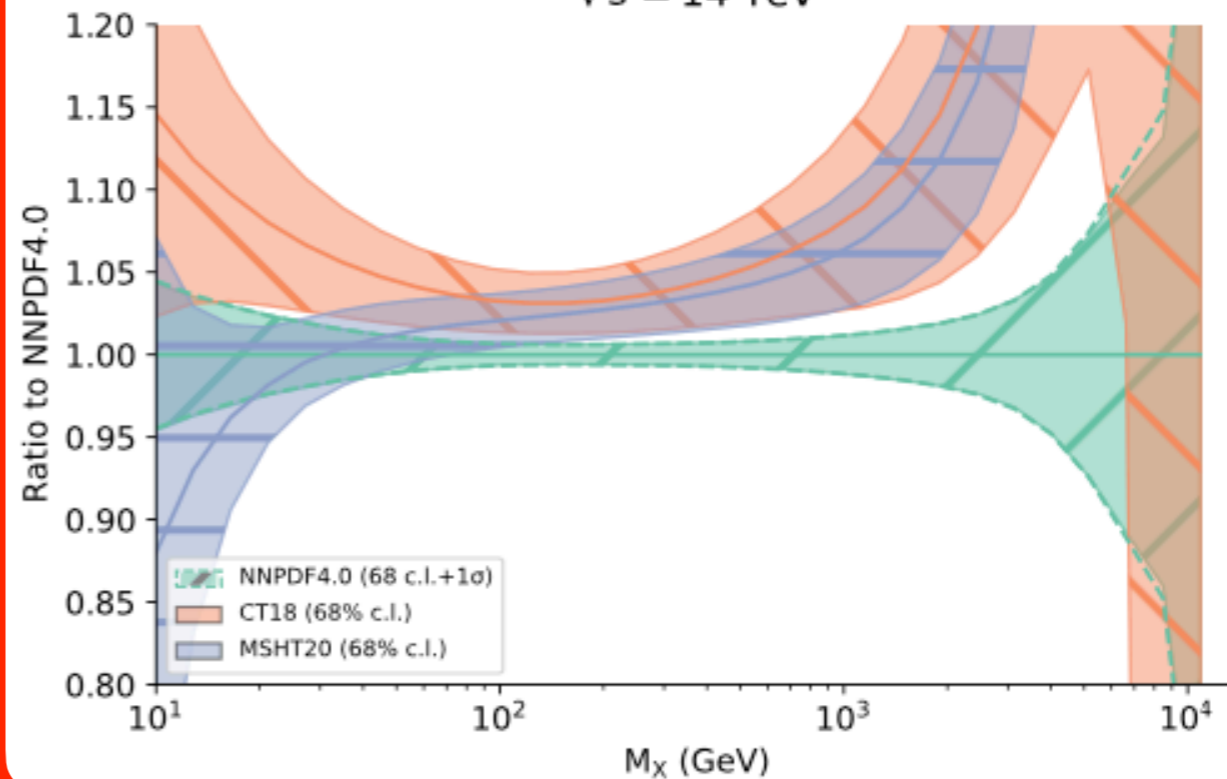
q $\bar{q}$  luminosity  
 $\sqrt{s} = 14$  TeV



gg luminosity  
 $\sqrt{s} = 14$  TeV



gg luminosity  
 $\sqrt{s} = 14$  TeV

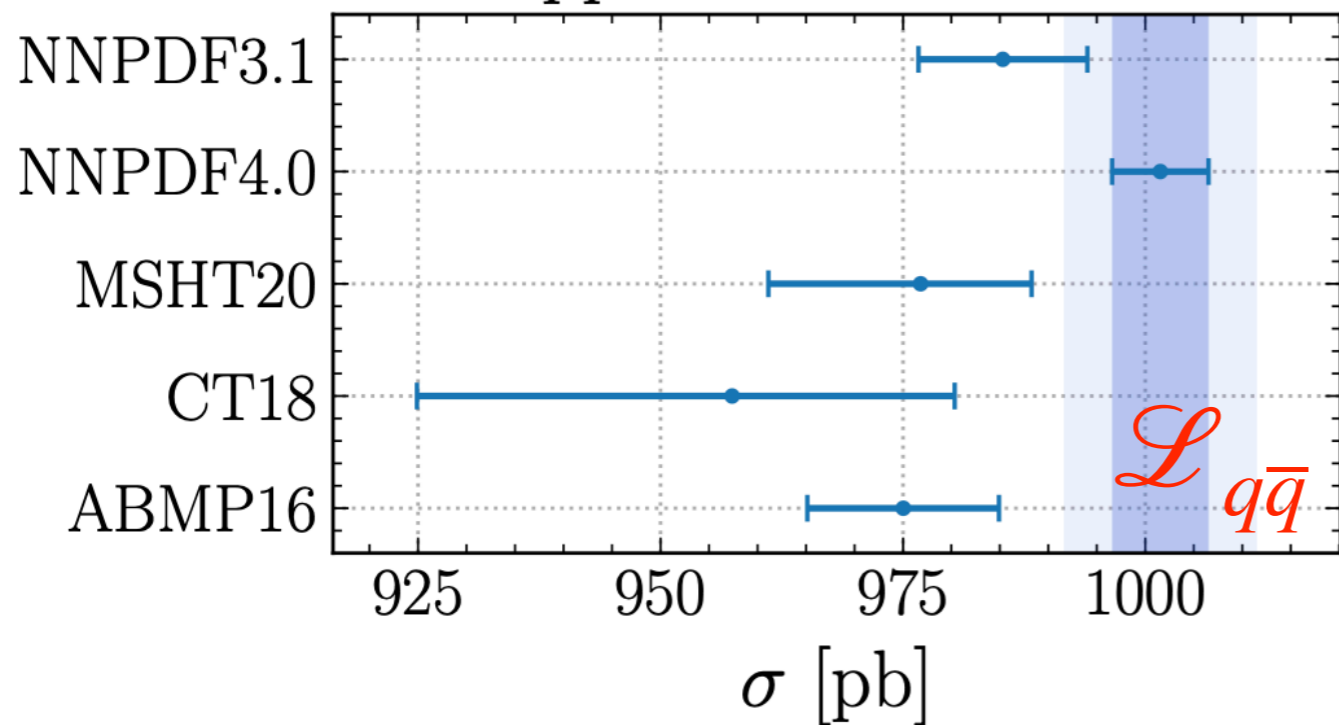


[E. Nocera's talk at DIS2021]

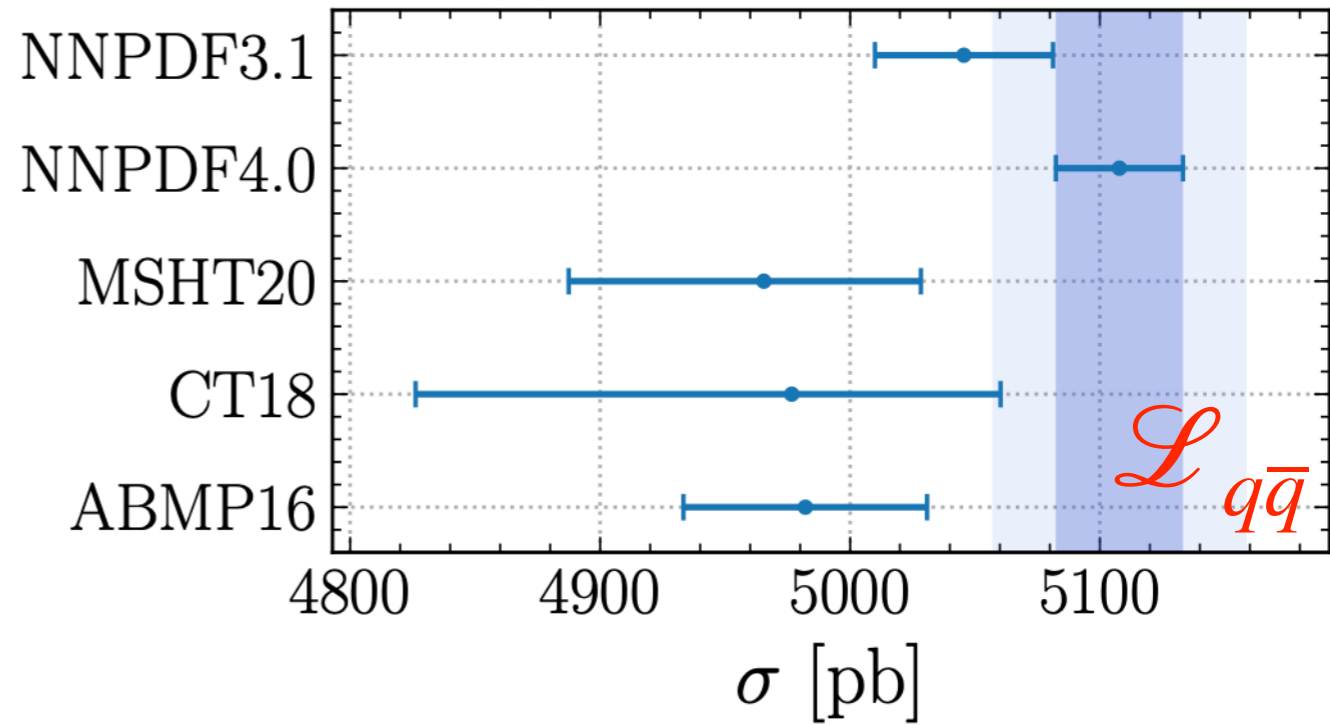


# A snapshot today

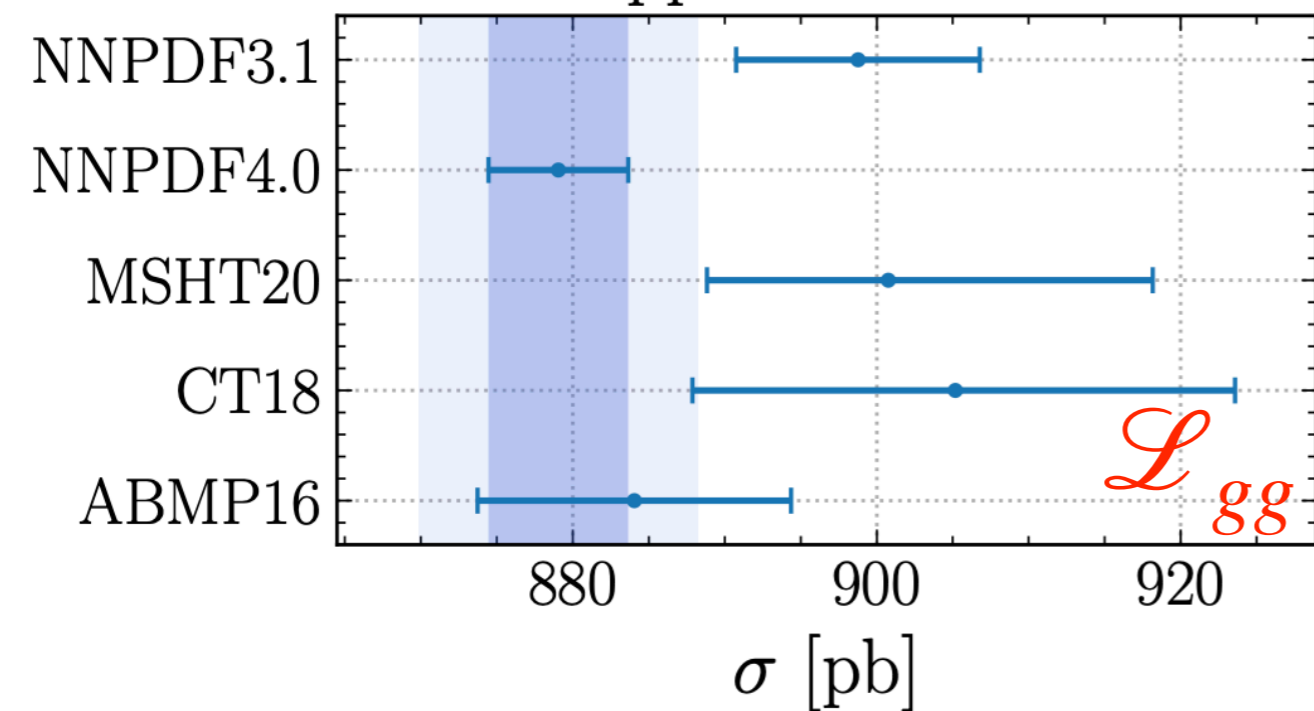
$$pp \rightarrow Z \rightarrow \ell\bar{\ell} + X$$



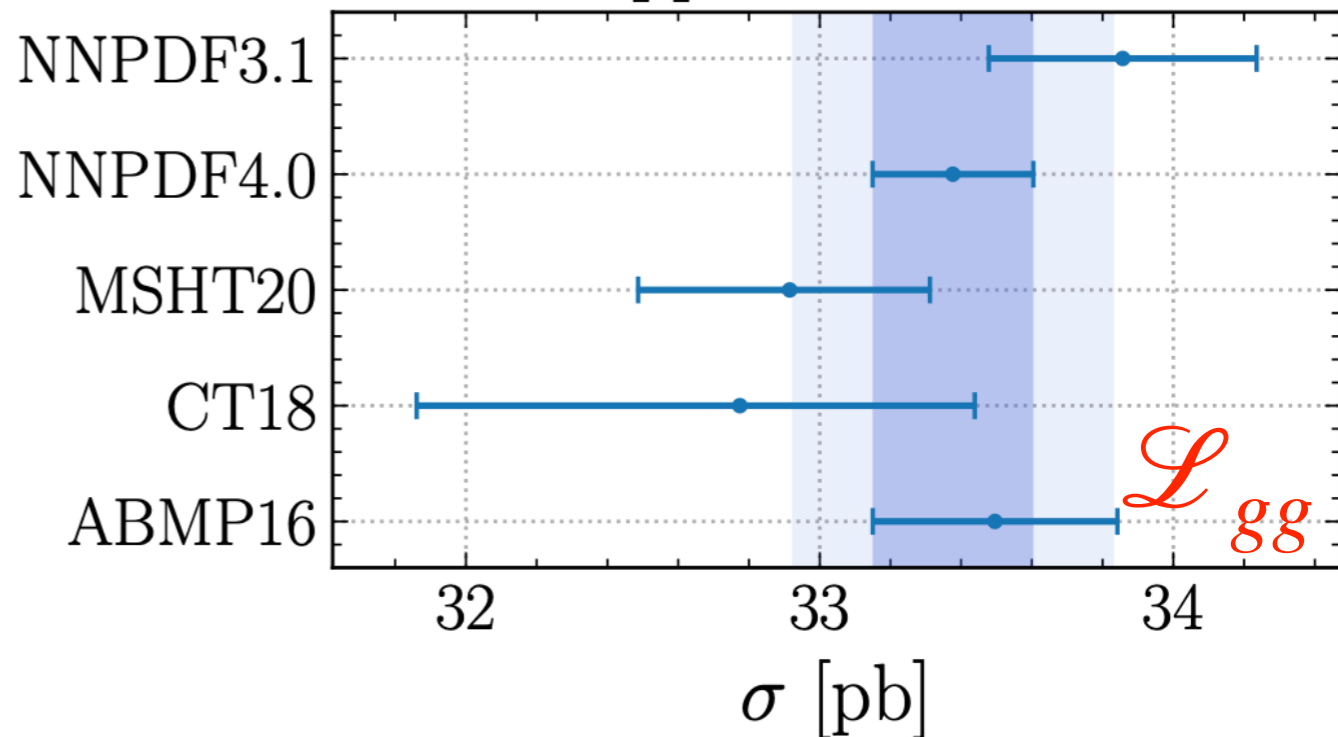
$$pp \rightarrow W^- \rightarrow \ell\bar{\nu}_\ell + X$$



$$pp \rightarrow t\bar{t} + X$$



$$pp \rightarrow H + X$$



# Conclusions

- Fitting PDFs requires making many choices:
  - data set.
  - Perturbative content:
    - DGLAP evolution,
    - hard cross sections.
  - Fitting methodology:
    - PDF parameterisation,
    - $\chi^2$  and error propagation,
    - minimisation and stopping.
- Different choices may lead to different results:
  - “Global” PDF fitters have reached a nice degree of agreement,
    - even though most recent fits present a larger departure as compared to the past.

**Backup**